Graduate Theses, Dissertations, and Problem Reports

2022

Electrochemical and mass spectrometry methods for identification of gunshot residues (GSR) in forensic investigations

Kourtney A. Dalzell
kadalzell@mix.wvu.edu

Electrochemical and mass spectrometry methods for identification of gunshot residues
(GSR) in forensic investigations

Kourtney A. Dalzell

Thesis submitted
to the Eberly College of Arts and Sciences
at West Virginia University

in partial fulfillment of the requirements for the degree of

Master of Science in
Forensic and Investigative Sciences

Luis E. Arroyo, Ph. D., Chair
Tatiana Trejos, Ph. D.
John Richardson, Ph. D.

Department of Forensic and Investigative Science

Morgantown, West Virginia
2022

Keywords: Gunshot residue, electrochemistry, distance determination, bullet hole
identification, mass spectrometry, forensics

ABSTRACT

Electrochemical and mass spectrometry methods for identification of gunshot residues (GSR) in forensic investigations

Kourtney A. Dalzell

Gun violence continues to be one of most significant challenges straining the USA society causing thousands of human lives lost every year. In 2020 alone, firearm-related incidents including homicide, accidents, and suicides, reached a staggering number of over 43,000.[1,2] With the increase in these types of incidents, several service areas in crime laboratories are heavily impacted by the number of cases run on a yearly basis. These include firearm examinations, gunshot residue (GSR) analysis, bullet hole identification, and shooting distance determination, which are crucial to support a criminal investigation and, overall, the justice system in our country. These areas are very resourceful for reconstructing firearm-related inquiries and evaluating the evidence under source (GSR present or absent) or activity (fired a gun or in the vicinity of the firing) propositions.

GSR particles are evaluated based on single-particle morphological and elemental analysis (e.g., lead, barium, and antimony) by Scanning Electron Microscopy Energy Dispersive Spectroscopy (SEM-EDS) following the ASTM 1588-20 method.[3–6] In addition to SEM-EDS, color tests are currently used to evaluate distance determination as per the recommendations given by the Scientific Working Group for Firearms and Toolmarks (SWGGUN) for nitrites, lead, barium, and copper.[7, 8,9]

Our research group has focused its attention on the development of emerging analytical tools that facilitate the detection of both inorganic (IGSR) and organic gunshot residues (OGSR) using electrochemistry (EC) along with data mining tools to support more objective data interpretation. This research aims to fill some of the gaps observed in existing technologies like color tests by offering faster and complementary methods to decrease subjectivity, cost, analysis time, to aid with triage and more cost-effective workflows at the crime scene and laboratory. The complementary OGSR information is anticipated to cause a breakthrough in the GSR analysis paradigm and respond to the current OSAC recommendations for this specialized area of work. [10–14]

To this end, the development of innovative sampling methods for distance determination and bullet hole identification were investigated to simultaneously gain spatial and chemical information via electrochemical detection. In the case of distance determination, a set of 30 calibrations and 45 unknown distance clothing samples on various light, dark, patterned, and bloodstained fabrics were assessed to compare the electrochemical performance against current techniques. Discriminant analysis statistical classification method was applied for the classification of the 45 unknowns resulting in an electrochemical method accuracy of 74% compared to color tests at 58%.

Bullet hole identification were investigated on 59 fabrics and other alternative substrates commonly found at crime scenes, such as wood, and drywall to assess potential interference and electrochemical performance from unknown shooting distance. Electrochemical methods successfully provided simultaneous detection of IGSR and OGSR with overall 98% accuracy using calibration thresholds for positive identification. OGSR results were confirmed using our research group's previously validated OGSR solvent extraction and LC-MS/MS method.

Transitions toward using portable technology probed investigation to compare the performance of portable and benchtop instrumentation for GSR analysis. A comparison of figures of merit and performance metrics found comparable results on the limits of detection, precision, linear dynamic range, and error rates, with 95.7% and 96.5% accuracies for identifying GSR using critical threshold analysis for benchtop and portable potentiostats, respectively.

Quick sample collection and screening allowed for fast electrochemical detection in 15 minutes for bullet hole and distance application. The advantage of this methodology is the developed analytical scheme can be easily incorporated within the current workflow to enhance reliability (i.e., physical measurements, color tests, or SEM-EDS) due to its non-destructive nature and highly selective and sensitive characteristics. The conclusions of this work demonstrate the fit-for-purpose of electrochemical detection expanding from GSR analysis to distance determination and bullet hole identification with fast detection using a low-cost platform for simultaneous IGSR and OGSR detection.

DEDICATION

Dedicated to my family whom I strive to make proud every day.

Mom and Dad – To the most hardworking people in the world. My greatest supporters throughout my life no matter what crazy idea I wanted to pursue. Thank you for all your love, advice, and wisdom. And lastly, thank you for believing in me and making me see the positive to every situation even when I could not see it myself. I am so grateful to have you both as my parents.

Taylor-- To the best sister a girl could ask for. Thank you for always being there to laugh, listen and talk. You are my main hype person, and I am so lucky to have a little sister that is so incredible, intelligent, and strong.

Kody – To the person I looked up to growing up. Thank you for always been there with a advice or a laugh via sock snapchat.

Aspen and Vail – Thanks for the endless kisses and excitement every time I come home.

I know we all do not get to see or be with each other as much as we'd like, but know you are with me every day.

This work is for you.

Big hugs, big love.

ACKNOWLEDGMENTS

It has taken a village to help me progress through my graduate school education. They are a lot of faculty and friends I would like to thank who have lent their unwavering support to me over the past years.

Dr. Arroyo -- Walking into your office three years ago, I truly never thought I'd be here. Thank you for seeing something in me that I didn't and believing I could make a good scientist. I am grateful for all the hours of teaching, grilling, and advice you have given me. It has made me a better student, researcher, and person. I look forward to what the next three years will bring with your guidance.

Dr. Trejos – So grateful I get to not only be a part of the Arroyo group, but also work with you and the GSR team. Thank you for always having an open door for me and offering your support and advice along the way.

Dr. Richardson – Thanks for welcoming me as an unfamiliar student and agreeing to be on my committee. I appreciate all the time, teaching, support you have given as I began this journey.

Courtney – I guess I'll start by apologizing for being scared of you in the beginning. I don't know how to put into words how much all the moments of talking, advice, coffee breaks, and lots of wine we've had over the years mean to me. So honored I get to call you my best friend and confuse everyone around us. Cheers to our next journeys because it's going to be a lot harder without you by my side.

Kylea, Colby, and Joe – For the countless laughs, memes, and adventures. For being together for big life moments. For becoming such a close-knit lab group and friends. Wouldn't want to get lost in the wood with anyone else. Glad we could take this unforgettable journey together.

Bill – Thanks for being my gym buddy, "research brother", and of course the FNAFs and laughs. Gotta catch 'em all…

GSR Team and Arroyo Group – So thankful I got to work and learn from all of you guys over the years.

FIS Department – For all the faculty I have gotten to learn from inside and outside of the classroom. Thank you for being the most welcoming and caring teachers. I am so grateful to have had the pleasure of being one of your students.

List of Abbreviations

Full Name	Abbreviation
2,4-Dinirotoluene	2,4-DNT
2,6-Dinitrotoluene	2,6-DNT
2-Nitrodiphenylamine	2-NDPA
4-Nitrodiphenylamine	4-NDPA
Abrasive Stripping Voltammetry	AbrSV
Acetonitrile	ACN
Akardite II	AKII
Alternative Light Source	ALS
Anodic Stripping Voltammetry	ASV
Antimony	Sb
Atomic Adsorption Spectroscopy	AAS
Barium	Ba
Box-Behnken design	BBD
Britton Robinson Buffer	BR
Collison Energy	CE
Copper	Cu
Counter Electrode	CE
Crime Scene Investigators	CSI
Current	i
Cyclic Voltammetry	CV
Desorption Electrospray Ionization Mass Spectrometry	DESI-MS
Differential Pulse Anodic Stripping Voltammetry	DPASV
Differential Pulse Cathodic Adsorptive Stripping Voltammetry	DPCAdSV
Diphenylamine	DPA
Discriminant Analysis	DA
Dithiooxamide test	DTO
Electron Ionization	EI
Electron Multiplier	EM
Electrospray Ionization	ESI
Ethyl Centralite	EC
European Network of Forensic Science Institutes	ENFSI
Flow Injection Amperometry	FI Amp
Fourier Transform Infrared Spectroscopy	FTIR
Gas Chromatography Mass Spectrometry	GC/MS
Glassy Carbon Electrode	GCE
Gold Mercury Film Electrode	Au-MFE
Gunshot Residue	GSR

Hanging Mercury Drop Electrode	HMDE
Infrared Spectroscopy	IR
Inorganic Gunshot Residue	IGSR
Institutional Review Board	IRB
Ion Mobility Spectroscopy	IMS
Laser Induced Breakdown Spectroscopy	LIBS
Lead	Pb
Limits of Detection	LOD
Liquid Chromatography	LC
Liquid Chromatography tandem Mass Spectrometry	LC-MS/MS
Lower Limits of Quantitation	LLOQ
Mass Spectrometry	MS
mass-to-charge ratio	m/z
Mercury coated Graphite Electrode	MCGE
Mercury Film Glassy Carbon Electrode	Hg-GCE
Methanol	MeOH
Methyl Centralite	MC
Microfluidic paper analytical device	µPAD
Microgram	µg
Microliter	µL
Milligram	mL
Milliliter	mL
Minute	min
Modified Griess Test	MGT
Nitrocellulose	NC
Nitroglycerin	NG
Nitroguanidine	NGd
N-Nitrosodiphenylamine	N-NDPA
Normal phase liquid chromatography	NPLC
Organic Gunshot Residue	OGSR
Organization of Scientific Areas Committee	OSAC
Parts per Billion	ppb
Parts per Million	ppm
Potential	E
Primer Gunshot Residue	pGSR
Principal Component Analysis	PCA
Principal Components	PC
Quadrupole 1	Q1
Quadrupole 2	q2

Quadrupole 3	Q3
Reference Electrode	RE
Relative Standard Deviation	%RSD
Regularized Discriminant Analysis	RDA
Retention Time	Rt
Reversed phase liquid chromatography	RPLC
Saturated Calomel Electrode	SCE
Scanning Electron Microscopy Energy Dispersive Spectrometry	SEM-EDS
Scientific Working Group for Firearms and Toolmarks	SWGGUN
Screen-printed Carbon Electrodes	SPCE
Screen-printed Electrodes	SPEs
Seconds	sec
Silver-Silver Chloride	Ag/AgCl
Solid Phase Microextraction Ion Mobility Spectroscopy	SPME-IMS
Square-Wave Anodic Stripping Voltammetry	SWASV
Square-wave Cathodic Adsorptive Stripping Voltammetry	SWCAdSV
Square-Wave Voltammetry	SWV
Time of Flight	TOF
Total Nitrite Pattern Visualization	TNV
Triple quadrupole mass spectrometry	QqQ
Ultra-High Pressure Liquid Chromatography	UPLC
Water	H2O
Working Electrode	WE

List of Figures

List of Tables

Chapter 4

Chapter 5

INTRODUCTION

As of 2020, the gun violence-related deaths in America reached an all-time high with over forty-three thousand deaths. The majority comprised approximately 58% suicides and 38% homicides.[1,2] Nationally, over 110 death occur per day in the United States where it is common to hear about gun violence whether it was a mass shooting, homicide, or suicide on the news, social media, or someone they knew personally. The tragedy of gun violence comes at a large cost not only to the individuals affected but to our country's economy, where 229 billion dollars is the estimated cost of gun violence to the American economy every year.[2] In our state, West Virginia ranks thirteenth in the United States for the highest gun death rate where on average there are 17.8 deaths per 100 thousand residents.[2] The cost to the West Virginia government and residents is over 1.6 billion dollars a year toward the care for resulting deaths and injuries to gun violence victims in the state.

With the ever-increasing trend in gun violence, the forensic community workload does not go untouched by the unfortunate outcomes of shooting-related crimes and events. Indeed, some states have implemented state-of-the-art systems to rapidly attend a shooting scene. To this end, technological improvements to the rapid acoustic gunshot detection have allowed the police to quickly be alerted to potential gunshots in a particular location with more reliability and accuracy.[15] These improvements have impacted the need for specialized trace analysts in gunshot residue (GSR), and to the development of rapid and complementary techniques to provide valuable information supporting and improving current practices.

Inorganic gunshot residue (IGSR) analysis is carried out by the gold standard scanning electron microscopy energy dispersive spectroscopy (SEM-EDS) following the standard ASTM E1588-20. The morphological identification of a GSR particle is one of the major advantages of this protocol. Once the particle is found, the analytical evaluation of the inorganic elements lead barium and antimony is conducted. However, some of the drawbacks of this method is the time required to complete the search and analysis of particles which can take many hours or even days to complete a report. This limitation has also boosted the interest of several researchers to find alternative methods and instrumentation to offer a more comprehensive evaluation of the GSR evidence. Within GSR analysis, sometimes the focus relates to evaluating the shooting distance and discerning a potential bullet hole. These two important areas are currently processed considering

both physical characteristics and colorimetric tests for lead, barium, and nitrites. Due to the subjective nature of these tests, modern and more informative methods are needed. Also, newer ammunition formulations do not contain lead and therefore, these updated methods should include not only the inorganic analysis of elements but also identifying organic constituents with confidence. The combination of both organic and inorganic analytical information represents an advantage to the analyst to gather stronger information for decision making and reporting. In fact, the organic gunshot residue analysis (OGSR) is currently recommended by the Organization of Scientific Area Committees (OSAC), where GC/MS and LC/MS are the recommended approaches.

This research work presented in this thesis aims to develop and provide smart, rapid, and low-cost methods for gunshot residue identification and distance determination to assist with evidence triage from a crime scene to the laboratory and enhancing the value of existing methodologies. Electrochemical and mass spectrometry techniques are proposed for evaluating their application to gunshot residue, distance determination and bullet hole identification. This work's structure is organized into five main chapters that outline the literature, objectives and tasks, and outcomes for the proposed methods.

Chapter 1 highlighted the theory, current practices, previous applications for gunshot residue, color tests, electrochemistry, and liquid chromatography-tandem mass spectrometry. This background information emphasizes the importance of this research by what has been done previously and the steps this research takes to address gaps in knowledge.

Chapter 2 outlines the motivation for this project, its respective goals, and objectives, and the tasks carried out to achieve the goals.

Chapter 3 addresses the first objective for distance determination by electrochemical detection as a solution for better screening and classification for shooting reconstruction purposes. Chapter 3 reports on the methods developed and used for distance determination, the finding of electrochemical methods compared to physical and color test, and the performance relative to different fabric material which may be encountered in actual casework.

Chapter 4 details the methods, outcomes, and conclusion for electrochemical analysis as a rapid screening for bullet hole identification. Chapter 4 assess the electrochemical detection for various substrates which are commonly found in or at crime scene which pose as difficult to analysis using current practices like color tests. Confirmation through mass spectrometry methods report OGSR presence compared to electrochemical results and proof of mass spectrometry application to bullet hole identification.

Chapter 5 describes the evaluation of portable and benchtop potentiostats for GSR detection. Potentiostats were evaluated using IGSR and OGSR standards and authentic non-shooter and shooter samples to determine the performance and accuracy of each electrochemical instrument.

Chapter 6 outlines the major conclusion from the overall project and recommendations or improvements for future work.

I. CHAPTER 1: LITERATURE REVIEW

1.1 Gunshot Residues (GSR)

During the discharge of ammunition from a firearm, a variety of residues are produced. A chemical reaction is set off by the low explosives consisting of the primer and propellant components inside the cartridge. The propellant is ignited by the primer, and it burns to create a high temperature and pressure setting in the firearm which in turn expels the bullet. The result of this event is a gaseous cloud which is rapid cooled as it interacts with the atmospheric temperature and pressure which settles in the surrounding area of the discharge, like the hands, nose, and clothing of an individual near this event.[3,16] Gunshot residues (GSR) are often referred to by where they origin from the ammunition: Primer Residues (pGSR) are residues generated from the primer mixtures, Inorganic GSR (IGSR) generated from the primer, projectile, cartridge case, and/or firearm, and Organic GSR (OGSR) generated from the propellant or primer mixture.[17,18] **Figure 1** demonstrates the anatomy of ammunition and the elemental and chemical sources from the cartridge case, projectile, and propellant.
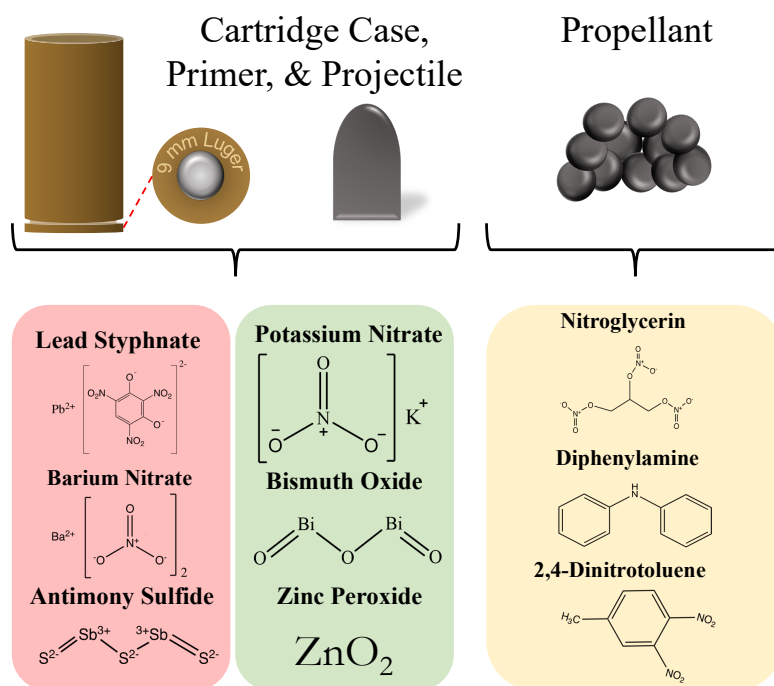
Figure 1.1. *Anatomy of ammunition and the common elements and chemical composition IGSR and OGSR compounds associated with the various components.*

1.1.1 Inorganic Gunshot Residues (IGSR)

The firing event begins with a primary explosive reaction which starts when the trigger is pulled, and the firing pin strikes the primer cup igniting lead styphnate. A rapid temperature increases due to oxygen-rich barium nitrate. At the high temperature, antimony sulfide is ignited, and the secondary explosive reaction of the smokeless powder propels the bullet through the barrel of the firearm. Therefore, IGSR comprises three main components of the primer composition (pGSR): the initiator (e.g., lead styphnate, $C_6HN_3O_8Pb$), the oxidizer (e.g., barium nitrate, $Ba(NO_3)_2$), and the fuel (e.g., antimony sulfide, Sb_2S_3). While the pGSR is the main component of IGSR, there are other sources that can contribute to other residue elements from the cartridge case, projectile, and firearm (see **Figure 1.1**). The other sources may contribute to additional metal or metal oxidizes, such as copper, aluminum, calcium, silicon, etc., depending on the composition of manufacturers.[18]

In forensic laboratories, scanning electron microscope energy dispersive spectroscopy (SEM-EDS) remains the gold standard for its capabilities to provide morphological and size of the particles as well as the elemental profiles of GSR particles and the classification scheme (**Table 1.1**).[18]

Table 1.1. *Interpretation scale for IGSR identification by SEM-EDS from the E1588-20 ASTM Standard.*[18]

Criteria for IGSR Detection	Interpretation for IGSR Identification		
Elemental Composition	Standard Ammunition	Non-toxic/Lead-Free Ammunition	Applies to either ammunition type
Characteristic of IGSR	Pb, Ba and Sb	Gd, Ti, Zn Ga, Cu, Ti	*additional elements incorporated*
Consistent with IGSR	Pb, Ba, Sb, Si Ba, Ca, Si Sb, Ba Pb, Sb Ba, Al Pb, Ba	Ti, Zn Sr	Al, Si, P, S, Cl, K, Ca, Fe, Ni, Cu, Zn, Zr, Sn
Commonly Associated with IGSR	Pb Sb Ba (sulfur can be present)		*Caution:* with barium sulfate and iron
Morphology **Spheroid**: 0.5-5 μm **Irregular**: 0.5-100+ μm Varies greatly and should not be the only criterion considered for GSR identification	Section 9.1.8 states "Additional classifications can be developed for specific types of primer compositions not included in the previous sections. Any new classification should aid in differentiating environmentally or occupationally produced particles that could be found in a sample from GSR. An assessment of the significance of these classifications shall be made in consideration of appropriate research and documentation"		

1.1.2 Organic Gunshot Residues (OGSR)

The composition of the propellant accounts for the main organic gunshot residues. The smokeless powders used in ammunition consist of a single base (nitrocellulose), a double base (nitrocellulose and nitroglycerin), and a triple base (nitrocellulose, nitroglycerin, and nitroguanidine) formulations as the explosives in the secondary explosion reaction.[19] Manufactures of these smokeless add other compounds like diphenylamine (DPA) and derivatives, 2,4-dinitrotoluene (2,4-DNT), acardite II (AKII), and ethyl centralite (EC) act as stabilizers, plasticizers, sensitizers and flash suppressors (**Figure 1.2**).[20,21] OGSR can sometimes be visible on the hands of an individual or target of firearm discharge as soot, unburnt, or partially burnt particles which can often be seen under a stereoscope at close shooting distances. Feeney and Vander Pyl highlight the common challenge with OGSR detection surrounds the persistence due to their physicochemical properties like absorption or evaporation into skin or air, in addition to, any activities like walking, running, or washing the target or skin hand which could affect the persistence due to the nature of OGSR compounds.[21]
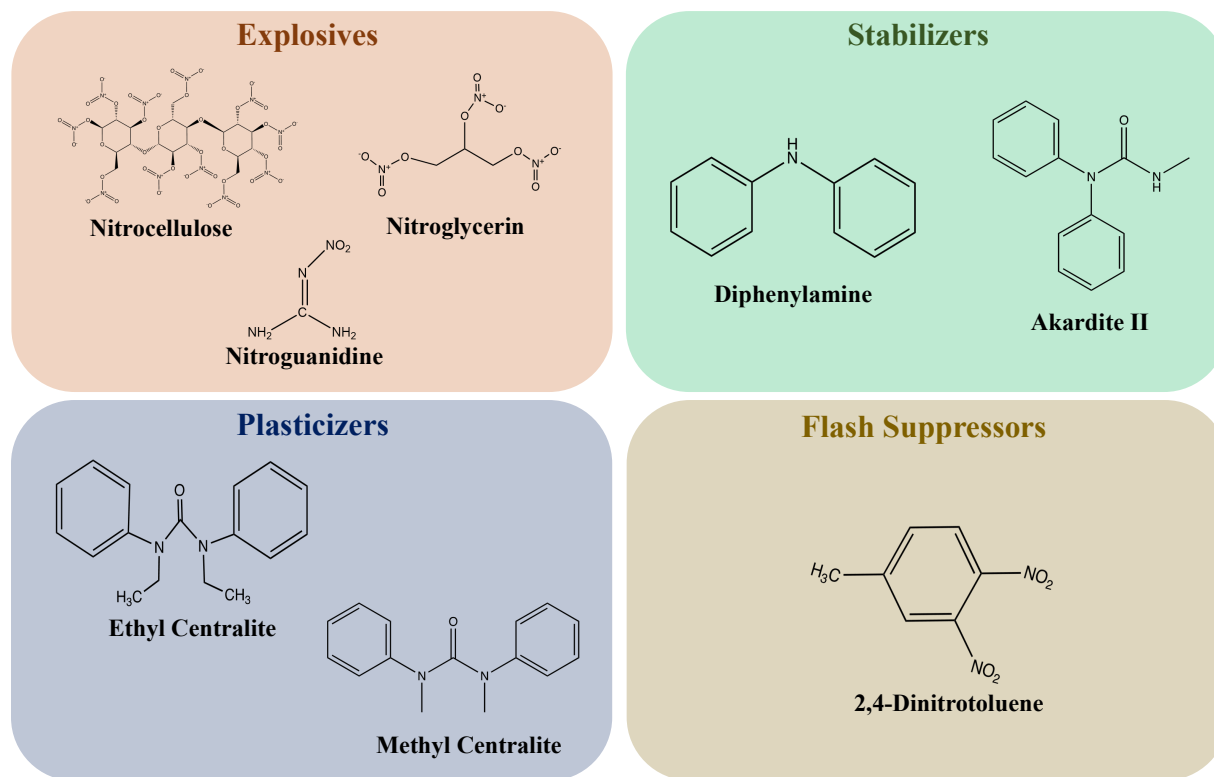
Figure 1.2. *Chemical structures of OGSR compounds and their function in smokeless powder formulations.*

Investigations into method of OGSR detection began in the 1960s with chromatographic methods.[22] In the past decades, instrumental improvements have allowed for more techniques to be included in research surrounding OGSR such as: liquid chromatography (LC), ion mobility spectroscopy (IMS), solid phase microextraction IMS (SPME-IMS), and desorption electrospray ionization mass spectrometry (DESI-MS). [22–25] Review articles by Goudsmits et al. in 2015 and Feeney et al. in 2020 reported over 100 different organic compounds that have been identified as commonly associated GSR using various instrumental methods with over 130 refereneces.[21,22] Appendix I, Table S1.1 provides a small subset of 37 manuscripts which report OGSR compounds detection from 1978 to 2020 using various analytical methods including LC-MS/MS, GC/MS, Raman spectroscopy, ion mobility spectroscopy (IMS), electrochemical detection, DESI-MS, etc. for the detection of OGSR compounds. These studies report research detecting compounds such as NG, EC, methyl centralite (MC), DPA, 2-, 4-, and N-nitrodiphenylamine and 2,4-DNT. Diphenylamine, ethyl centralite, and 2,4-dinitrotoluene most frequently reported where compounds like 2,6-DNT and acardite II less frequently studied.[10,11,21,23–50]

The standard method for OGSR identification includes the ASTM 2998-16 defining smokeless powders, terminology, and acceptable instrumental methods for analysis as gas chromatography-mass spectrometry (GC/MS), Fourier Transform Infrared Spectroscopy (FTIR), and Liquid Chromatography mass spectrometry (LC/MS).[19] Currently, the organization of scientific areas committee (OSAC) has published, "Standard practice for collection, preservation, and analysis of organic gunshot residue." At this time, the document is undergoing the process of becoming an ASTM standard which provides terminology, and procedures for the collection and preservation of organic gunshot residue. Additionally, the document provides procedures for GC and LC-MS analysis as well as the classification scheme of OGSR compounds into Category 1 (NG, EC, MC, 2-,4-NDPA) and Category 2 (NC, DPA, 2,4-DNT, AKII) and criteria for identification of OGSR being characteristic or consistent with gunshot residues.[17]

1.1.3 Current Needs

The discipline's standards and guidelines offer excellent methodologies and interpretation of GSR evidence by using confirmatory methods. Current research in GSR aims to add complementary information via the creation of screening techniques to aid in sample collection decision-making

processes, reduce backlogs, and decrease the time of analysis. Additionally, methods that perform simultaneous IGSR and OGSR detection could improve triage and workflow at the crime scene and laboratory.

Some limitations of SEM-EDS related to the speed of analysis which creates a bottleneck from the number of samples, and the automated search time, which can take anywhere from 3-8 hours.[51] Moreover, the interpretations of SEM-EDS analysis data must now consider potential environmental contamination originating from materials handled by fireworks operators and electricians, components present in airbags, or brake pads, all of which can potentially lead to false-positive results due to these activities creating GSR-like particles.[8,9] The rise in new non-leaded ammunition has expanded the suite of elements present in the novel formulations, including bismuth, titanium, potassium, and copper, which increases the difficulty in interpretations of the SEM-EDS results (**Figure 1**). These limitations of SEM-EDS and the inclusion of new formulations of ammunition have led to investigations in the quest for new screening and confirmatory methods.[52,53]

Highlighted in Harris et al., reported a study of CCI Blazer lead-free ammunition discussing the interpretation of SEM-EDS and the memory effect firearms can have when using leaded and lead-free primer ammunition in the same firearm. The authors found CCI Blazer contains a profile of tetracene, diazo dinitrophenol, and strontium from direct analysis of the ammunition. Test fires from using multiple ammunition and firearms found the presence of carry-over of traditional ammunition when the lead-free ammunition was used in the firearm.[5] This thesis highlights some of the challenges that new lead-free ammunition can make for analysts when interpreting SEM-EDS results concerning memory effect of the firearm and the current changes in the ammunition markets.

1.2 Colorimetric Tests for GSR

Crime scene investigations often carry out crime scene reconstruction to help answer investigative questions involving how an event took place. During investigations that involve a firearm, questions commonly asked by investigators to forensic personnel concern the identification of bullet holes, shooting positioning, distance from the target, and more about the relevance of GSR being present or not. At a crime scene, the discharge event of a bullet from a firearm may leave

gunshot residues (GSR) on a target depending on the distance or unidentified surface damage that could be used in the reconstruction of shooting distance and bullet hole identification. The Scientific Working Group of Firearms and Toolmark Identification (SWGGUN) and the European Network of Forensic Science Institutes (ENFSI) best practices standards analysis methods in these situations follow an analytical scheme through physical and visual examination, microscopic examination, and colorimetric tests.[7,54] The ranges used for distance determination look at the patterns of firearm discharge residues, soot, bullet wipe, and bullet hole size for close-, mid-, and long-range shots, typically from contact to 36 inches **(Figure 1.3)**. Additionally, bullet hole patterns can be observed with microscope analysis for starburst or circular bullet entrance and exit hole at close- and long-range firing, in addition to, burns, melting, flakes, and soot surrounding the bullet wipe, especially at close to mid-range shots. Like color tests for seized drug analysis, there are colorimetric methods to enhance GSR on a substrate by using chemical reactions that produce a visual color depending on the element or functional group of interest. According to the SWGGUN and ENFSI best practice guidelines for gunshot residue detection, there are three colorimetric tests that can be performed for shooting distance determination in the following order: modified Griess (MGT), dithiooxamide (DTO), and sodium rhodizonate.[7,54]
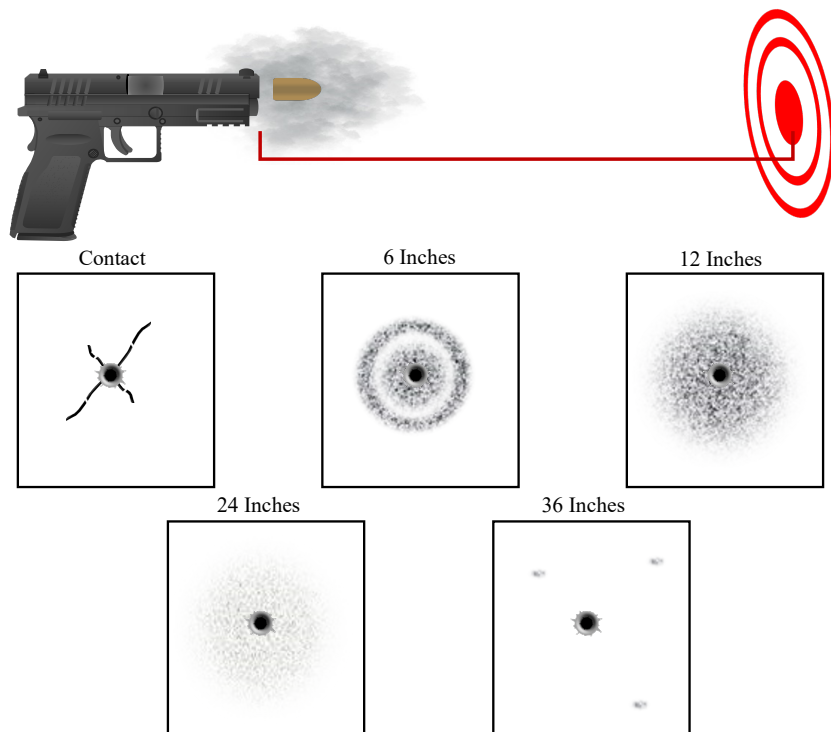
Figure 1.3. *Graphic representation of the distribution patterns of GSR on a target at various close- and long-range distances with typically physical characteristic observations.*

1.2.1 Modified Griess Test

Nitrite detection is performed using the Modified Griess Test (MGT), which targets compounds from the propellant, like nitro compounds that may have been expelled onto the clothing or other surfaces. The color change occurs on photographic paper that has been soaked in alpha-naphthol and sulfanilic acid. Sodium nitrite swabs soaked in dilute acetic acid are placed in four corners of the paper to assure the paper acts as a positive control for the analysis. The sample is placed on the photographic paper, so the area of interest is facedown, and a cheesecloth dampened with dilute acetic acid is placed on the back of the sample, where pressure and heat are applied using an iron until dry. When the sample is removed, an orange azo dye color change is produced by the heating of the nitrites and acetic acid to form nitrous acid, which reacts with the sulfanilic acid to produce a diazonium compound that in the presence of alpha-naphthol produces an orange-colored dye (**Figure 1.4**).[55]
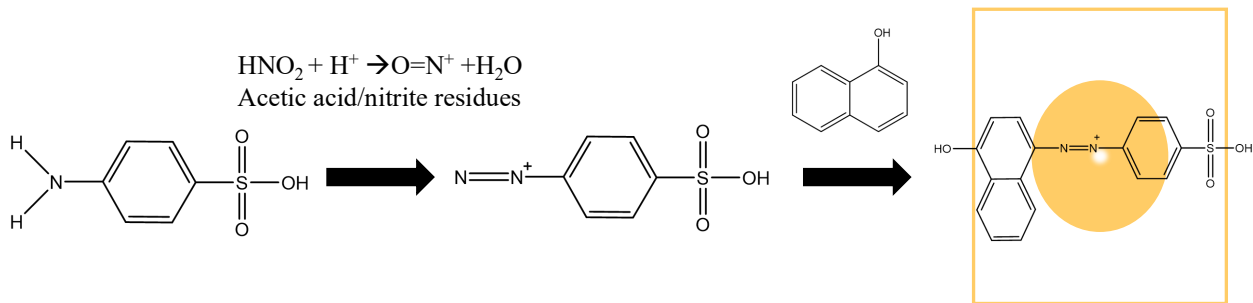
Figure 1.4. *Chemical reaction of the Modified Griess Test.*

1.2.2 Sodium Rhodizonate Test

Lead and barium are two common elements originating from the primer and projectiles that can produce residues on a substrate. The sodium rhodizonate test evaluates the presence of lead and barium by generating a reddish-violet color change.[56] Often the method is carried out using a Bashinski transfer method where filter paper is wet with dilute acetic acid and placed on the area of interest. Similar to the Griess test, both pressure and heat are applied using a hot iron to transfer the lead and barium deposits to the filter paper. Then, the sodium rhodizonate method is used in the filter paper rather than the actual sample or piece of evidence. Continuous spray bottles apply the reagents in the following order to the filter paper: saturated sodium rhodizonate in water, sodium bitartrate and tartaric acid buffer pH 2.8, and dilute hydrochloric acid. A pinkish violet

color change followed the complexes that are formed when barium or lead reacts with the sodium rhodizonate salt (**Figure 1.5**).[56]
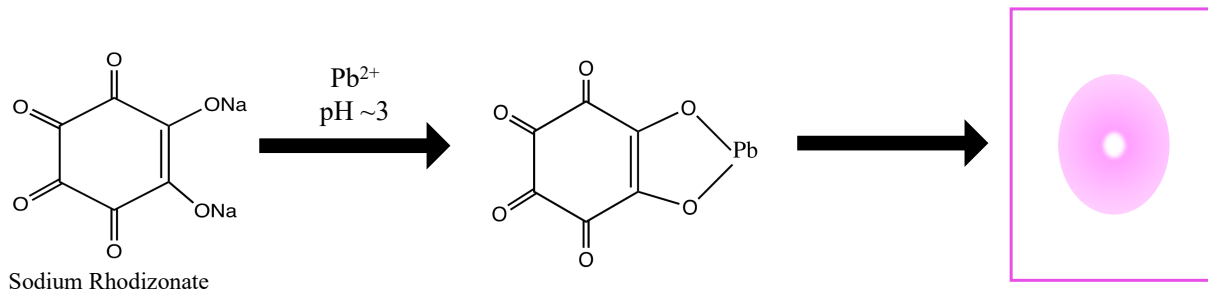
Figure 1.5. *Chemical reaction of the Sodium Rhodizonate Test.*

1.2.3   Current Needs

Colorimetric methods have several advantages for laboratories, including simplicity, speed, and low-cost testing for IGSR and nitrites, however, they have been the subject of criticism over the years due to challenges with subjectivity. Some of the major limitations of existing colorimetric methods include a) the presence of false positives generated by environmental sources, b) evaluation of difficult-to-manipulate substrates like clothing, walls, and ceilings, and c) lacking confirmatory and/or screening capability in laboratory and crime scene settings. Many variables like ammunition type, bullet type, and angle of firing can influence the bullet hole shape and distribution of GSR on the target, which can make analysis difficult and subjective for the analyst.[57,58] Additionally, environmental contamination can cause false positives with the colorimetric method due to factors like the presence of trace and minor elements in soil particles, face make-up, airbags detonation components, fireworks, and mechanical work that can produce similar elements like lead, barium, and antimony.[8,9,59,60] To illustrate the difficulty of analyzing substrates found in crime scenes, dark or bodily fluid-soaked fabric obscures the visualization of GSR by CSIs and forensic personnel. Additionally, other substrates like wood, drywall, and glass are commonly involved in a shooting event and may not be able to be examined onsite or brought back to the laboratory for analysis. Besides these challenges, the colorimetric methods have been investigated to address issues and interferences that occur during the analysis of samples or evidence.

Research has been developed in recent years to investigate the use of the modified Griess and sodium rhodizonate tests, focusing on improving visualization and detection, especially

surrounding their use for long-range shooting distance, loss from sample handling, and overpowering lead patterns.[61] Recently, in 2019, Berger et al. compare the traditional MGT to the total nitrite pattern visualization method (TNV) developed by Glattstein et al. The comparison looked at the method application to address the incubation time of the additional alkaline hydrolysis step, bloody substrates, and long-distance ranges. Berger's group found that a reduction in incubation time can aid in the speed of analysis and nitrite patterns detected up to 36 inches, however, there was no improvement with detection on bloody substrates.

A limitation of the sodium rhodizonate test involves the rapid decomposition of the salt complexes which results in a fading of the violet color change. Studies from Bartsch et al. have found over a nine-month period, that the lifespan of the sodium rhodizonate color can be preserved by removing the excess HCl during the analysis.[62] Another study by Andreola et al., investigated the use of HCl in the sodium rhodizonate test on human skin. The study used 88 histological specimens from 6 cases involving firearm injuries and concluded that HCl improved the significance of the color test due to the nonspecific nature of sodium rhodizonate. The author also looked at stability over 6 months which noticed sample discoloration over the time period, but observations could still be made from 6-month-old samples.[63] Recently, researchers from Thailand reported using digital imaging and micro-fluidic paper as an analytical device employing rhodizonate reagents for the detection of lead from four different fabric substrates. While imagining could detect up to 40 cm distances on all fabrics, the μPAD device performed better with detection up to 60 cm and found thicker fabrics retained more GSR than thinner fabrics.[64]

New technologies for distance determination have been investigated using XRF, AAS, LIBS, FTIR, and micro-fluidic paper as alternatives to the current practices.[10,12,64–66] In 2006, Berendes reported using a Midex M XRF system which allows mapping of a 20x20 cm area with no sample preparation for Pb and Ba detection of leaded primer as well as Ti, K, and Ga for non-toxic ammunition formulations.[65] Gagliano-Candela reported Atomic Absorption Spectroscopy (AAS) for lead detection around bullet holes from test shots fired ranging from 5-100 cm distances onto filter paper.[67] A study by Sharma and Lahiri looked at using FTIR instrumentation for distance determination of organic GSR using 3-9 cm firing distances and transmission mode to measure at various distance away from the bullet hole on the target.[10] Other researchers have investigated the

issue surrounding the analysis of skin and dark fabric substrates using alternative light sources (ALS) and multi-spectral imaging and scanning electron microscopy.[68–70]

In 2018, our research group reported the use of Laser-Induced Breakdown Spectroscopy (LIBS) in GSR detection with applications including both hand and distance determination.[12,14,66,71] Vander Pyl reported 100% accuracies for the classification of distance determination ranges using LIBS methods compared to physical measurements and colorimetric testing.[66] An additional study by Vander Pyl looked at the distance estimation and bullet hole application of LIBS to dark and patterned fabrics, bodily fluid-soaked fabrics, as well as common crime scene substrates like wood, glass, and drywall. LIBS detection was still achievable, and LIBS offered a superior classification of true shooting distances over physical and colorimetric testing.[12]

Research work presented above focuses on improvement to the colorimetric methods or discusses alternative techniques for IGSR or OGSR detection. This research thesis explores the electrochemical detection to provide a fast, simple analysis which can perform simultaneous IGSR and OGSR detection for the application of bullet hole and distance determination. This method merges IGSR and OGSR detection into a single low-cost screening platform which can be produce spatial and chemical information necessary for identification and classification of samples.

1.3 Electrochemistry

In the United States, electrochemistry has been an instrumental analytical technique used in various industries such as medical, biomechanics, thermodynamics, and other fields. A fundamental definition of electrochemistry by Heineman, is "the measurement of electrical signals associated with a chemical system into an electrochemical cell".[72] Observation of the electrochemical system involves applying a potential (E) or voltage to produce a change in current (i) through the transfer of electrons typically produced by a redox reaction to observe the oxidation and reduction of the analyte of interest. The movement of electrons that produces the current can be useful in the determination of the concentration of the species by Faraday's equation and taking the derivative of it to relate to the current.

$$Q = nFN, \tag{1}$$

Where Q is the charge in Coulombs, n is the number of electrons involved in the redox reaction, N is the number of moles electrolyzed, and F is faradays constants (96,485 C/mol).[72]

So current equals,

$$i = \frac{dQ}{dt} = nF\frac{dN}{dt}, \tag{2}$$

Where dN/dt is the addition of the rate of the reaction at the electrochemical interface.[72]

A common electrochemical cell often discussed in textbooks is a galvanic cell which consists of two electrodes, a cathode, and an anode, in an electrolyte solution, allowing for electron transfer in two half-reactions of reduction and oxidation. These traditional electrochemical cells use a large volume of supporting electrolyte and sample to contain the separate working, reference, and auxiliary electrodes in a beaker to perform electrochemical detection. These large solid-state electrodes have specific functions in electrochemical detection, the first being the surface of the working electrode (WE) where the potential or voltage is applied to detect the movement of current from the redox reaction. The most widely used WE is the hanging drop mercury electrode (HDME) due to its wide potential range and high sensitivity, although other materials like glassy carbon, silver, gold and boron-doped diamond are commonly used working electrodes.[45,73,74, 72] While the HDME affords superior detection of a broad array of analytes, many analysts have turned away from that electrode use due to the harmful nature of mercury. The reference electrode is a known electrochemical reaction used to measure potential against the WE, typically using a saturated calomel electrode (SCE), or Silver-Silver Chloride (Ag/AgCl). The auxiliary or counter electrode has the opposite potential applied to sustain electrolysis by allowing the flow of current through inert metals like platinum, palladium, or copper as some examples. [72] Innovations in modern electrochemical cells have transitioned to screen-printed electrodes that combine a traditional electrode unit into a small-single platform containing: the working (WE), reference (RE), and counter or auxiliary electrodes (CE). The advantages of these electrode configurations are they provide small, disposable, cheap, and reduced sample volumes (see **Figure 1.6**).

$$O + e^- \leftrightarrow R$$

$$Pb^{2+}$$

$$Pb_s$$

Metrohm
110

C.E.

W.E.

R.E.

10 x 34 mm
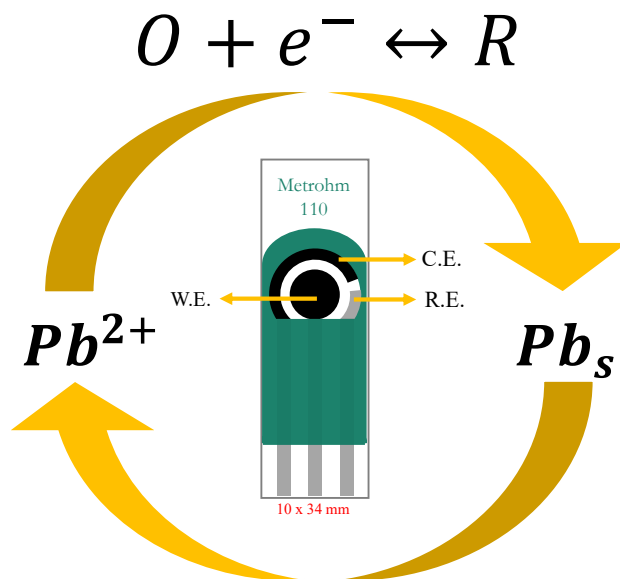
Figure 1.6. Graphic of the movement of electrons for the oxidation and reduction of Pb and anatomy of Screen-printed Electrodes (SPEs) for positioning the WE, RE, and CE.

Other requirements in performing an electrochemical experiment include the electroanalytical technique and potentiostat. There are many different electroanalytical techniques developed to measure the potential, current, and charge relationships in the electrochemical cell. Two common techniques that establish the relationship between current and an applied potential will be discussed. Cyclic voltammetry (CV) is a highly versatile technique that use changes of potential over time to observe the current in two directions, shown in **Figure 1.7A and C**. Linear forward, and reserve scans change the applied anodic and cathodic potentials resulting in the observation of reduction and oxidation peaks of the species of interest which is why a CV is often used to determine if a species is electrochemically active.[75] Furthermore, other electrochemical techniques can achieve higher specificity and lower detection limits and involve pulse techniques. For instance, square-wave voltammetry (SWV) is a frequently used pulse technique for the advantages of speed of analysis, detection limits, and reducing noise by limiting the non-faradic current. The excitation signal of an SWV is a staircase with a defined step to measure the difference between the forward pulse and backward pulse to determine the net current depicted on the right in **Figures 1.7B and D**. Stripping techniques are commonly used in trace metal detection by using an electrochemical deposition followed by the measurement technique.[72,76] These voltammetric techniques are easily carried out by the potentiostats which house the electrical system for signal

application and detection. Modern potentiostats have been made smaller than their predecessors that offer new applications due to the portability of these new instruments.[77,78]
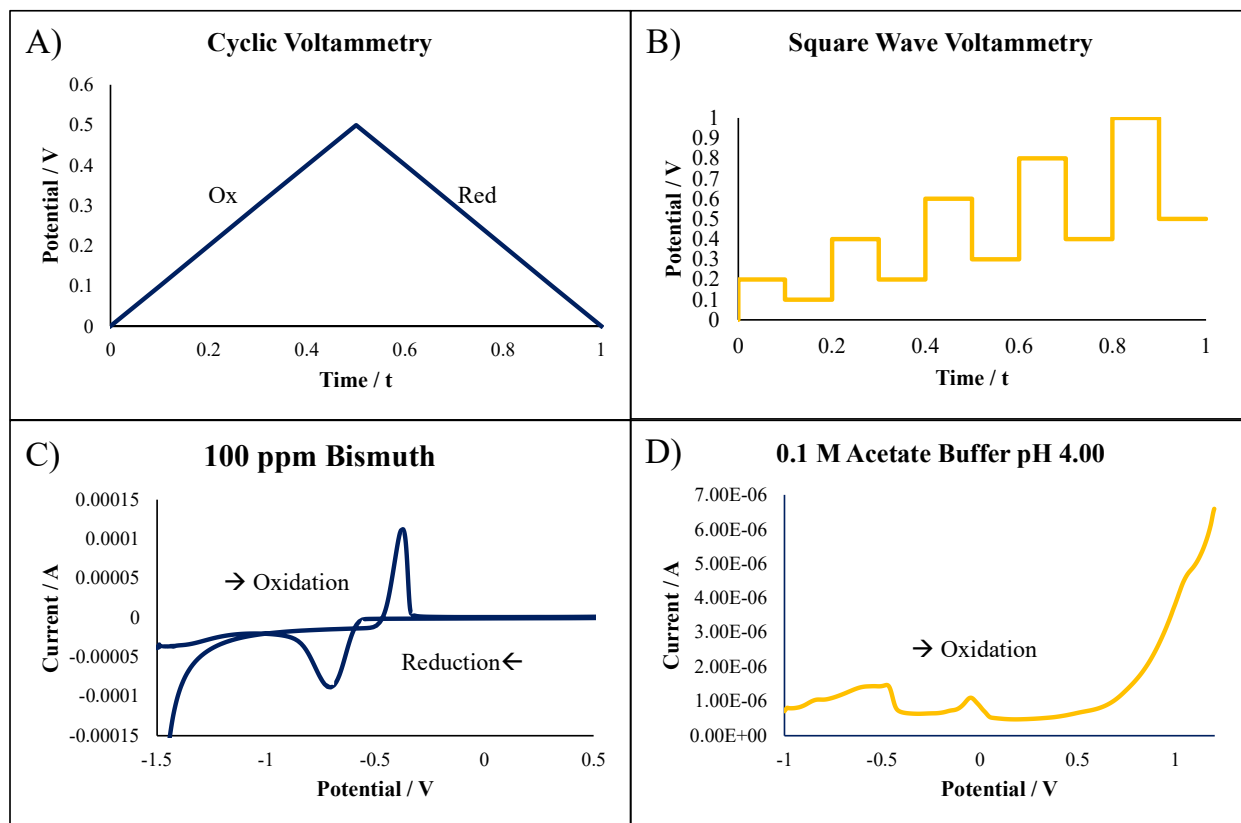
Figure 1.7. *The excitation potential waveforms for A) cyclic voltammetry and B) square-wave voltammetry and example voltammograms of C) 100 ppm Bismuth using CV and D) 0.1 M Acetate Buffer pH 4.0 using SWV.*

1.3.1 Applications to GSR Using Electrochemistry

The application of electrochemistry to gunshot residue detection has been investigated since 1977, when Konanur and Van Loon utilized anodic stripping voltammetry for lead and antimony identification. [79] The authors evaluated the hands of non-shooters and shooters by using mercury-coated graphite electrodes to analyze washes from shooter and non-shooter individual hands. They reported that lead and antimony oxidized at -0.50 V and -0.24 V, respectively, and used standard addition (100 ppm and 10 ppm) to quantify samples. Hands of those who had not fired a firearm resulted in ranges of from 0.43-16 µg and after firing from 0.25-115 µg.[79] From this initial research, the next two decades investigated anodic stripping voltammetry (ASV) for single and multi-metal detection and organic explosive substances detection.[80–84] To highlight a few manuscripts during

this time, Bratin et al., evaluated the reduction of nitroglycerin, 2,4-dinitrotoluene, and diphenylamine using glassy carbon and gold mercury film electrodes to identify and determine electron transfers occurring for nitro aromatics, nitramine, and nitro ester group compounds by cyclic voltammetry.[81] Shifting to metal compounds, Briner et al. investigated the use of mercury film glassy carbon electrodes for antimony detection between 10-120 ng from the hands of potential shooters using swabs and ASV electrochemical method.[82]

Electrochemical improvements have shifted to using electrode modifications, simultaneous IGSR and OGSR detection, portable potentiostats, and chemometric treatment of electrochemical data. De Deonato et al., introduced a fast detection using batch injection analysis coupled with ASV to detect IGSR elements on a hanging mercury drop electrode (HMDE). The author determined that taping, lifting, and extraction was an adequate method for lead detection in the hand of the shooter where the different areas of the hand were compared using a revolver and pistol firearm.[85] Arduini et al. provide a review of using bismuth-modified electrodes on various working electrode substrates for lead detection in various applications.[86] In 2012, Vuki et al., demonstrated the capability of detecting IGSR and OGSR in an electrochemical run-on mercury film electrodes using CV and cyclic-SWV on a portable electrochemical potentiostat. The authors were able to detect the oxidation and reduction of Pb, Sb, DNT, and NG in a single scan.[45] Salles in 2012 evaluated lead detection from four different firearms and six different ammunitions were detected on gold microelectrodes with a limit of detection of 1.7 nmolL^{-1}.[87] O'Mahony and Wang have published a "swipe and scan" electrochemical detection method and a review article on electrochemical methods for forensic application of GSR which developed a rapid sampling method by swiping the hand of a shooter with working electrode of an SPE for lead, antimony, and copper detection.[88,89] More recently, our own research group has also published an electrochemical method for simultaneous IGSR and OGSR detection applied to a large population of data sets of non-shooter and shooter samples analyzed using screen-printed carbon electrodes and square-wave anodic stripping voltammetry.[11,71] Ott et al. analyzed large population data sets using critical thresholds and machine learning as a chemometric method for interpreting the classification of a positive GSR sample. The trends in electrochemical detection for GSR have been considered by Harshey, who looks at the historical developments in electrochemical techniques, electrode sensors, and changes in the GSR landscape and interpretations using these

technologies.[90] One of these trends is the portability of electrochemical methods for field employment which electrochemistry is highlighted in de Araujo's article as a review of portable platforms in forensics.[78] **Table 1.2** demonstrates the historical progress of electrochemical detection techniques from 1977 to 2020 for GSR applications. These works provide the foundation for electrochemical detection fit for purpose for GSR detection, and how the advances in technology has improved analysis, portability, and sensitivity to continue research for transitioning these methods by forensic laboratories.

Table 1.2. *14 manuscripts highlighting electrochemical techniques reported for GSR applications from 1977 to 2020.*

Author	Year	Sampling	Scan Methods	Working Electrode	Analytes	Reported sample concentration or LOD
Konanur and Van Loon[79]	1977	Washing	ASV	MCGE	Pb, Sb	10 ug of Pb and 16 ug of Sb
Liu et al.[84]	1980	Washing	ASV	Tailor-made Polarograph	Zn, Pb, Cu, Sb	0.5, 1.36, 0.02 , 0.08 ug (Zn, Pb, Cu, Sb)
Bratin and Kissinger[81]	1981	Swabbing and Extraction	CV	Au-MFE & GCE	Nitramines, TNT, NG, 2,4-DNT, 2,6-DNT, PETN	NR
Briner et al.[82]	1985	Swabs	ASV	Hg-GCE	Sb	10-120 ng
Woolever and Dewald[80]	2001	Swabs	DPASV	GCE	Ba, Pb	144.5 & 255.8 ng (Ba, Pb)
DeDeonato et al.[85]	2005	Swabs, washing, and Adhesive Tape	DPASV	BIA-HMDE	Pb	20 ppb
Erden et al.[91]	2011	Adhesive Tape	DPCAdSV & SWCAdSV	HMDE	Pb, Sb	2.0E-09-3.0E-07 M (Pb) 2.0E-09-7.0E-07 M (Sb)
O'Mahony et al.[92]	2012	Abrasive	AbrSV	SPCE	Pb, Sb, Cu	NR
Salles et al.[35]	2012	Swab	SWV	Au microelectrode	Pb	1.8 nmolL^{-1}
Vuki et al.[93]	2012	N/A	CV, C-SWV, & SWV	GCE & Hg-GCE	Zn, Ba, Pb, Sb, NG, DNT, DPA	NR
O'Mahony et al.[94]	2014	Abrasive	SWV	Carbon Tape-SPCE	Pb, Sb, Cu	NR
Trejos et al.[71]	2018	Adhesive Tape	SWASV	SPCE	Pb, Sb, DNT, NG	0.1-1 ppm
Promsuwan et al.[95]	2020	Swabs	FI Amp	Pd-GCM/GCE	Nitrite	0.03 umolL^{-1}
Ott et al.[11]	2020	Adhesive Tape	SWV	SPCE	Pb, Sb, Cu, DNT, DPA, NG, EC	0.012-0.462 ppm

1.4 Liquid Chromatography-Tandem Mass Spectrometry (LC-MS/MS)

1.4.1   Liquid Chromatography

Chromatographic techniques are often coupled with mass spectrometry techniques as a means to not only separate analytes of interest but to provide confirmation of their identity. A widely used chromatographic method is liquid chromatography, a technique where compounds of interest are separated in liquid mobile phases through their interaction with a stationary phase (column). There are several parameters that can influence the resolution of the analytes, such as column packing, mobile phases, flow rate, solvent mixtures, and analyte physicochemical properties. Columns are usually packed with porous particles (composed of silica, alumina, or ion-exchange resin, depending on the application) and are available in various diameters ranging from 3-10 μm, although modern packing technology includes sub-2-micron particle sizes for ultra-high-pressure liquid chromatography (UPLC). Organic and aqueous solvents for the mobile phases are chosen based on polarity for the species of interest that can be eluted in isocratic or gradient elution to gain better separation. With these considerations, liquid chromatography is often carried out using either normal-phase (NPLC) or reverse-phase liquid chromatography (RPLC) for separation. The operation of NPLC uses a highly polar stationary phase relative to the mobile phase, but more commonly used is RPLC speaking to the relatively nonpolar stationary phase and polar mobile phases. In reverse-phase chromatography, the order of elution comprises more polar compounds eluting faster than relatively nonpolar compounds. Liquid chromatography is a popular technique due to the sensitivity, adaptability, automation, and capability of a broad array detecting non-volatile or thermally unstable compounds.[96–98]

1.4.2   Mass Spectrometry (QqQ)

Mass spectrometry (MS) is often coupled to chromatographic techniques like gas or liquid chromatography to obtain information on the separated compounds' molecular mass, elemental composition, and structural information. Mass spectrometry is a highly discriminatory technique because it has the power to identify and quantify unknown substances as well as determine the structure of the molecules. A mass spectrometer typically includes three main components: 1) ionization source, 2) mass analyzer, and 3) detector.

The ionization sources are classified into hard and soft ionization sources that employ different sources of atoms, electrons, high electrical fields, etc. to cause the fragmentation of an analyte molecule. A hard ionization technique commonly used is electron ionization (EI) to produce ion fragments through the use of filaments that produce energized electrons typically accelerated at 70 V.[96] Fenn and Tanaka won the 2002 Nobel Prize for their development of a soft desorption ionization method called electrospray ionization (ESI). This ionization technique takes place under ambient pressure and temperature where samples are pumped through a capillary needle at a few μm per second, where a cylindrical electrode surrounds the needle, which is charged around several kilovolts. The charged spray of fine droplets undergoes desolvation through a capillary to evaporate the solvent from the droplets and adhere the charge to the molecule. The Rayleigh limit is when these droplets reach their charge density due to the evaporation of solvent resulting in a Coulombic explosion where the droplet is split into smaller droplets. This process repeats until a charged analyte molecule is left.[96] In the Agilent Jetstream ESI source, an additional dry gas (nitrogen) is added to aid in desolvation and noise before ions enter the sampling capillaries.

Various mass analyzers are available for the separation of mass-to-charge ratios, such as a quadrupole mass analyzer, time of flight (TOF), and ion-trap analyzers. In this section, only quadrupole mass analyzers will be discussed because one was used in this research. A triple quadrupole mass analyzer or filter (QqQ) performs similarly to a single quadrupole with the ability to be more selective in the masses monitored. In a single quadrupole, alternating dc and radio frequencies are applied to each pair of rods. A constant ratio between the rod voltages is kept as they increase where the ions are accelerated towards a potential difference of 5-10 V. Non-specific ions will collide or exit the path of the quadrupole while ions the targeted masses will pass through the quadrupole to the detector. In a QqQ setup, the first quadrupole (Q1) allows only selected precursor ions to pass to the collision cell. The hexapole collision cell (q2) improves the transmission of ions from the first quadrupole to the second while bombarding the precursor ions with collision gas, and high-pressure nitrogen, to form smaller product ions and neutral fragments. The third quadrupole (Q3) is a mass filter, which main purpose is selecting only monitored product ions.

Lastly, ion detectors mainly rely on electron multipliers with two common layouts, discrete and continuous. Both electron multipliers (EM) function in a similar way, positive ion or electrons strike the surface of a dynode electrons are emitted which are drawn to the next dynode with increasing voltage gradient. The difference between discrete and continuous are discrete EM have limited number of dynodes where a continuous EM is shaped like a horn to allow better signals since an exponential number of electrons are emitted with each strike along the EM. Electron multipliers are a better detection method due to their rapid detection capability, reliability, and robustness. The components discussed in this section for the MS have been presented in box diagram form in **Figure 1.8**.
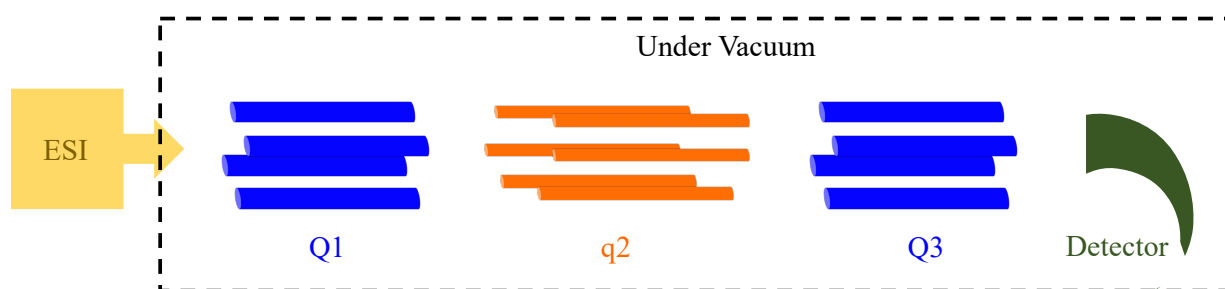
Figure 1.8. *Box diagram of a triple quadrupole mass spectrometer schematic.*

1.4.3   Applications of Mass Spectrometry to GSR analysis

Liquid Chromatography-Tandem Mass Spectrometry is undergoing review to be considered a standard practice technique for confirmatory testing for OGSR by OSAC.[17] This progress has come about by contribution from several research groups which have reported the use of liquid chromatography-tandem mass spectrometry (LC-MS/MS) as a method of detecting smokeless powders and GSR from hand samples. For instance, Tong et al., in 2001, assessed a quantitative LC-MS/MS method for OGSR compounds from swabbing hands with percent recoveries from 79-83%.[46] In 2007, Belgium researchers, Laza et al., expanded the panel of common smokeless powder stabilizers to include diphenylamine and derivatives, ethyl and methyl centralite, and acardite II detection from authentic samples ranging from 0-50 nmolL^{-1}.[25] In 2016, a study by Ali et al. performed an investigation into the amount of pGSR in police stations, vehicles, and personnel as well as the transfer using LC-MS/MS analysis with the SEM-EDS carbon adhesive stubs as the collection medium. Following, the stubs were analyzed by SEM-EDS, then LC-MS/MS were many commonly associated with particles found on the individual's samples, and

ethyl centralite was detected, however, typically below the LLOQ.[48] In more recent investigations, Bell and Feeney has developed methods not only for the detection of OGSR by LC-MS/MS and IGSR using guest host chemistry and ligand binding. [50] Further research by Feeney applied these methods to large non-shooter and shooter populations, evaluating post-shooting activities, a combination of instrumentation, and interpretations and classification of samples using machine learning algorithms.[98–100] This work will expand the current research by furthering LC-MS/MS analysis application to bullet hole identification by improving reliability in OGSR detection as a confirmatory technique.

II.   CHAPTER 2: OBJECTIVES OF OVERALL PROJECT

2.1 Motivation of the Project

Bullet hole identification and shooting distance determination are two critical areas within GSR that require improvements in their current analytical workflow. Specific challenges to bullet hole ID and distance estimation involve difficulty analyzing larger or immovable substrates, high false-positive rates, and sample destruction. This research work will focus on developing novel strategies to provide smarter analytical solutions that overcome existing limitations by offering faster and non-destructive methods that can facilitate the measurement and chemical characterization of GSR particles.

This thesis proposes electrochemistry as a reliable screening technique that offers rapid, simultaneous IGSR and OGSR detections that are minimally destructive for the identification of elements and compounds related to GSR as a practical screening method for distance estimation, bullet hole identification, and portable GSR screening applications. To achieve these goals, three objectives were developed, and their respective tasks for completion are detailed below.

2.2 Goals and Objectives

The overall goal of this thesis was to develop novel sampling and screening methods for simultaneous IGSR and OGSR detection as adaptable and rapid analytical methods for entrance hole identification and distance determination and evaluate the reliability of portable electrochemical potentiostats for GSR analysis. This main objective was carried out by three specific objectives as stated below and depicted in **Figure 2.1**:

1. Development of a modern approach for distance determination using electrochemical methods for simultaneous inorganic and organic GSR detection from fabric.

2. Development of a rapid sampling and electrochemical technique for the identification of bullet holes from common substrates found at crime scenes.

3. A comparison study of the performance and capabilities of benchtop and portable potentiostats for inorganic and organic gunshot residue detection.

Figure 2.1. *Graphical representation of the overall objectives and goals of this thesis.*

2.3 Objectives and Task

Objective 1: Development of a modern approach for distance determination using electrochemical methods for simultaneous inorganic and organic GSR detection from fabric. This objective will target the development of a sensitive and specific method for the detection of GSR, reduction of subjectivity in the interpretation, and the incorporation of statistical approaches for distance determination analysis. In addition to providing faster sampling and analysis methods than the current colorimetric techniques that require exposure to corrosive chemicals. In objective one, the developed electrochemical method will be compared to the performance of current colorimetric techniques to assess the identification and classification of shooting distance estimation by evaluating of unknown shooting distances on fabric substrates. These substrates will simulate case-work scenarios by evaluating colored and patterned and bloodstained clothing which replicate more difficult assessments for the analyst.

Task 1.1: To utilize electrochemistry for distance determination, the first task targets the development of the sample collection, extraction, and electrochemical methods for obtaining compound and distance determination information from the fabric samples. An investigation into developing a collection method from around the bullet hole using SEM-EDS aluminum stubs and carbon adhesive tape as currently accepted sampling methods to gain spatial information from the samples. The extraction and electrochemical methods for GSR detection were modified from previous electrochemical GSR detection by our research group.[11]

Task 1.2: The second task will focus on the collection and analysis of authentic fabric samples assessed using both electrochemistry and current practices in the field on white and colored/patterned samples. Physical measurements, electrochemistry, and color tests (Modified Griess and Sodium Rhodizonate) will be carried out in this respective order on calibration and unknown distance. A total of 30 calibration samples will be collected, consisting of five shooting distances completed in triplicate on white fabric. Evaluation of 35 unknown samples will be subsequently divided up into 10 replicates on white fabric, and 5 replicates of each different color or pattern fabric (orange, red, navy, dark, and light patterns). Following the collection and analysis of samples, the electrochemical method will be evaluated for identification of GSR analytes, graphic interpretation of the data, and statistical classification methods to compare the current practices.

Task 1.3: Like task 1.2, the third task focuses on the performance of the electrochemical method for distance determination on blood-stained fabric. Physical measurements, electrochemistry, and color tests (Modified Griess and Sodium Rhodizonate) will be carried out in this respective order on another set of three shooting distance calibrations and 5 replicates of bloodstained white fabric compared to 5 replicates of non-bloodstained white fabric. Additional, interference assessment of the blood to electrochemical detection of GSR was evaluated. The same data analysis discussed in task 1.2 will be performed for this bloodstained comparison population.

Objective 2: **Development of a rapid sampling and electrochemical technique for the identification of bullet holes from common substrates found at crime scenes.**
This study utilized the previously mentioned fabric samples as the first sample subset for method development, difficult bullet hole visualization, and potential interference. Additionally, an assessment of the electrochemical method will be carried out on a set of hard substrates (wood and drywall) for bullet hole recognition. In this research, LC-MS/MS will be performed as confirmation for OGSR presence in the samples. Data analysis includes the identification of GSR analytes via their voltammograms reporting the respective number of positive analytes, performance measures, and comparing electrochemistry and LC-MS/MS results for the samples.

Task 2.1: For the bullet hole identification, the first task consists in developing a rapid sampling method to collect from the bullet wipe and analyze electrochemically. This task implemented the use of SEM aluminum stubs and carbon adhesive tape similar to task 1.1.

Task 2.2: Collection of authentic samples for fabric and hard substrate population performed. The fabric samples collected in task 1.2 will be assessed for bullet hole identification purposes using the same calibration and unknown sample sizes and materials. Additionally, 7 replicates of wood and 7 replicates of drywall substrates will be collected, shooting at a known distance as a proof of concept and assessment of potential interferences. Electrochemical data will be evaluated via voltammograms and using the average lowest calibrator as the threshold for positive IGSR and OGSR calls. Respective negative control for each material will be assessed as true negative and for any potential interferences with electrochemical detection.

Task 2.3: The sample sets used bullet hole identification will be assessed via mass spectrometry methods as a confirmation of OGSR presence. This third task explores the application of mass spectrometry methods which are in progress of a standard in GSR analysis to

bullet hole identification. [17] As a confirmation method, only the 45-fabric unknown distance, and 14 hard substrate samples will be assessed via the mass spectrometry approach.

Objective 3: A comparison study of the performance and capabilities of benchtop and portable potentiostats for inorganic and organic gunshot residue detection.
Demonstrating the portability and reliability of electrochemical instruments as a feasible screening technique for crime laboratories by a comparison study between benchtop and portable potentiostats for GSR detection. This third objective focused on using the PalmSens4 potentiostat as the portable electrochemical instrument to compare to the Metrohm Autolab potentiostat.

    Task 3.1: The first task evaluates of IGSR and OGSR standards on the portable and benchtop potentiostats. Assessment of performance characteristics for both potentiostats including potential windows, linearity, R^2, repeatability, and limits of detections for a panel of 7 common IGSR and OGSR.

    Task 3.2: The second task aimed at evaluating authentic non-shooter and shooter samples to assess the performance of the individual potentiostat on the same sample. A total of 350 authentic samples will be separated into 200 background non-shooters and 150 shooter samples comprised of 100 leaded primer ammunition and 50 lead-free primer ammunition to replicate real-life case scenarios.

    Task 3.3: Data analysis exercised graphical visualization, significance testing, and critical thresholds to assess the data. Performance characteristics of task 3.1 will be subjected to significant tests for comparison of potentiostats using standards. Critical threshold analysis will be considered for evaluation of positive GSR calls and performance measures to evaluate the accuracies of each potentiostat.

III.   CHAPTER 3: DETERMINATION OF SHOOTING DISTANCE BY ELECTROCHEMICAL DETECTION

3.1 Overview

This chapter investigates innovative sampling methods in combination with electrochemical GSR detection for the application of crime scene reconstruction as a novel approach to shooting distance estimation. This study focuses on both the development of a fast, novel sampling method to obtain spatial and chemical information from simultaneous IGSR and OGSR detection and the exploration of the statistical classification of the shooting distance. Common challenges in the current distance determination discipline were targeted by evaluating emerging protocols in comparison with existing colorimetric methods and improvements to interpretation approaches. A total of 75 samples were collected during this study, including 30 calibration samples (6 replicates of 5 shooting distances on white fabric), 15 white fabric, 25 colored/patterned fabrics, and 5 blood-stained white fabric samples. All the unknowns were shot at a distance that was kept blind to the analyst to minimize bias. Stub samples were collected using a lightbox and acetate template of the interval collection pattern using a carbon adhesive tape on an aluminum SEM stub. All samples were evaluated for physical measurements prior to analysis, and color tests, modified Griess and sodium rhodizonate, were performed on the samples after sampling for electrochemical testing. Macro-spatial mapping and bar graphs were used to visualize GSR patterns in the IGSR and OGSR compounds detected by electrochemistry using the predetermined sample collection intervals. Classification of shooting distance was performed using principal component analysis (PCA) followed by discriminant analysis (DA).

These developed techniques applied to distance determination provide a rapid method for IGSR and OGSR detection with the for macro-spatial mapping and distance classification while adding the advantage of being non-destructive, allowing color testing after electrochemical analysis, if needed. **Figure 3.1** demonstrates the goals, investigative question, number of samples, and analytical techniques performed in completion of this research.
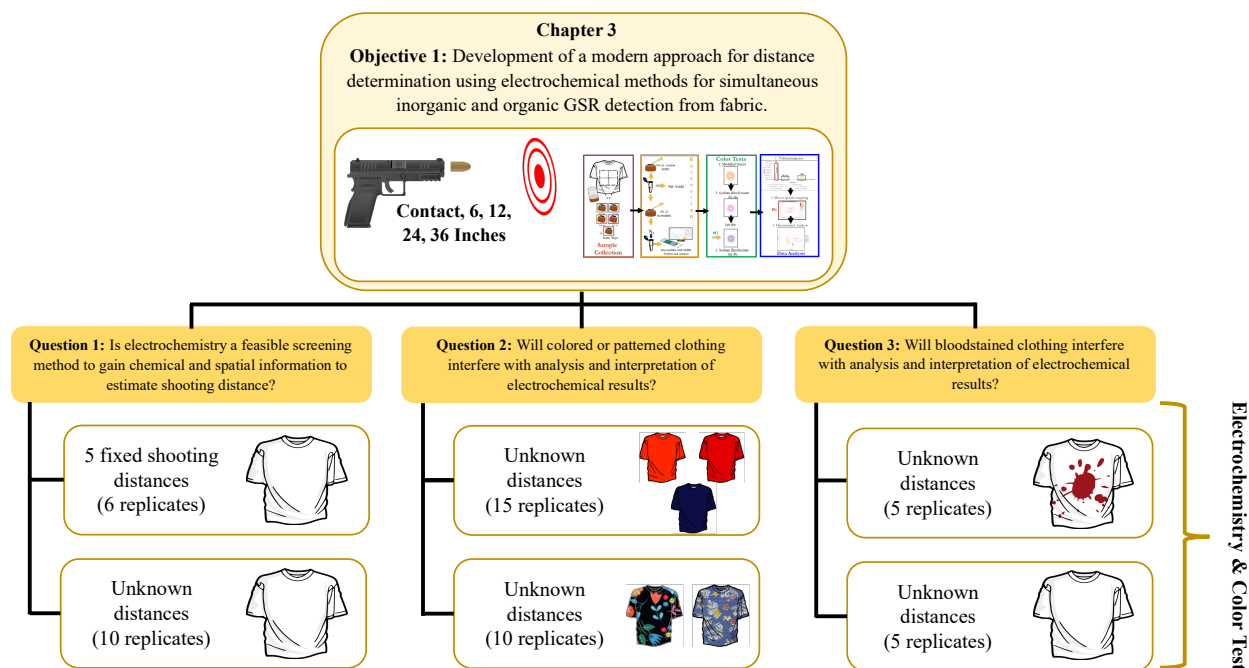
Figure 3.1. *Graphical representation of Chapter 3 objective, tasks, and experimental design.*

3.2 Materials and Methods

3.2.1   Reagents and Standards

Glacial acetic acid (HPLC grade), sodium acetate anhydrous and acetonitrile (Optima) were obtained from Fisher Scientific (Fair Lawn, NJ). Lead, copper, and antimony standards were purchased from Ultra Scientific (Kingstown, RI). Nitroglycerin and 2,4-dinitrotoluene standards were acquired from AccuStandard (New Haven, CT). Ethyl centralite (1,3-diethyl-diphenylurea 99%) and diphenylamine were purchased from Sigma-Aldrich (St. Louis, MO) and SPEX Certiprep (Metuchen, NJ), respectively. Ultrapure 18.2 MΩ water was obtained from a Millipore Direct-Q® UV water purification system (Billerica, MA). Compressed nitrogen was obtained from Matheson Tri-Gas, Inc. (Irving, TX).

Positive quality controls for the electrochemical instrumentation were created using the above mentioned IGSR and OGSR standards to make two high concentrations of IGSR and OGSR mixtures consisting of 2 ppm Pb, 0.2 ppm Cu, 8 ppm Sb, and 10 ppm of OGSR (2,4-DNT, and DPA OR NG, and EC). These 10-ppm control were then diluted in a 1:4 ratio to make a low concentration control for 0.5 ppm Pb, 0.05 ppm Cu, and 2 ppm Sb and 2.5 ppm of OGSR analytes.

Color test reagents for the modified Griess test included sulfanilic acid (Sigma Aldrich, MO), alpha-naphthol (Alfa Asear, MA), methanol (Fischer Chemical, PA), desensitized everyday HP Photographic paper (Palo Alto, CA), sodium nitrite (Acro Organic-Thermo Fischer Scientific, MA), and acetic acid (Fischer Scientific, NH). Reagents to perform the sodium rhodizonate test included sodium rhodizonate (Sigma Aldrich, MO), sodium bicarbonate (Sigma Aldrich, MO), tartaric acid (Alfa Aesar, MA), hydrochloric acid (Fischer Scientific, NH), Whatman benchkote paper (Sigma Aldrich, MO) and an ultrafine continuous mister (Amazon.com, Inc).

3.2.2   Electrodes and Instrumentation

Determination of buffer pH was carried out using a Mettler Toledo FiveEasy pH meter (Columbus, OH). Electrochemical instrumentation utilized for measurements and data analysis was the Autolab PGSTAT128N potentiostat with the NOVA software version 2.14 from Metrohm Inc, USA. Commercial screen-printed carbon electrodes (model DRP-110) were utilized for electrochemical measurements purchased from Metrohm DropSens, USA.

3.2.3   Sample Preparation and Collection of Fabric Substrates

All shooting collection was performed at the West Virginia University Ballistics laboratory under controlled conditions. Winchester .40 caliber ammunition was fired at the fabric samples using a Springfield XD9 firearm (manufactured in Croatia). Fabrics were cut into 8 x 11-inch pieces, and collection was performed by pinning fabric backed with manila paper to a self-healing shooting block. Two sets of calibration curves (total of 30 samples on 100% white cotton fabric) consisting of 5 shooting distance were completed in triplicate at contact, 6-, 12-, 24-, and 36-inches using a measuring tape and floor markers prior to collection. To avoid cross-contamination, individuals performing the shooting were not the same as those handling and storing the samples.

A total of 45 unknown fabric samples comprised of 20 white 100% cotton lint-free cloth samples (Electron Microscopy Sciences), five of each color orange, red, navy, light patterned, and dark patterned 100% cotton fabric (Waverly Inspirations, Bentonville, AR) were shot at unknown distances that were blind to the analyst performing analysis.

3.2.4   Application of Blood to White Cotton Fabric

Half of the 20 white cotton fabrics were used to assess the effect of bloodied fabric on the electrochemical detection of GSR and any potential interferences that may result. Five were used as controls and left as pristine (non-blood) samples, while blood was applied to the other five white cotton fabric samples after the shooting to simulate the bleeding of an injured individual. Nitrile gloves and lab coats were worn during sample handling, collection, and application of whole human blood (UTAK blank whole blood, Valencia, CA). Application of blood was performed in a Biological Safety Cabinet fume hood with protected layers of butcher paper and Wypall Wipers® on all surfaces and cleaned with a 70% ethanol solution before and after use. Continuous spray bottles were used to apply the blood to the unknown samples until the soot pattern was less observable. Samples were air-dried for approximately 2 hours in the hood before returning them for storage in a pre-labeled butcher paper and placed in a clean biological safety hood until analysis.

3.2.5   Sampling Methodology for Distance Determination

For distance determination, four sampling approaches were explored in order to gain spatial information for the classification of shooting distance in addition to the GSR analytes detected. The established sampling method employed typical SEM aluminum stubs (13 mm) with carbon adhesive tape (Ted Pella, CA) to sample the bullet wipe and 4 predetermined intervals around the bullet wipe, resulting in the collection of 5 stubs per sample. As depicted in **Figure 3.2**, the intervals for sampling were conducted at the bullet wipe and 4 positions moving away from the bullet wipe, including bullet wipe to 2 cm, 2-4 cm, 4-6 cm, and 6-8 cm and repeated in the north, south, east, and west directions by dabbing about 2 times in each position. To keep this sampling consistent, a lightbox and acetate paper with the sampling template were used to visualize the sampling strategy for consistency between samples since the bullet hole was not always centered on the fabric. This was performed on all samples, including the 30 calibration curves samples and 45 unknown fabric samples totaling 375 stubs used for electrochemical analysis.
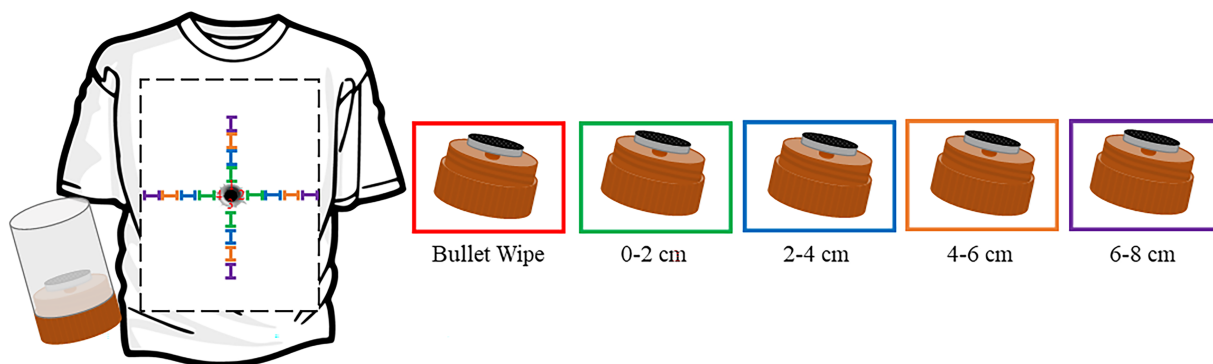
Figure 3.2. *Graphical demonstration of sampling collection intervals and application to fabric samples for distance determination.*

3.2.6 Stub Extraction

Minor changes were made to the extraction procedure described in Ott et al., where a two-step washing of the stub surface was employed to collect IGSR and OGSR extracts from the carbon adhesive. [11] The extraction volumes were increased to 100 µL to cover the entire stub surface, as demonstrated in **Figure 3.3**. A 50 µL aliquot from the extraction method was used to perform electrochemical analysis and the remaining 50 µL could be saved if the analysis needed to be repeated.
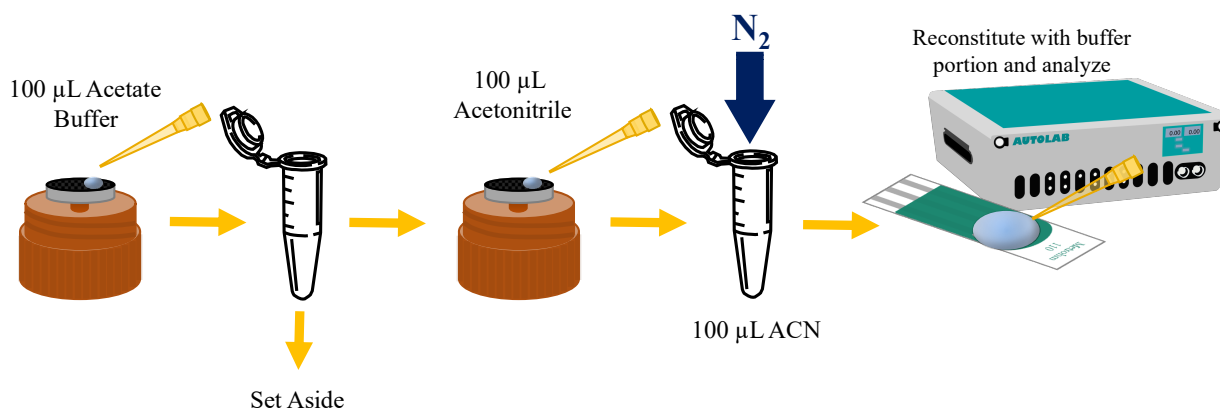
Figure 3.3. *GSR Extraction procedure for SEM aluminum stubs used in the assessment of electrochemical detection for distance determination.*

3.2.7 Square-wave Anodic Stripping Voltammetry

Electrochemical analysis was performed using a square-wave anodic stripping voltammetry method (SWASV). A preconcentration/deposition step was applied first at -0.95 V for a deposition

time of 120 seconds. Following preconcentration, an anodic sweep was applied via the SWASV method from -1.0 V to +1.2 V to strip/oxidize the analytes from the surface of the electrode resulting in the generation of oxidation peaks. Additional SWASV parameters can be found in **Table 3.1**.

Table 3.1. *SWASV parameters for the analysis of GSR-related elements and compounds using the Metrohm Autolab potentiostat.*

Parameter	Value/Unit
Deposition Time	120 s
Deposition Potential	-0.95 V
Start Potential	-1.0 V
End Potential	1.2 V
Potential Step	0.004 V
Amplitude	0.025 V
Frequency	8 Hz

Several quality controls were run pre- and post-analysis to ensure the performance of the electrochemical instrument and the quality of sample collection and extraction procedures. Positive controls included 10 and 2.5 ppm mixtures of GSR quality control mixtures and a tailor-made pGSR (IGSR) standard.[101] Negative controls included an acetate buffer pH 4.00, stubs collected from the pristine unused fabrics, and an extraction control (blank carbon adhesive stub).

3.2.8 Electrochemical Data Analysis

A total of 375 voltammograms were accumulated and data analysis included exporting peak potential and peak current areas from the NOVA 2.1.4 software to Microsoft excel 2016 (Version 16.55, Microsoft Corporation) for plotting, graphing, and initial data analysis. Chemical heat map plots and discriminant analysis were completed using JMP 16.0.0 software (SAS Institute Inc., NC).

3.2.9 Physical Examination and Color Tests

Fabric samples were photographically documented prior to electrochemical sampling and post colorimetric testing using a Nikon D7200 camera. Several measurements including bullet hole width, length, soot area, and the number of particles were estimated from photographs using ImageJ software (version 1.53, National Institute of Health, MD).

The chemical color tests, modified Griess and sodium rhodizonate were performed according to Dillion on all fabric samples.[55,56] The results of colorimetric testing were used to cross-validate the results for distance determination by electrochemical analysis. The ImageJ program was used to measure the resulting color on the photographic paper following these two tests.

3.2.10 Overall Analytical Procedure

The analytical scheme for fabric samples progressed from least to the most destructive techniques. The samples followed the analytical procedure except for the blood-stained samples, which had additional sample preparation steps. Photography of all samples prior to any analysis was completed first, followed by stub collection for the electrochemical assessment. Then, stubs could be analyzed by electrochemistry while the modified Griess and sodium rhodizonate were performed on the samples. Color test results were also documented by photography after analysis as well. The analytical scheme is demonstrated graphically in **Figure 3.4**.
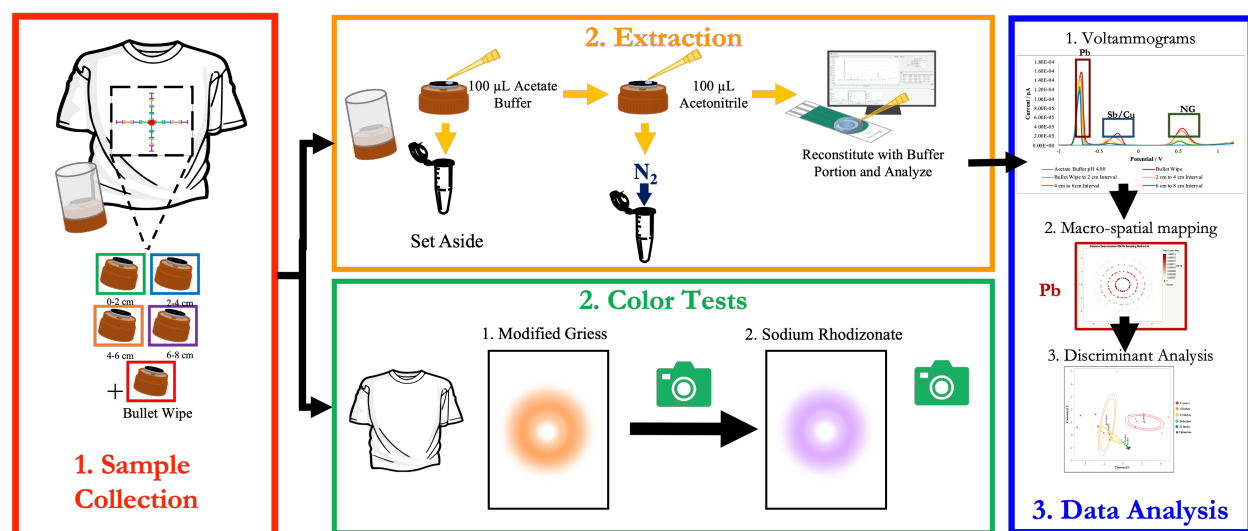
Figure 3.4. *Analytical scheme followed for electrochemical and colorimetric tests completed on all calibration and unknown distance determination samples.*

3.3 Results and Discussion

The motivation for the study in Chapter 3 was to assess the capabilities and reliability of electrochemical detection of GSR in combination with statistical methods for the identification and classification of unknown distance determination samples in comparison to existing

colorimetric techniques. Due to the detailed analytical scheme, the main objectives of this chapter are divided into electrochemical, physical and color tests, and statistical results. The first task was the development and assessment of electrochemical detection for the IGSR and OGSR analytes using standards for the performance characteristics reported in *section 3.3.1*. The second and third tasks were divided throughout multiple sections: *Sections 3.3.2-3.3.7* for the analysis of 35 unknown white, colored, and patterned samples, and *Sections 3.3.8-3.3.11* for the unknown distance determination of blood-stained fabrics. These sections follow a similar flow by first addressing the evaluation of samples by electrochemistry which entails data visualization methods and statistical classification of the unknown distance samples. Following the electrochemical results, the physical and color test findings detail the measurements and distance classifications using the current practice protocols. Finally, the last sections report the accuracies of the novel electrochemical and statistical approaches compared to the traditional methodologies

3.3.1   Method Development of Electrochemical Detection

Figures of merit were determined for the Metrohm Autolab potentiostat through calibration curves of the 7 monitored IGSR and OGSR analytes (IGSR: lead, antimony, and copper OGSR: 2,4-DNT, DPA, NG, and EC). Standards were analyzed in triplicate for five-point calibration curves to assess potential windows, linear dynamic ranges, repeatability, R^2, and limits of detection (LOD). The potentiostat performing analysis has been used in previous research by our group where we have reported the performance characteristics in **Table 3.2** as well as Chapter 5 of this work.[11,102]

Table 3.2. *Performance characteristics of the Metrohm Autolab potentiostat for IGSR and OGSR analytes on SPCEs.*

IGSR	Potential (V)	Linear Range (µg/mL)	R^2	Repeatability (%RSD, n=3)	LOD (µg/mL)
Lead	-0.784 ± 0.035	0.10 to 2.0	0.999	4.4	0.055 ± 0.01
Antimony	-0.401 ± 0.027	0.75 to 7.5	0.986	10	0.183 ± 0.07
Copper	-0.292 ± 0.053	0.05 to 1.0	0.990	2.3	0.012 ± 0.001
OGSR	Potential (V)	Linear Range (µg/mL)	R^2	Repeatability (%RSD, n=3)	LOD (µg/mL)
2,4-Dinitrotoluene*	−0.132 ± 0.032	1.0 to 20	0.982	5.6	0.200 ± 0.03
Diphenylamine	0.406 ± 0.018	1.0 to 8.0	0.987	6.2	0.462 ± 0.06
Nitroglycerin	0.509 ± 0.010	0.50 to 8.0	0.998	10	0.147 ± 0.08
Ethyl centralite	1.03 ± 0.045	0.50 to 8.0	0.998	8.0	0.450 ± 0.09

*2,4-dinitrotoluene was assessed by peak current height.

Assessment of the standards demonstrates acceptable linear ranges over the 5 calibration points with an R^2 value greater than 0.99. Repeatability over the three replicates was below 10% for all analytes, with copper having the lowest relative standard deviation (%RSD) at 2.3%. Limits of detection fell below approximately 500 ppb for IGSR and OGSR. Copper was the most sensitive, with an LOD of 12 ppb, whereas most of the other analytes' LOD range between 100 and 500 ppb. Excellent sensitivity and specificity were demonstrated by the potentiostat for IGSR and OGSR analysis, where LOD ranges for the sodium rhodizonate test are in the thousand nanogram range.[66]

3.3.2   Evaluation of White, Colored, and Patterned Unknown Samples via Electrochemical Detection

The electrochemical SWASV technique was performed on all 75 samples for the 5 stub collection intervals resulting in 375 voltammetric data files. Initial data processing involved peak integration and potential window evaluation for the identification of positive analyte calls. While the positive calls were investigated in the identification of bullet holes (Chapter 4), this chapter focuses on using peak current area from the collection intervals to develop GSR visualization methods and statistical classification of shooting distance. Two visualization methods explored were bar graphs and macro-spatial heat maps created in the Excel and JMP software. Statistical methodologies investigated discriminant analysis to predict the distance classification of the unknown shooting distances by the peak current areas.

3.3.3 Macro-spatial Mapping for Shooting Distance Determination

Specific shooting distances often leave a visual pattern in the GSR on the target of interest in a shooting event as the distance of the shot affects the distribution and physical characteristics of GSR on the target. Colorimetric methods produce similar results with the color change for lead and nitrites; however, these tests use hazardous chemicals and require obtaining photographic records of the observations since the tests are subject to fading over time. Bar graphs and macro-spatial heat maps address this issue by creating a permanent visualization of the GSR patterns. The calibration distance chosen for this study aimed at defining the typical patterns at contact, short-range (6 and 12 inches), and long-range (24 and 36 inches) shooting distances. For each sample, five voltammograms were integrated for the peak current areas of IGSR and OGSR present in the respective stub collection interval distances described in methods *section 3.2.3*. The peak current area can also be thought of as intensity for this purpose of mapping. Two graphical visualization methods, bar graphs and heat maps, were completed on the calibration and unknown samples. Bar graphs were created by plotting the collection interval against the peak current area for the 5 calibration shooting distances for every GSR analyte detected. **Figure 3.5** demonstrates a bar graph for one of the six shooting distance calibration curves for lead. In the figure, the bullet hole stub produced the highest intensities for lead, with a decreasing trend the farther away the stub is collected from the bullet hole on the same sample. Concurrently, a similar decreasing trend is seen with lead as the shooting distances get farther away. Appendix II contains all bar graphs created for calibration and unknown samples for lead, copper, and nitroglycerin.
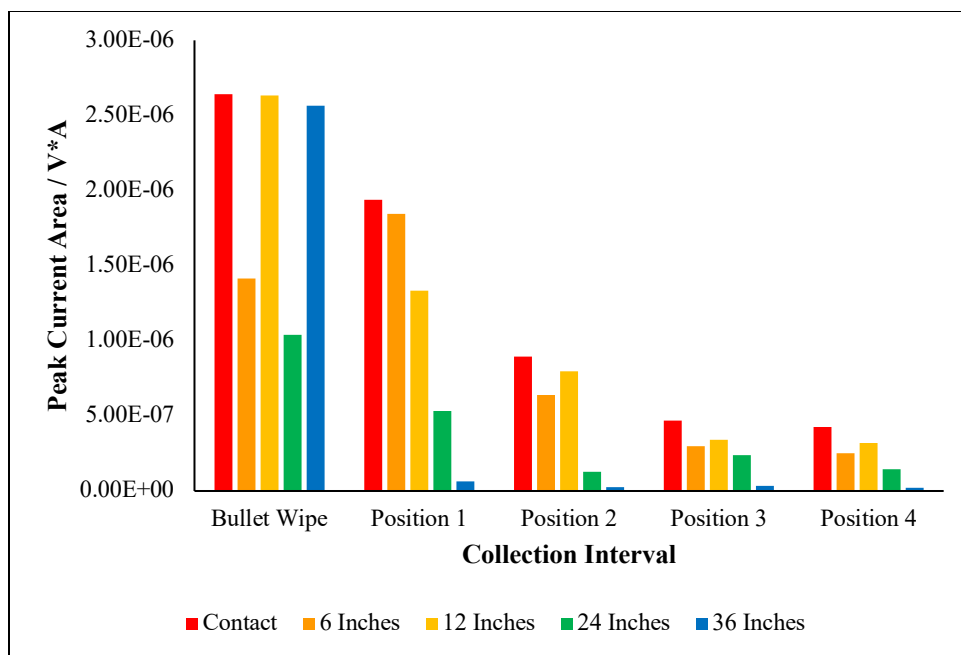
Figure 3.5. *Example bar graph of peak current areas for lead observed in a shooting distance calibration curve, displaying the collection interval for the bullet wipe, position 1 (bullet wipe-2cm), position 2 (2-4cm), position 3 (4-6), and position 4 (6-8cm) on the x axis and the peak current area on the y axis where the shooting distance are color coded: contact (red), 6 inches (orange), 12 inches (yellow), 24 inches (green), and 36 inches (blue).*

Heat maps created in JMP software utilized the peak current areas overlayed on an x and y-axis, representative of five collection intervals to extrapolate the intensity in a circular pattern for macro-spatial heat maps of the GSR pattern. Lead, copper, and nitroglycerin heat maps were created for all calibration and unknown samples if identified by the voltammetric data (Appendix II). **Figure 3.6** established the heat maps created for lead, copper, and nitroglycerin for an example shooting distance calibration curve. Details like an intense bullet hole region for lead can be seen throughout all shooting distances, while surrounding intervals decrease in intensity the further away the fabric was shot. A comparable trend was seen in the copper and nitroglycerin heat maps. An interesting visual in the 6-inch shooting distance for Pb and NG was the defined intensity in the bullet hole to 2 cm interval, which aligns with a large amount of gunpowder seen on the actual samples. To provide an example of how the voltammetric data is converted to heat maps, **Figure 3.7** exhibits the voltammograms collected for an unknown shooting distance on a white fabric sample and the respective heat maps created for lead and nitroglycerin.

The creation of heat maps from the voltammetric data is useful for the application of electrochemistry to the colored and patterned fabric where the GSR pattern is difficult or

unobservable to the naked eye. This sampling for electrochemical analysis provides a method of visualizing IGSR and OGSR through a rapid analysis method as demonstrated in **Figure 3.8**.
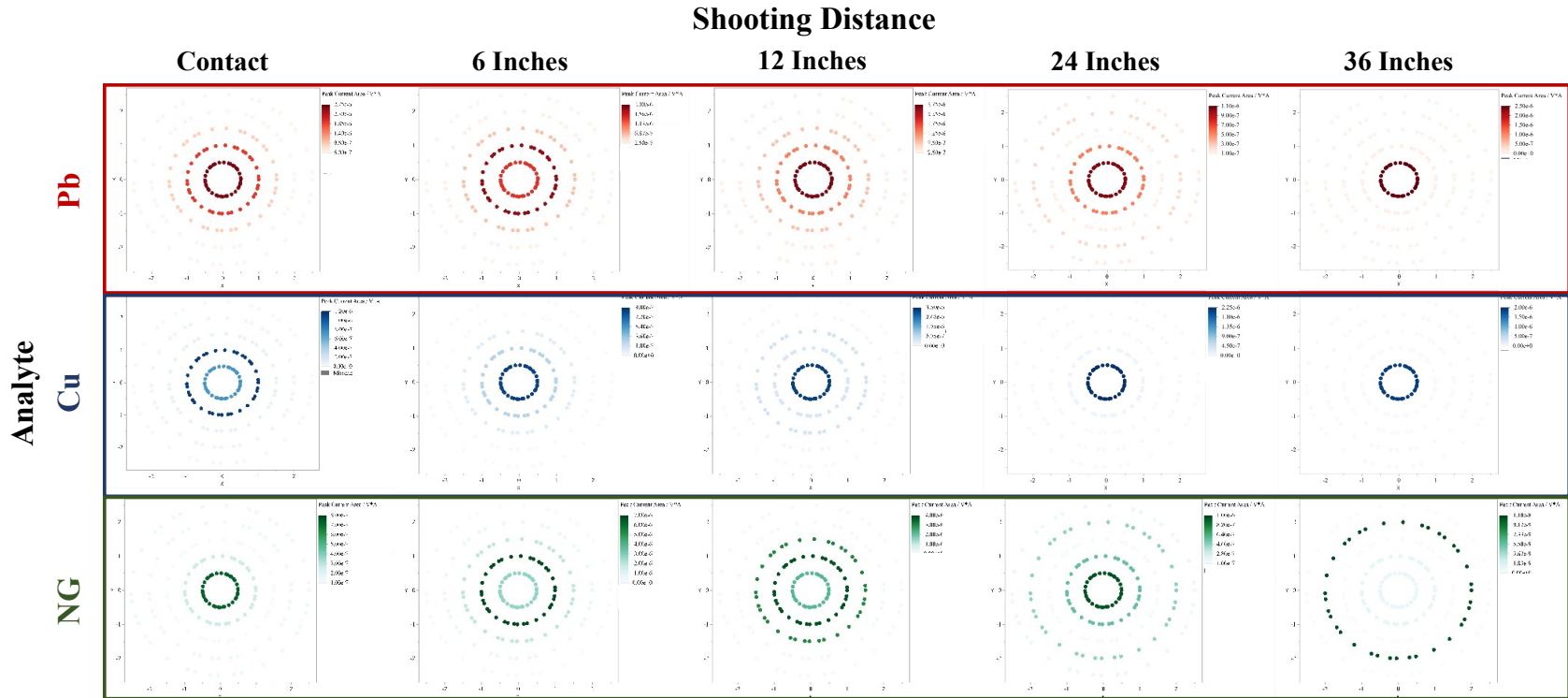
Figure 3.6. *Macro-spatial heat maps created for lead (red), copper (blue), and nitroglycerin (green) for the shooting distance calibration curve at contact, 6-, 12-, 24-, and 36-inches distances defined from left to right at the top of the heat maps.*
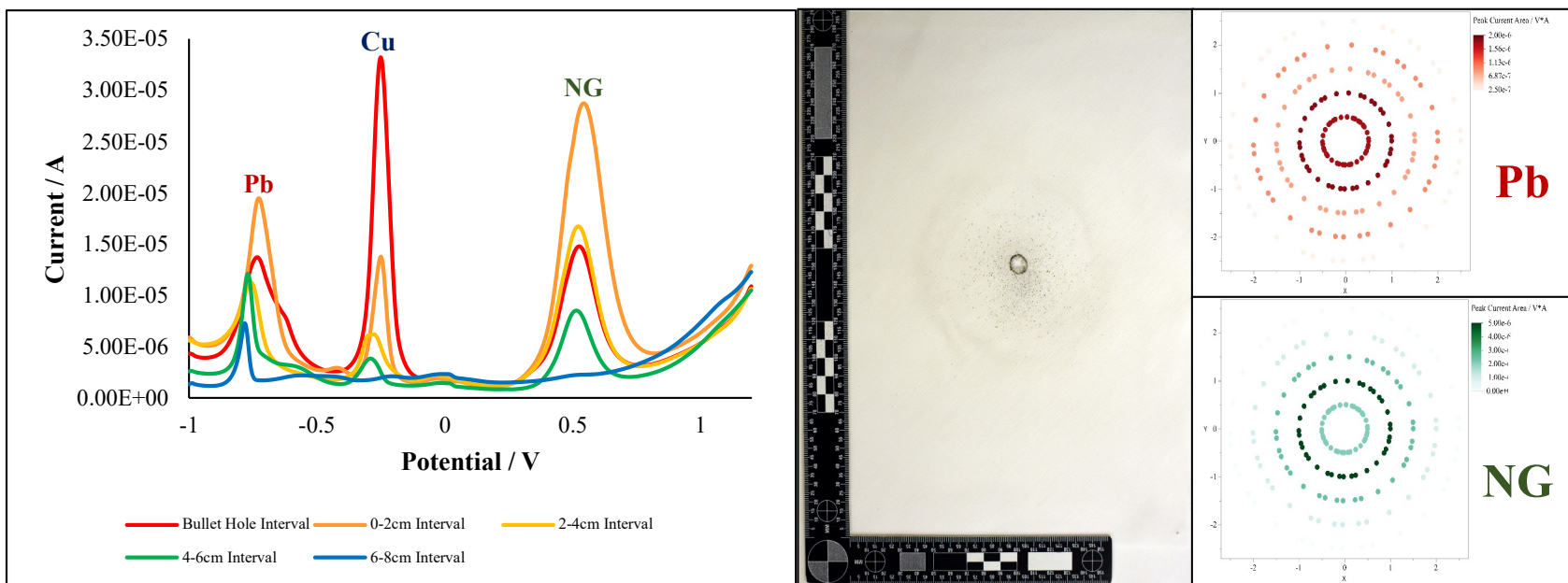
Figure 3.7. *Voltammogram (left), sample photograph (middle), and lead (red) and nitroglycerin (green) heat maps (right) observed from an unknown shooting distance on white fabric.*
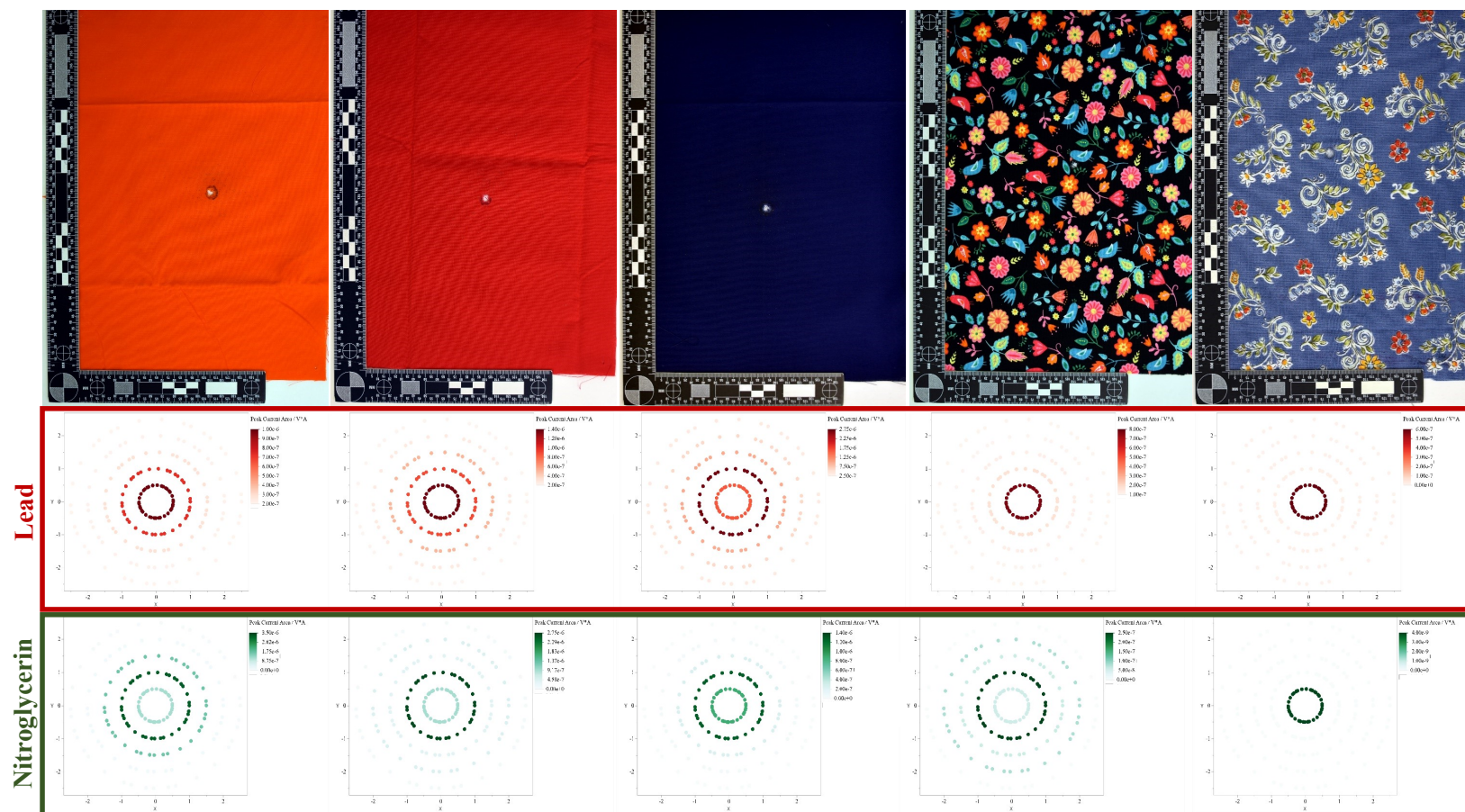
Figure 3.8. *Orange, red, navy, dark and light patterned fabric sample with their respective lead (red) and nitroglycerin (green) heats maps created to visualize GSR pattern observed from electrochemical analysis.*

3.3.4 Shooting Distance Evaluation of White, Colored, and Patterned Fabric by Physical Measurements and Color Tests

If shooting distance determination is required in an investigation, examination by physical measurements and color tests is commonly performed on the targeted substrate. The analytical scheme follows physical measurements taken from the sample, including the bullet orifice length and width, soot dimensions, gunpowder area, and the number of particles visible on the substrate. When possible, a shooting distance calibration curve is obtained for the analyst to use for comparison of the unknown to known shooting distances to make their classification. However, this analysis introduces some subjectivity to the classification process, and many times, if the clothing is dark or patterned, the physical observations can be difficult to discern. **Table 3.3** provides the physical measurement taken from the first 3 replicates of the shooting distance calibration curves and white, orange, red, navy, dark, and light patterned unknowns.

In addition to physical measurements, all calibration and unknown samples were assessed by the modified Griess and sodium rhodizonate color tests. In this study, the stub collection for electrochemical analysis was performed prior to colorimetric methods as described in the analytical scheme from S*ection 3.2.10*. The preliminary testing completed prior to data collection demonstrated that stubbing the fabric before color testing does not interfere with the results, as shown in **Figure 3.9**. All positive controls for the modified Griess (one in each corner of the photographic paper) had positive results before sample application. After application of the Griess reagent, samples were air dried before preforming a Bashinski transfer using Benchkote filter paper. This preserved the integrity of the sample for the sodium rhodizonate test. Color tests were performed on unfired fabric of the same dimensions and fabric type to act as negative controls to evaluate potential interference from the fabric dyes or other constituents. Visual observation and measurements from color test analysis, included the area of Griess color changes, Griess particle distance, and inner and outer color change area of the sodium rhodizonate test. **Table 3.4** provides the measurements taken for calibration sets 1-3 and 35 unknown shooting distance samples.

Table 3.3. *Physical measurements of the shooting calibration set 1-3 and unknowns 1-35 for bullet hole length and width, soot area, gunpowder area, and gun particle counts where unobservable features were denoted by N/A.*

Distance	Sample ID	Bullet Hole LxW (cm)	Soot Area (cm³)	Gunpowder Area (cm³)	Gun Particle Count
Contact	Cal White Set 1	2.9 x 1.9	N/A	1.31	25
Contact	Cal White Set 2	1.1 x 1.0	17.8	6.88	33
Contact	Cal White Set 3	0.96 x 1.1	14.6	2.75	103
6 Inches	Cal White Set 1	0.85 x 0.95	N/A	10.1	274
6 Inches	Cal White Set 2	0.82 x 0.84	8.38	2.53	183
6 Inches	Cal White Set 3	0.97 x 0.93	10.6	2.43	232
12 Inches	Cal White Set 1	0.96 x 1.0	N/A	8.88	436
12 Inches	Cal White Set 2	0.98 x 0.90	N/A	6.19	169
12 Inches	Cal White Set 3	0.83 x 0.80	N/A	5.36	204
24 Inches	Cal White Set 1	0.87 x 0.85	N/A	N/A	186
24 Inches	Cal White Set 2	0.93 x 0.84	N/A	N/A	71
24 Inches	Cal White Set 3	0.92 x 0.98	N/A	N/A	44
36 Inches	Cal White Set 1	0.90 x 0.91	N/A	N/A	22
36 Inches	Cal White Set 2	0.87 x 0.84	N/A	N/A	11
36 Inches	Cal White Set 3	1.0 x 0.94	N/A	N/A	25
Unknown 1	White	0.82 x 0.90	10.1	3.06	183
Unknown 2	White	0.92 x 0.88	N/A	6.25	159
Unknown 3	White	1.0 x 1.0	10.9	2.12	175
Unknown 4	White	0.95 x 0.94	N/A	5.2	171
Unknown 5	White	1.0 x 0.98	8.83	2.63	158
Unknown 6	White	0.91 x 0.96	N/A	N/A	36
Unknown 7	White	0.92 x 0.93	N/A	N/A	26
Unknown 8	White	0.92 x 0.97	N/A	N/A	19
Unknown 9	White	0.88 x 0.85	N/A	N/A	16
Unknown 10	White	0.89 x 0.87	N/A	N/A	9
Unknown 11	Orange	0.93 x 0.87	N/A	N/A	30
Unknown 12	Orange	0.87 x 0.70	N/A	N/A	27
Unknown 13	Orange	0.78 x 0.72	N/A	N/A	28
Unknown 14	Orange	0.93 x 0.65	N/A	N/A	36
Unknown 15	Orange	1.0 x 0.95	N/A	N/A	127
Unknown 16	Red	0.63 x 0.77	N/A	N/A	32
Unknown 17	Red	0.87 x 0.98	N/A	N/A	44
Unknown 18	Red	0.87 x 0.98	N/A	N/A	78
Unknown 19	Red	0.84 x 0.80	N/A	N/A	123
Unknown 20	Red	0.85 x 0.89	N/A	N/A	81
Unknown 21	Navy	0.83 x 0.91	N/A	N/A	60
Unknown 22	Navy	0.38 x 0.40	N/A	N/A	76
Unknown 23	Navy	1.0 x 1.1	N/A	N/A	74
Unknown 24	Navy	0.75 x 0.78	N/A	N/A	54
Unknown 25	Navy	0.92 x 0.95	N/A	N/A	62
Unknown 26	Dark Pattern	0.72 x 0.72	N/A	N/A	5
Unknown 27	Dark Pattern	0.75 x 0.77	N/A	N/A	3
Unknown 28	Dark Pattern	0.72 x 0.78	N/A	N/A	2
Unknown 29	Dark Pattern	0.82 x 0.91	N/A	N/A	5
Unknown 30	Dark Pattern	8.2 x 10.1	N/A	2.48	2
Unknown 31	Light Pattern	0.89 x 0.72	N/A	N/A	N/A
Unknown 32	Light Pattern	0.83 x 0.75	N/A	N/A	N/A
Unknown 33	Light Pattern	0.78 x 0.71	N/A	N/A	N/A
Unknown 34	Light Pattern	0.88 x 0.81	N/A	N/A	N/A
Unknown 35	Light Pattern	0.89 x 0.77	N/A	N/A	1

Shooting Distance

| Contact | 6 Inches | 12 Inches | 24 Inches | 36 Inches |

Samples

Modified Griess

Sodium Rhodizonate
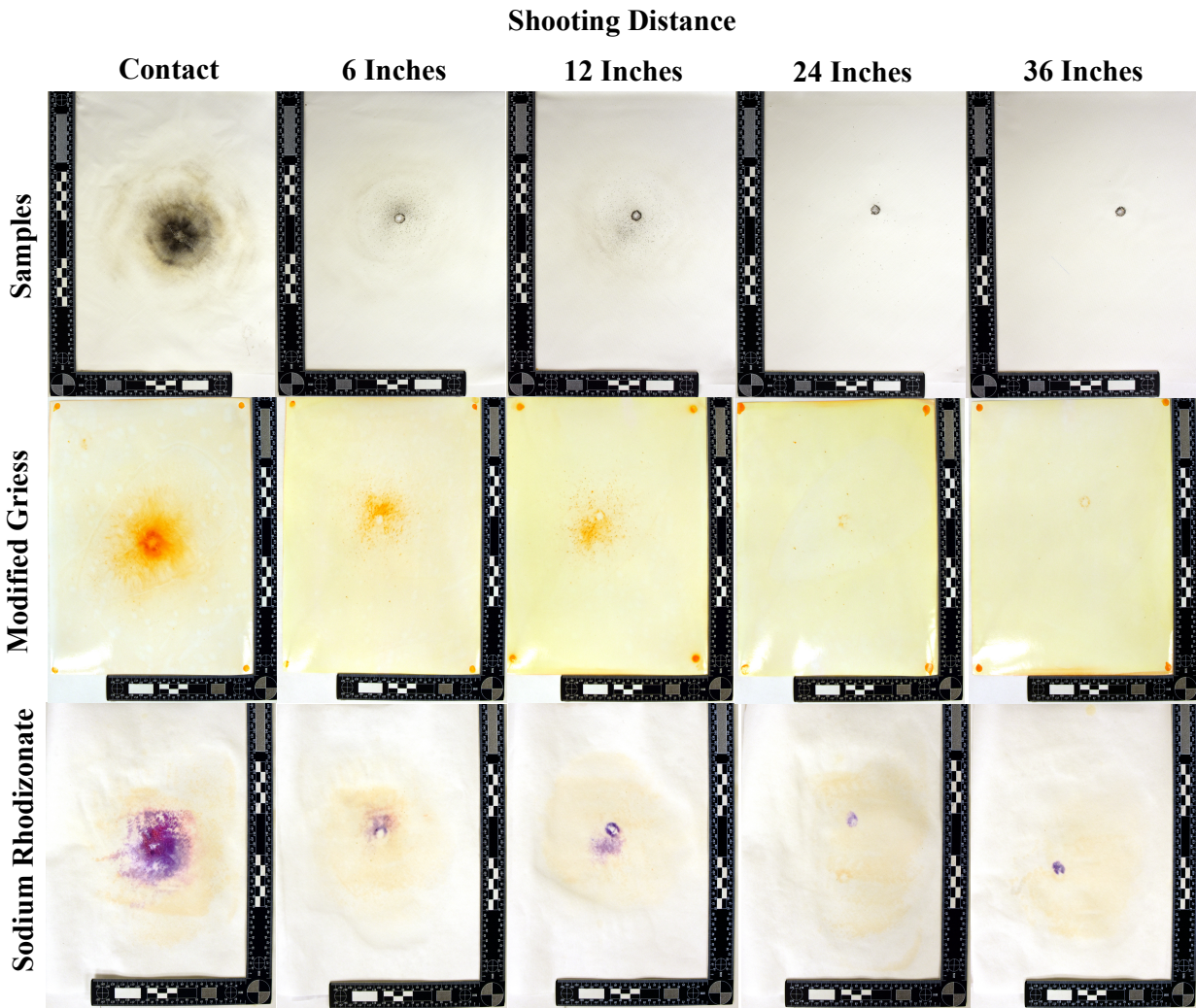
Figure 3.9. *Example sample photographs (top), modified Griess(middle), and sodium rhodizonate (bottom) results from shooting calibration curve set 2 with the five shooting distances defined at the top of the figure.*

Table 3.4. *Color test measurements of the shooting calibration set 1-3 and unknowns 1-35 for area of Griess color, Griess particle distance, and inner and outer sodium rhodizonate color where unobservable features were denoted by N/A.*

Distance	Sample ID	Area of Griess Color (cm^3)	Griess Particle Distance (cm)	Outer Sodium Rhodizonate Area (cm^3)	Inner Sodium Rhodizonate Area (cm^3)
Contact	Cal White Set 1	1.4	11.2	0.0	0.8
Contact	Cal White Set 2	2.4	13.4	0.8	N/A
Contact	Cal White Set 3	2.2	12.5	2.9	0.1
6 Inches	Cal White Set 1	13.3	117.9	1.0	0.1
6 Inches	Cal White Set 2	1.6	10.2	1.0	0.1
6 Inches	Cal White Set 3	1.5	10.5	1.9	0.1
12 Inches	Cal White Set 1	1.5	12.7	0.6	0.2
12 Inches	Cal White Set 2	1.7	7.7	1.1	0.2
12 Inches	Cal White Set 3	1.4	9.8	0.7	0.2
24 Inches	Cal White Set 1	N/A	11.3	N/A	0.2
24 Inches	Cal White Set 2	N/A	11.4	N/A	0.1
24 Inches	Cal White Set 3	N/A	11.9	N/A	0.1
36 Inches	Cal White Set 1	N/A	14.8	N/A	0.1
36 Inches	Cal White Set 2	N/A	13.2	N/A	0.1
36 Inches	Cal White Set 3	N/A	13.1	N/A	N/A
Unknown 1	White	1.1	10.3	0.6	0.2
Unknown 2	White	1.6	10.9	N/A	0.2
Unknown 3	White	1.1	13.7	0.8	0.2
Unknown 4	White	1.1	9.4	1.7	0.1
Unknown 5	White	1.2	10.5	1.0	0.2
Unknown 6	White	N/A	13.6	N/A	0.1
Unknown 7	White	N/A	10.8	N/A	0.2
Unknown 8	White	N/A	14.7	N/A	0.1
Unknown 9	White	N/A	6.6	N/A	0.1
Unknown 10	White	N/A	6.0	N/A	0.1
Unknown 11	Orange	N/A	13.5	N/A	0.1
Unknown 12	Orange	N/A	15.1	N/A	0.1
Unknown 13	Orange	N/A	11.5	N/A	0.1
Unknown 14	Orange	N/A	12.4	N/A	0.1
Unknown 15	Orange	1.6	11.6	N/A	0.1
Unknown 16	Red	N/A	14.7	N/A	N/A
Unknown 17	Red	N/A	15.5	N/A	N/A
Unknown 18	Red	N/A	11.9	N/A	0.1
Unknown 19	Red	N/A	11.4	N/A	0.1
Unknown 20	Red	N/A	11.0	N/A	0.1
Unknown 21	Navy	0.8	5.9	0.5	0.1
Unknown 22	Navy	0.4	9.6	N/A	0.1
Unknown 23	Navy	0.5	11.2	N/A	0.1
Unknown 24	Navy	N/A	9.7	N/A	N/A
Unknown 25	Navy	0.6	8.4	N/A	0.1
Unknown 26	Dark Pattern	N/A	9.6	N/A	N/A
Unknown 27	Dark Pattern	N/A	9.5	N/A	N/A
Unknown 28	Dark Pattern	N/A	7.5	N/A	N/A
Unknown 29	Dark Pattern	N/A	8.5	N/A	N/A
Unknown 30	Dark Pattern	0.6	12.6	N/A	0.3
Unknown 31	Light Pattern	N/A	12.4	N/A	0.1
Unknown 32	Light Pattern	N/A	9.5	N/A	0.1
Unknown 33	Light Pattern	N/A	11.8	N/A	0.1
Unknown 34	Light Pattern	N/A	12.6	N/A	0.1
Unknown 35	Light Pattern	N/A	9.6	N/A	0.1

3.3.5   Shooting Distance Prediction Using Statistical Methods for Electrochemical Data

Statistical techniques were explored to provide a more objective approach for the classification of shooting distance via the electrochemical data and included principal component analysis (PCA) and discriminant analysis (DA). Principal component analysis is often used for identifying relationships and data reduction while maximizing the variation within the dataset by extracting orthogonal sources of variation, the principal components. Moreover, PCA often results in a fortuitous outcome of grouping classes as a visual benefit of the data reduction process.[103] PCA was the first step in data processing where a PCA plot was constructed over the collection intervals for lead, copper, and nitroglycerin integrated peak current areas. While antimony and diphenylamine were present in the voltammetric data, they were less prevalent in the specimens analyzed and were therefore excluded from the statistical analysis. In addition to the integrated analytes, two bullet hole qualifiers were added as variables to account for the tearing or ripping of the fabric and soot morphology for contact shooting distances. These variables were described as bullet hole diameter to account for the tearing of contact shots and bullet hole morphology to account for when there was tearing of contact shot or a dark soot pattern with star-like shape. All six shooting calibration sets were used to assemble PCA plots to assess light colored fabric (white and orange unknowns) and dark or pattern fabric (red, navy, dark and light pattern unknowns). Utilizing the five collection intervals and the bullet hole qualifiers, less than 65% of the variation was captured using the first two principal components (PC) for the light dark color, and patterned clothing data set. To increase the amount of captured variation, the data sets were reduced to include the two bullet hole qualifiers, and only the collection intervals 2-6cm for lead, copper, and nitroglycerin. The bullet hole and 6-8 cm were excluded based on observations from bar graphs where the bullet hole demonstrated variable signal intensity no matter the shooting distance introducing unnecessary noise. For the 6-8cm collection interval, one GSR analyte was often not identified, most often nitroglycerin, so it was left out due to an inadequate number of data points for statistical input. Following analysis on the reduced data sets, the variation captured by the first two PCs for light, dark color, and patterned clothing increased to 77.5% and 69.9%, and 75.7%, respectively.

The first two principal components from PCA were used as the variables to create canonical plots and discriminant analysis for the classification of light and dark clothing unknowns (**Figures 3.10, 3.11, and 3.12**). Discriminant analysis is a supervised pattern recognition method, or hard classification method which targets maximizing between-class variation and minimizing within-class variation for an object to be classified into their pre-defined and mutually exclusive classes. The data separation uses a single vector, or canonical, to maximize the between and the within-class ratio between the individual and central data points to create the model for classification.[103] For this study, regularized discriminant analysis (RDA) was applied as the statistical model to compensate for a small sample size population. In the case of the light and dark/pattern clothing RDA, the six calibration curves were entered as the training set and the unknowns as the validation or test sets. The model outcomes determined the first and second predictions for RDA. However, for some unknown samples, a second prediction was not provided in the output, so the analyst referred to the next closest square distance to make the secondary class prediction. For light and dark color, and patterned clothing, misclassification rates in the training set were 0%, 7%, and 7%, respectively. These misclassifications mostly occurred between the 6 and 12 shooting distances and the 24 and 36 distances. **Figures 3.10, 3.11, and 3.12** show canonical plots demonstrating the difficulty the model has in separating the closer shooting distances from each other. The shooting distance ranges for the unknown samples were created by using the first prediction and the second prediction class determine the classification range. Unknowns did not include samples with star-like tearing from a contact shot since physical characteristics can easily inform a contact classification.

The statistical interpretation for electrochemical data input for PCA and DA is intended to support GSR findings. Predictor reduction demonstrates how most of the variability in samples occurs between the 2–6-inch collection intervals from the bullet wipe. Additionally, physical characteristics like bullet hole factor adds important information to electrochemical detection features. The model's difficulty with grouping close shooting distances maybe caused by the small sample population or a limited number of predictors; however, these challenges provide expansion for future work. Overall, the model proved that the sampling method and electrochemical data are effective in creating statistical models for distance classification.
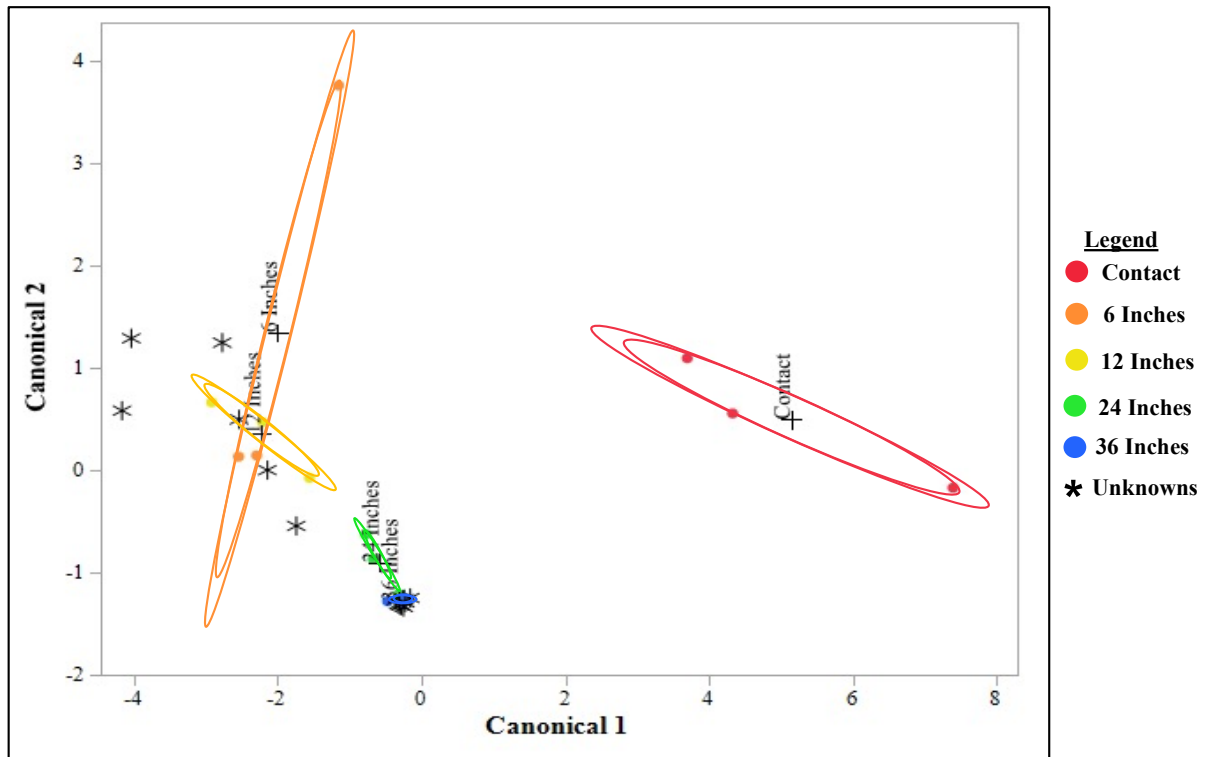
Figure 3.10. *Canonical plot for the white calibration samples with light-colored fabric unknowns (white unknowns 1-10 and orange unknowns 11-15). Unknowns have a true shooting distance of either 14, 28, or 38 inches. (the + represents the multivariate mean for each distance class, the outer ellipses represent the 50% contour of observations for each distance class, and the inner ellipses represent the 95% confidence interval for each distance class.)*
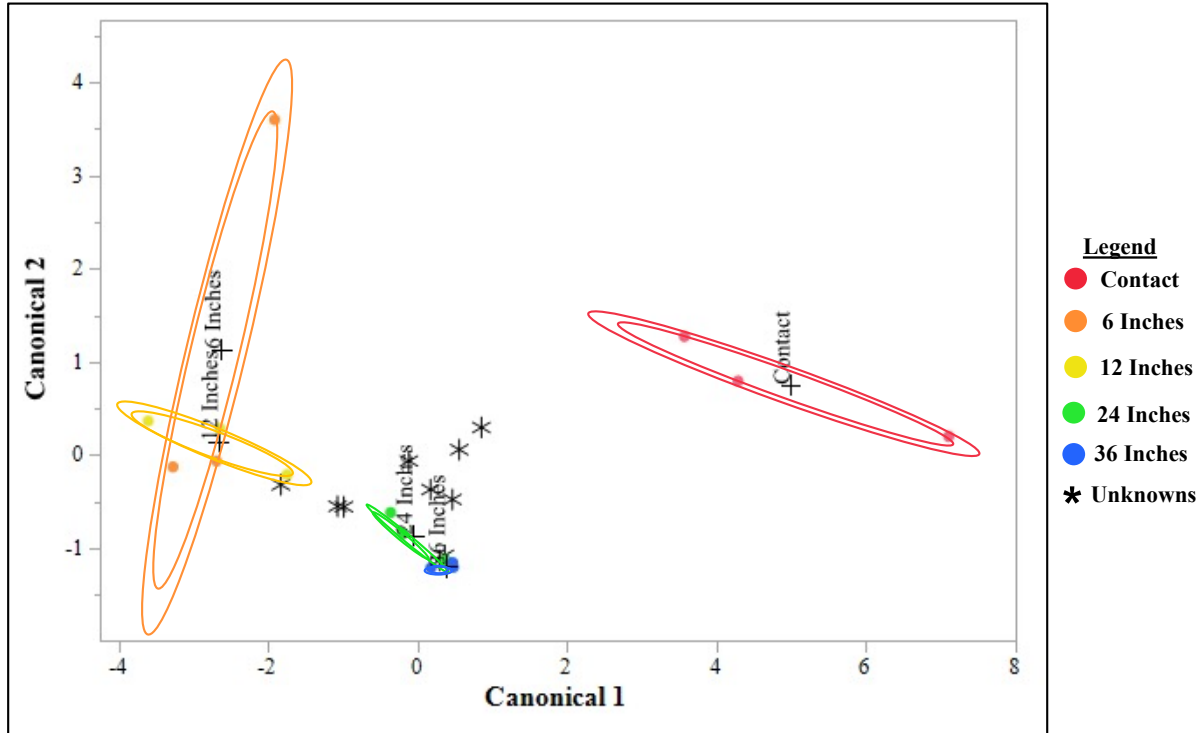
Figure 3.11. *Canonical plot for the white calibration samples with dark-colored fabric unknowns (red unknowns 16-20 and navy unknowns 21-25). Unknowns have a true shooting distance of either 6, 8, 12, 14, 24, 26 or 36 inches. (the + represents the multivariate mean for each distance class, the outer ellipses represent the 50% contour of observations for each distance class, and the inner ellipses represent the 95% confidence interval for each distance class.)*
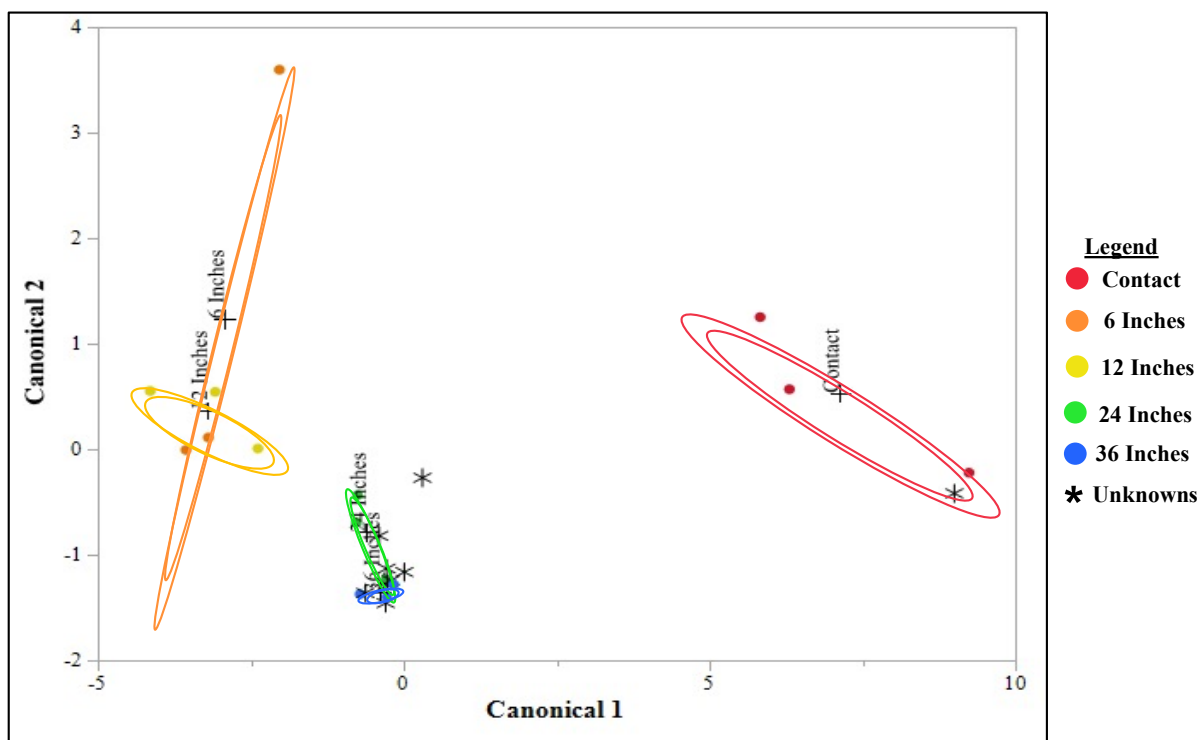
Figure 3.12. Canonical plot for the white calibration samples with dark-colored fabric unknowns (dark pattern unknowns 26-30 and light pattern unknowns 31-35). Unknowns have a true shooting distance of either 6, 8, 12, 14, 24, 26 or 36 inches. (the + represents the multivariate mean for each distance class, the outer ellipses represent the 50% contour of observations for each distance class, and the inner ellipses represent the 95% confidence interval for each distance class.)

3.3.6 Statistical Approaches and Assessment of Method Accuracy

Reporting the interpretation from distance determination can provide important investigative information to determine whether a firearm discharged at a close-, mid-, or long-range which becomes relevant when investigators (medical examiners), are deciding whether a shooting was a suicide, homicide, or accident. A typical report does not include a single distance, but rather a range of the shooting distance. The classification by ranges include contact, 6 inches, 12 inches, 24 inches, and 36 inches where a proper range falls between 1 increment of shooting distance (i.e., 6-12 inches). A misclassification within this study was identified if the test set resulted from the actual distance being outside of the determined range or if the range was too large (i.e., more than one range increment such as contact to 12 inches). This criterion was used to determine the accuracy of the classification by discriminant analysis for electrochemistry compared to physical measurements, and color tests. Electrochemical data performed as well as the physical measures but exhibited superior accuracy compared to color test for the light-colored clothing (**Table 3.5**).

51

For the first white fabric unknown samples, the true shooting of 14 inches was predicted by the models as 12 inches for all five samples. Taking into consideration several factors including shooting variation and the appearance of the samples, it was reasonable to use a plus or minus 2-inch uncertainty range when assessing the true shooting distance to classify the samples. The uncertainty accounts for any misalignment of the shooter during firing since these were shot using floor markers and any movement of arms/hands forward or backward as the projectile is discharged can cause variations of the muzzle-to-target true distance. Additionally, the data shows that when the firing distance is slightly outside a calibration range the model has more difficulty with the classification. This is demonstrated by the next five white clothing fabrics which had a true distance of 28 or 38 inches, and the DA was able to classify 5 out of 5 samples correctly when considering the range uncertainty. The white fabric unknown distance resulted in 91% accuracies across all methods. Electrochemical classification for the unknown orange fabrics found to be 100% correct compared to the physical measurements and color test, which resulted in prediction accuracy of 83% or below. For the 15 light colored unknowns, discriminant analysis provided 94% accuracy compared to 82% and 88% for physical measurements and color tests, respectively.

As shown in **table 3.6**, a slight decreased accuracy was observed for the statistical classification by DA for the dark and patterned clothing (overall accuracy of 85%). However, the EC performance was superior to physical measurements and color test (60% accuracy). Poor accuracy was seen for the red and navy fabric unknown subset. Again, the model prediction capabilities struggled for the samples on the edges of the calibration distances where two true shooting distances were 14 inches. All prediction methods, EC, physical, and color testing had difficulties estimating shooting distances on these fabrics (accuracy 58%, 42% and 33% for EC, physical and color test)/ The results were more affected on red versus navy samples, therefore further investigation on potential interference from fabric dyes is recommended. On the other hand, the algorithm's performance resulted in higher accuracies for the patterned subset with 83% accuracy for EC compared to 58% and 67% for the other conventional techniques. The performance of the electrochemical method demonstrates how dark and patterned clothing makes physical measurements and color tests more difficult for the analyst to interpret, adding subjectivity to the distance estimation. **Tables 3.5 and 3.6** provide the summary of accuracies of the light and dark

52

clothing data sets for classification by DA, physical measurements, and color tests, in addition to, the actual shooting distance and a comment regarding whether the sample was correctly classified.

The analysis of light and dark-colored clothing indicated how performance between methods may be affected by the substrate being evaluated. The model for electrochemical detection demonstrated better accuracies for light-colored, and dark- and patterned fabrics over physical measurements and color tests. Nonetheless, as discussed above, the model's performance struggled with red and navy fabrics or when the true distance was outside the calibration distance ranges, which can be observed in **Tables 3.5 and 3.6**. These results provide a proof of concept on how electrochemical detection can provide more objective outcomes, particularly as the GSR visualization in conventional methods decreases.

Table 3.5. *Summary of classifications by electrochemical, physical measurements, and colorimetric methods for light colored unknowns. (RTL = range too large, Bolded # = model's first prediction, non-bolded # = model's second prediction)*

Unknown Sample ID/ Substrate		Discriminant Analysis by EC Classification Range	Actual Distance	Correctly Classified?	Visual/Physical Classification Range	Correctly by Visual/Physical?	Color Test Classification Range	Correctly Range by Color Tests?
Unknown 1	White	6-**12**	14	Yes	6-12	Yes	12-36	RTL
Unknown 2	White	6-**12**	14	Yes	6-12	Yes	6-12	Yes
Unknown 3	White	6-**12**	14	Yes	6-12	Yes	6-12	Yes
Unknown 4	White	Contact-**12**	14	RTL	6-12	Yes	6-12	Yes
Unknown 5	White	6-**12**	14	Yes	Contact-12	RTL	6-12	Yes
Unknown 6	White	24-**36**	28	Yes	24-36	Yes	24-36	Yes
Unknown 7	White	24-**36**	28	Yes	24-36	Yes	24-36	Yes
Unknown 8	White	24-**36**	28	Yes	24-36	Yes	24-36	Yes
Unknown 9	White	24-**36**	28	Yes	24-36	Yes	24-36	Yes
Unknown 10	White	24-**36**	38	Yes	24-36	Yes	24-36	Yes
Accuracy of White Unknowns		91%			91%		91%	
Unknown 11	Orange	24-**36**	38	Yes	24-36	Yes	24-36	Yes
Unknown 12	Orange	24-**36**	38	Yes	24-36	Yes	24-36	Yes
Unknown 13	Orange	24-**36**	38	Yes	12-36	RTL	24-36	Yes
Unknown 14	Orange	**24**-36	38	Yes	24-36	Yes	24-36	Yes
Unknown 15	Orange	6-**12**	14	Yes	Contact-12	RTL	6-24	RTL
Accuracy of Orange Unknowns		100%			67%		83%	
Overall Accuracy		94%			82%		88%	

54

Table 3.6. Summary of classifications by electrochemical, physical measurements, and colorimetric methods for dark and patterned unknowns. (RTL = range too large, Bolded # = model's first prediction, non-bolded # = model's second prediction)

Unknown Sample ID		Discriminant Analysis by EC Classification Range	Actual Distance	Correctly Classified?	Visual/Physical Classification Range	Correctly by Visual/Physical?	Color Test Classification Range	Correctly by Color Tests?
Unknown 16	Red	**24**-36	14	No	24-36	No	24-36	No
Unknown 17	Red	**24**-36	14	No	12-36	RTL	24-36	No
Unknown 18	Red	**12**-24	6	No	24-36	No	12-24	No
Unknown 19	Red	**12**-24	6	No	6-12	Yes	12-36	RTL
Unknown 20	Red	6-**12**	6	Yes	6-24	RTL	6-12	Yes
Unknown 21	Navy	6-**12**	12	Yes	6-12	Yes	12-24	Yes
Unknown 22	Navy	**12**-24	12	Yes	12-24	Yes	12-36	RTL
Unknown 23	Navy	6-**12**	12	Yes	Contact-12	RTL	24-36	No
Unknown 24	Navy	**12**-24	12	Yes	12-36	RTL	24-36	No
Unknown 25	Navy	Contact-**12**	12	RTL	24-36	No	12-36	RTL
Accuracy of Dark Color Unknowns			58%			42%		33%
Unknown 26	Dark Pattern	**24**-36	12	No	24-36	No	24-36	No
Unknown 27	Dark Pattern	24-**36**	24	Yes	24-36	Yes	24-36	Yes
Unknown 28	Dark Pattern	24-**36**	24	Yes	24-36	Yes	24-36	Yes
Unknown 29	Dark Pattern	24-**36**	24	Yes	12-24	Yes	24-36	Yes
Unknown 30	Dark Pattern	**Contact**	Contact	Yes	Contact-6	Yes	Contact-6	Yes
Unknown 31	Light Pattern	24-**36**	24	Yes	6-24	RTL	24-36	Yes
Unknown 32	Light Pattern	24-**36**	36	Yes	6-24	RTL	24-36	Yes
Unknown 33	Light Pattern	**12**-24	8	No	24-36	No	24-36	No
Unknown 34	Light Pattern	12-**24**	14	Yes	24-36	No	24-36	No
Unknown 35	Light Pattern	24-**36**	26	Yes	24-36	Yes	12-36	RTL
Accuracy of Patterned Unknowns			83%			58%		67%
Accuracy			85%			60%		60%

55

3.3.7 Evaluation of Bloodstained and Non-Bloodstained Unknown via Electrochemical Detection

Assessment of the performance of the voltammetry method included bloodstained clothing to evaluate the potential interference from the blood and how this additional factor could change the results of the GSR visualization methods and statistical classification. For this study, distance predictions on five bloodstained samples were compared to 15 non-bloodstained white fabric samples to compare the capabilities of electrochemical detection and evaluate potential interference from blood. The application of blood to the five samples was achieved as explained in the methods *Section 3.2.4*, which was the only additional step taken prior to carrying out the analytical procedure in *Section 3.2.10*. Electrochemical detection of GSR was achieved for both bloodstained and non-bloodstained fabric in addition to completing graphical visualization and distance classification.

3.3.8 Macro-spatial Mapping for Shooting Distance Determination on Bloodstained Fabric

Similar to *Section 3.3.3*, bar graph plots and heats maps were generated through the conversion of the peak current areas to graphical depictions of the intensity for the IGSR and OGSR analytes by the different collection intervals. **Figure 3.13** provides bar graphs of an unknown bloodstained (unknown 37) and a non-bloodstained (unknown 41) sample for the collection intervals of the integrated areas for lead, copper, and nitroglycerin. These bar graphs provide a simple and easy way to visualize the intensity of the compounds as the sampling distance from the bullet hole increases. In the bloodstained samples, the two most prevalent compounds were lead and nitroglycerin, which both had a decreasing trend from the 2-8 cm collection intervals. In contrast to the non-bloodstained unknown, the decreasing intensity trend was seen from the bullet wipe to 8 cm interval.

Heat maps were created for the same unknowns shown in F**igure 3.13** to provide another visual comparison of bloodstained and non-bloodstained fabric. The bloodstained fabric diminishes the observation of a GSR pattern on the substrate, however, plotting the peak current area from electrochemical detection overcame this challenge. **Figure 3.14** demonstrates the voltammograms,

visual photograph, and heat maps for the unknown samples. The trends between the two unknowns discussed for the bar graphs can also be observed by looking at the heat maps. Plotting using the two methods highlights how electrochemical detection overcomes undiscernible GSR patterns on these complex materials without concerns like bloodstain transfer to color test paper apparatuses.
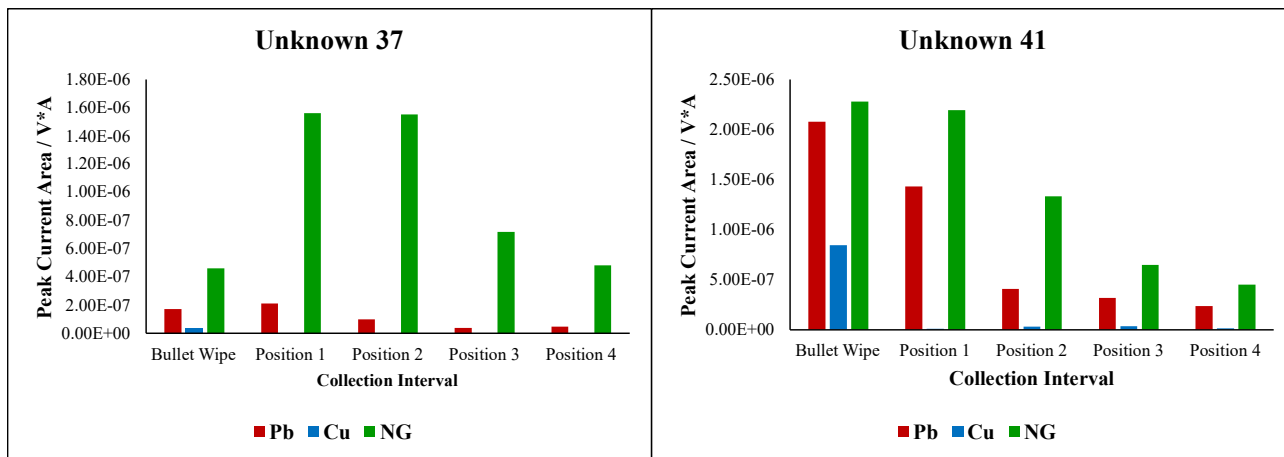
Figure 3.13. *Example bar graph of the peak current areas for lead (red), copper (-blue), and nitroglycerin's (green) peak current areas observed in an unknown bloodstained (37) and non-bloodstained (41) sample exhibiting the collection interval for the bullet wipe, position 1 (bullet wipe-2cm), position 2 (2-4cm), position 3 (4-6), and position 4 (6-8cm) on the x axis and the peak current area on the y-axis.*
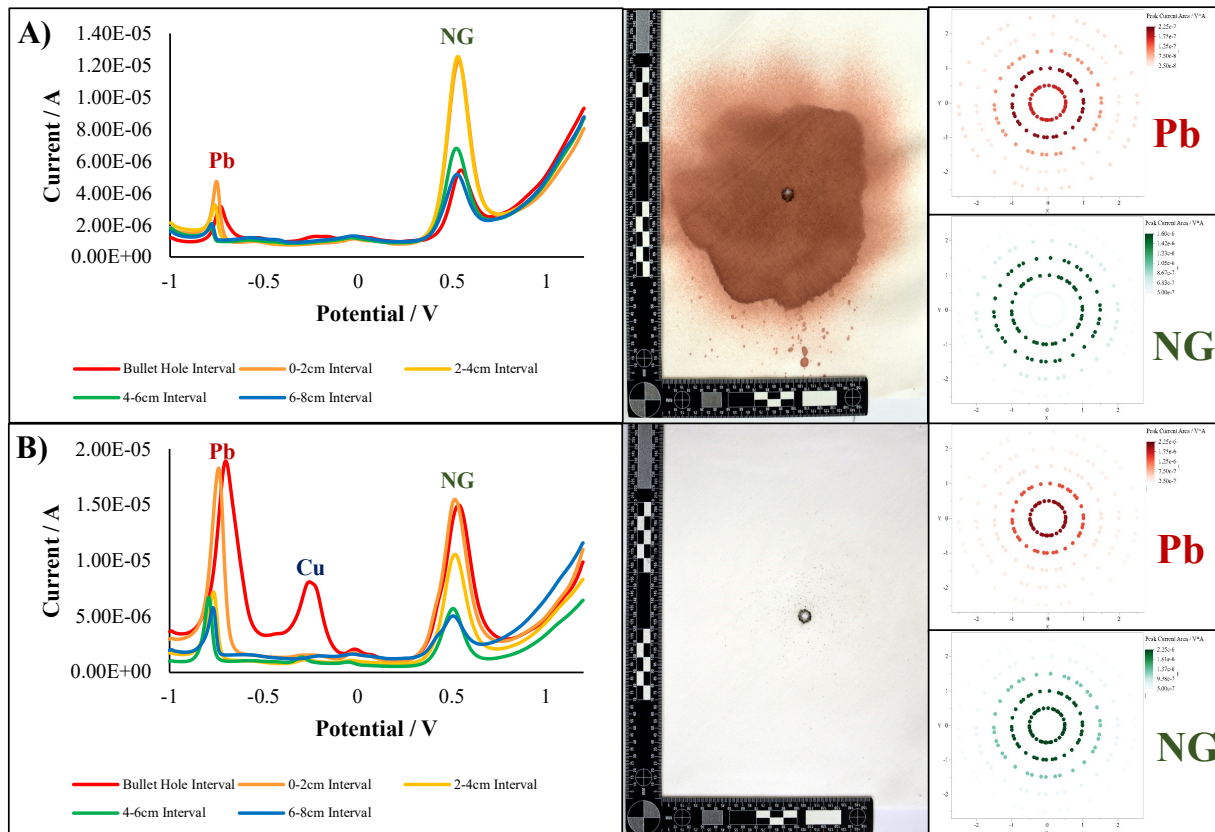
Figure 3.14. *Voltammograms (left), sample photographs (middle), and heat maps (right) observed for an unknown shooting distance for A) bloodstained and B) non-bloodstained fabrics. The heat maps demonstrate lead (red) and nitroglycerin (green) distribution on the fabric samples.*

3.3.9 Shooting Distance Evaluation by Physical Measurements and Color Tests on the Bloodstained Fabric

Traditional practices for physical measurement and color tests for distance determination were performed on the second triplicate set of shooting distance calibration curves, bloodstained, and non-bloodstained samples. Compared to the pristine white calibration curve and 5 unknown distances, the soot patterns were harder to discern on the bloodstained samples. The variability and difficulty in making measurements showcase one of the limitations of visual assessment for distance determination. In the case of the bloodstained samples, the bullet hole dimensions, and particle counts were evaluated for all five samples. From **Table 3.7**, the particle counts found from the bloodstained samples were smaller than the pristine white unknowns, where particles could be easily visualized on the fabric.

When dealing with difficult interferences from dark or blood-stained samples, color tests were more reliable than visual examination and measurements. **Table 3.8** exhibits the measurements taken from the modified Griess and sodium rhodizonate results completed on the samples. As per the analytical procedure, the sampling collection for electrochemical detection was executed prior to the color tests, which, as shown, does not affect the results. Positives were performed on the four corners of the Griess paper before sample analysis, and negative control were all negative for reaction with the modified Griess and sodium rhodizonate tests. Evaluation of physical and colorimetric methods allows for comparison to the electrochemical results. These results demonstrated how blood application on a substrate produces more non-observable features by the analyst.

Table 3.7. *Physical measurements of the shooting calibration set 4-6 and unknowns 36-45 for bullet hole length and width, soot area, gunpowder area, and gun particle counts where unobservable features were denoted by N/A.*

Distance	Sample ID	Bullet Hole LxW (cm)	Soot Area (cm³)	Gunpowder Area (cm³)	Gun Particle Count
Contact	Cal White Set 4	0.92 x 0.96	11.5	1.38	20
Contact	Cal White Set 5	1.0 x 0.98	10.2	0.98	24
Contact	Cal White Set 6	0.95 x 0.96	6.74	2.39	23
6 Inches	Cal White Set 4	1.0 x 0.98	N/A	N/A	244
6 Inches	Cal White Set 5	1.0 x 0.95	6.81	1.43	190
6 Inches	Cal White Set 6	1.0 x 0.98	4.82	1.59	190
12 Inches	Cal White Set 4	1.1 x 1.1	N/A	N/A	141
12 Inches	Cal White Set 5	1.1 x 1.0	N/A	N/A	186
12 Inches	Cal White Set 6	1.0 x 0.99	N/A	N/A	123
24 Inches	Cal White Set 4	1.0 x 0.99	N/A	N/A	44
24 Inches	Cal White Set 5	1.0 x 0.97	N/A	N/A	82
24 Inches	Cal White Set 6	1.0 x 1.0	N/A	N/A	34
36 Inches	Cal White Set 4	1.1 x 1.0	N/A	N/A	19
36 Inches	Cal White Set 5	0.98 x 0.96	N/A	N/A	11
36 Inches	Cal White Set 6	0.94 x 0.94	N/A	N/A	13
Unknown 36	Blood	0.97 x 0.91	N/A	N/A	34
Unknown 37	Blood	1.0 x 0.90	N/A	N/A	61
Unknown 38	Blood	0.97 x 0.97	N/A	N/A	32
Unknown 39	Blood	0.99 x 0.89	N/A	N/A	28
Unknown 40	Blood	1.0 x 0.92	N/A	N/A	26
Unknown 41	Non-blood	0.97 x 0.95	N/A	N/A	161
Unknown 42	Non-blood	0.88 x 0.93	N/A	N/A	94
Unknown 43	Non-blood	1.0 x 1.0	N/A	N/A	96
Unknown 44	Non-blood	0.93 x 0.83	N/A	N/A	59
Unknown 45	Non-blood	0.95 x 0.925	N/A	N/A	79

Table 3.8. *Color test measurements of the shooting calibration sets 4-6 and unknowns 36-45 for the area of Griess color, Griess particle distance, and inner and outer sodium rhodizonate color where unobservable features were denoted by N/A.*

Distance	Sample ID	Area of Griess Color (cm³)	Griess Particle Distance (cm)	Outer Sodium Rhodizonate Area (cm³)	Inner Sodium Rhodizonate Area (cm³)
Contact	Cal White Set 4	1.4	11.2	0.0	0.8
Contact	Cal White Set 5	2.4	13.4	0.8	N/A
Contact	Cal White Set 6	2.2	12.5	2.9	0.1
6 Inches	Cal White Set 4	13.3	117.9	1.0	0.1
6 Inches	Cal White Set 5	1.6	10.2	1.0	0.1
6 Inches	Cal White Set 6	1.5	10.5	1.9	0.1
12 Inches	Cal White Set 4	1.5	12.7	0.6	0.2
12 Inches	Cal White Set 5	1.7	7.7	1.1	0.2
12 Inches	Cal White Set 6	1.4	9.8	0.7	0.2
24 Inches	Cal White Set 4	N/A	11.3	N/A	0.2
24 Inches	Cal White Set 5	N/A	11.4	N/A	0.1
24 Inches	Cal White Set 6	N/A	11.9	N/A	0.1
36 Inches	Cal White Set 4	N/A	14.8	N/A	0.1
36 Inches	Cal White Set 5	N/A	13.2	N/A	0.1
36 Inches	Cal White Set 6	N/A	13.1	N/A	N/A
Unknown 36	Blood	0.17	8.18	N/A	0.09
Unknown 37	Blood	0.22	8.01	N/A	0.08
Unknown 38	Blood	0.14	8.10	N/A	0.13
Unknown 39	Blood	0.19	9.65	N/A	0.09
Unknown 40	Blood	N/A	10.45	N/A	0.08
Unknown 41	Non-blood	0.18	12.57	N/A	0.16
Unknown 42	Non-blood	N/A	12.82	N/A	0.10
Unknown 43	Non-blood	0.15	12.13	N/A	0.12
Unknown 44	Non-blood	N/A	11.15	N/A	0.12
Unknown 45	Non-blood	N/A	12.17	N/A	0.10

3.3.10 Shooting Prediction, Statistical Approaches, and Method Accuracies for Bloodstained Fabric

PCA and DA were again used for statistical analysis to classify the shooting distance for the bloodstained sample set. Following the similar procedure as *Section 3.3.5*, PCA plots were constructed using the integrated peak current areas for lead, copper, and nitroglycerin for the 2-8 cm collection interval range. The bullet hole interval and bullet hole diameter predictors were excluded from statistical analysis due to introducing unnecessary noise or no variation in the diameters was seen in the data. Again, a bullet hole morphology was added to account for the star-like characteristic tearing and soot patterns of contact shots. The calibration curves, bloodstained, and non-bloodstained unknowns were used to calculate PC which captured variation from 78.1% using the first three principal components.

The resulting principal components were the variables used for discriminant analysis of the electrochemical method (**Figure 3.15**). RDA was used with three calibration curves entered as the training set and the bloodstained or non-bloodstained unknowns were used as the validation or test sets. Misclassification rates for the DA model training set was 13% where two samples of the calibration where incorrectly classified into their true distance class, while the unknown test set produced high misidentification rates (67%). True distances included three of the bloodstained samples fired at 6 or 10 inches, which DA was able to classify correctly only one sample by the electrochemical method. Conversely, the known distance for the non-bloodstained samples varied from 10 to 38 inches and resulted in 81% of unknowns being correctly classified in the appropriate distance range.
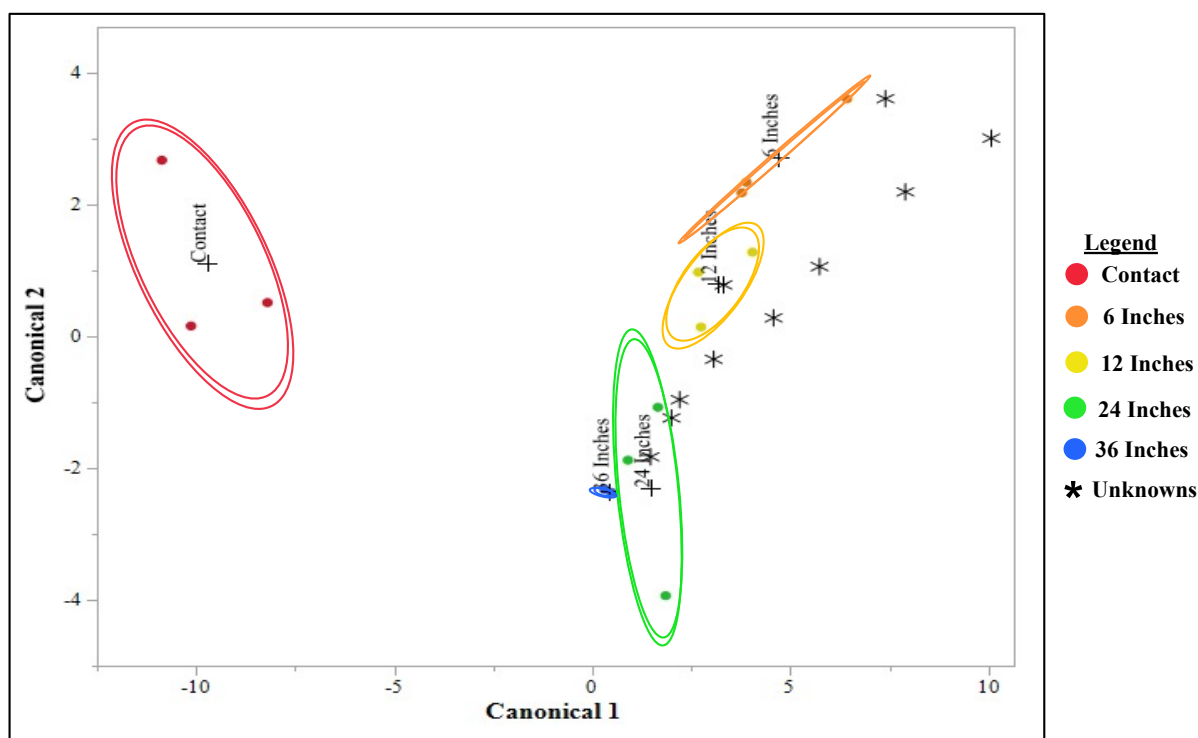
Figure 3.15. *Canonical plot for the white calibration samples with bloodstained fabric unknowns, 36-40 and non-bloodstained unknowns 41-45. Unknowns have true shooting distance of either 6, 10, or 20 inches. (the + represent the multivariate mean for each distance class, the outer ellipses represent the 50% contour of observations for each distance class, and the inner ellipses represent the 95% confidence interval for each distance class.)*

Reporting criterion followed the same protocol as described in *Section 3.3.6* for determining the accuracy of the classification by discriminant analysis for electrochemistry compared to physical measurements and color tests. As specified in T**able 3.9**, the electrochemical method had poor

performance similar to physical measurements and colorimetric methods with 33%, 50%, and 33% accuracy, respectively for the bloodstained samples. In **Table 3.9**, most bloodstained samples were classified having too large of range. However, it should be noted that the electrochemical method the true distance fell within the ranges provided by the statistical analysis, but a boarder range of uncertainty is provided in the output. A potential cause of this larger uncertainty range is the lack of copper identified in the bloodstained samples whereas copper was found in a great frequency of the pristine white samples. This increase in performance is demonstrated where the 15 pristine white samples classified by the electrochemical method resulted in 81% accuracy on par with physical measurements and color test at 81% and 69%, respectively. **Table 3.9** outlines the results of classification by methods and the overall accuracy of the 20 unknown distances for bloodstained sample set, where electrochemical detection achieved an overall 68% accuracy. The blood interference will be the subject of future work as it is intriguing what is the culprit of prediction error on these stained samples. A potential cause is that the blood is producing the distortion of the GSR on the fabric, and thus future experiments comparing results of blood application before and after shooting may help determining the need of using calibration standards stained with blood.

Electrochemical detection of IGSR and OGSR compounds emphasizes how this method was combined with statistical approaches to offer a more objective interpretation than physical measurement or color tests when involving more complex materials. The model was able to make correct predictions despite struggling to differentiate distance classes like 6- and 12-inch. As a proof-of-concept, electrochemical data affords many benefits as a quick, disposable platform that lessens the risk to the analyst with these biohazardous substrates. Further, statistical models developed provided a more objective approach to distance determination.

3.4 Conclusions

Distance determination plays a vital role in investigations concerning firearm-related suicides, homicides, and accidental deaths. The range of the shooting distance can provide investigative leads and aid in crime scene reconstruction. Physical measurements and colorimetric tests are the current practice carried out on appropriate materials that have been involved in a shooting event. These practices provide important physical characteristics and colorimetric mapping of the lead and nitrite present. However, these tests have lengthy procedures with corrosive chemicals and can fade over time and are destructive to the evidence. Additionally, complex materials like dark,

patterned, or bloody clothing can disrupt the confidence the analyst has in interpreting the results for reporting a distance range. This gap in knowledge was the target of this research to provide a fast collection method in combination with a rapid screening method for complementary spatial and chemical information and a more objective statistical classification method.

The developed sampling method utilizing SEM aluminum stubs and carbon adhesive tape allowed for multiple stubs to be easily collected from around a bullet hole for screening analysis and without interfering with colorimetric methods. Additionally, the collection stub offers the potential for less contamination at the crime scene or laboratory settings and the ability to collect controls from the surrounding material. This collection method provided an excellent sampling of GSR in under a minute per interval, saving crime scene investigators time when processing a shooting-related crime scene.

Little sample preparation is needed for electrochemical analysis, where a sample can be extracted and analyzed in approximately 5 minutes. The electrochemical method allows for minimal destruction to the sample and is a faster, safer analysis method for the analyst.

The electrochemical analysis demonstrates a fit-for-purpose method for distance determination applications. The electrochemical data obtained allowed for the creation of permanent bar graphs and heat maps to visualize the gunshot residue patterns. The heat map created by the electrochemical data was successful for difficult clothing materials like the dark, patterned and bloodstained fabric and performed better than the naked-eye or color tests, where less features were noticed by the analyst when taking measurements from these types of fabrics.

Discriminant analysis using electrochemical data performed as equally well as the current practices for light-colored clothing, showing a 94% accuracy. The statistical classification struggled with differentiating the 6- to 12-inche and 24- to 36-inch distance classes. This issue may be overcome by using smaller stubs for collection and adding additional intervals between 2-6 cm from the bullet wipe, as well as, exploring more statistical classification methods like neural networks to recognize more patterns in the voltammetric data. For more complex materials, electrochemical classification had better performance with 85% accuracy for dark colors and patterned, and 68% for bloodstained unknown distance samples. Assessment of the 45 unknowns' samples, resulted

in an overall accuracy for the electrochemical method of 74%, while color tests resulted in an overall accuracy of 58%. Overall, the methods developed were able to provide a simple analytical scheme to add electrochemical analysis to current practices and provide simultaneous IGSR and OGSR detection, spatial, and chemical information.

Table 3.9. *Summary of classifications by electrochemical analysis, physical measurements, and colorimetric methods for bloodstained and pristine white fabric unknowns. (RTL = range too large, Bolded # = model's first prediction, non-bolded # = model's second prediction)*

Unknown Sample ID		Discriminant Analysis by EC Classification Range	Actual Distance	Correctly Classified?	Visual/Physical Classification Range	Correctly by Visual/Physical?	Color Test Classification Range	Correctly Range by Color Tests?
Unknown 36	Blood	12-**24**	6	No	6-24	RTL	Contact-12	RTL
Unknown 37	Blood	6-**24**	6	RTL	12-24	No	6-24	RTL
Unknown 38	Blood	6-**24**	6	RTL	6-12	Yes	6-12	Yes
Unknown 39	Blood	6-**24**	10	RTL	12-24	No	12-36	RTL
Unknown 40	Blood	12-**24**	10	Yes	6-12	Yes	12-24	No
Accuracy of Bloodstained Unknowns		33%			50%		33%	
Unknown 1	White	6-**12**	14	Yes	6-12	Yes	12-36	RTL
Unknown 2	White	6-**12**	14	Yes	6-12	Yes	6-12	Yes
Unknown 3	White	6-**12**	14	Yes	6-12	Yes	6-12	Yes
Unknown 4	White	Contact-**12**	14	RTL	6-12	Yes	6-12	Yes
Unknown 5	White	6-**12**	14	Yes	Contact-12	RTL	6-12	Yes
Unknown 6	White	24-**36**	28	Yes	24-36	Yes	24-36	Yes
Unknown 7	White	24-**36**	28	Yes	24-36	Yes	24-36	Yes
Unknown 8	White	24-**36**	28	Yes	24-36	Yes	24-36	Yes
Unknown 9	White	24-**36**	28	Yes	24-36	Yes	24-36	Yes
Unknown 10	White	24-**36**	38	Yes	24-36	Yes	24-36	Yes
Unknown 41	White	**6**-12	10	Yes	6-24	RTL	6-24	RTL
Unknown 42	White	6-**12**	20	No	12-24	Yes	12-36	RTL
Unknown 43	White	**12**-24	20	Yes	12-24	Yes	12-24	Yes
Unknown 44	White	12-**24**	20	Yes	12-24	Yes	24-36	No
Unknown 45	White	6-**12**	20	No	24-36	No	24-36	No
Accuracy of White Unknowns		81%			81%		69%	
Accuracy		68%			73%		59%	

IV. CHAPTER 4: ELECTROCHEMICAL AND MASS SPECTROMETRY METHODS FOR BULLET HOLE IDENTIFICATION

4.1 Overview

The objective of this chapter was to provide a practical, rapid approach for the application of electrochemical detection of GSR for the screening of potential bullet entrance holes on various substrates common in firearm-related events. This quick approach utilized a single carbon adhesive GSR collection stub to sample the bullet wipe from fabric, wood, and drywall substrates and assessed by electrochemistry. This work employed electrochemical techniques to all 59 samples consisting of several types of materials broken down into 15 white fabrics, 25 colored and pattern fabrics, 5 bloodstained fabrics, 7 wood, and 7 drywall samples (**Figure 4.1**). Electrochemistry provided an adequate tool for detecting IGSR and OGSR from all of the different substrates. Additionally, as confirmatory analysis, all 59 samples were analyzed by liquid chromatography-tandem mass spectrometry to confirm the presence of OGSR from the bullet wipe. While some materials demonstrated background current interferences, electrochemical detection resulted in 98% accuracy for the correct identification of a bullet entrance orifice.
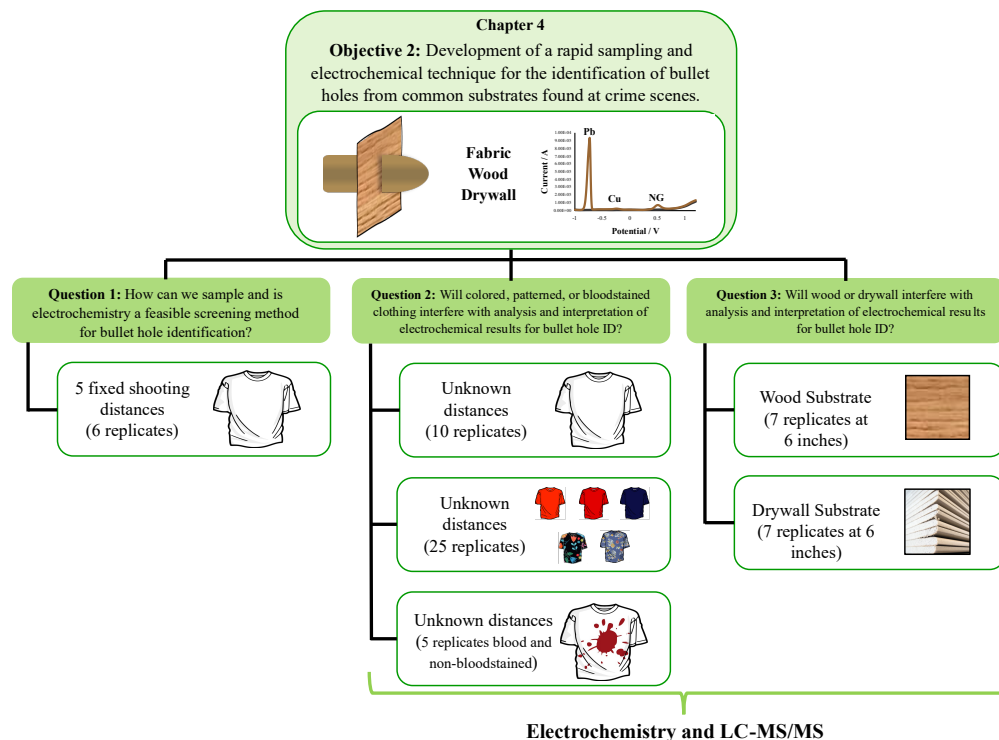
Figure 4.1. *Graphical representation of the objective, tasks, and experimental design for Chapter 4.*

4.2 Materials and Methods

The fabric samples collected for distance determination included white, colored and patterned, and bloodstained clothing were also analyzed for bullet hole identification. The materials and methods from *sections 3.2.1-4* and *3.2.6-8* were used to assess the fabric samples in this chapter. Other substrates, wood and drywall, were collected as described in the section below.

4.2.1   Reagents, Standards, and Instrumentation

Please refer to *section 3.2.1* for reagents and standards used for electrochemical analysis, neat standards, and quality controls used to perform analysis in this part of the study. Additional reagents for LC-MS/MS analysis included Optima® LC-MS grade Methanol, Acetonitrile and water containing 0.1% Formic acid were obtained from Thermo-Fisher Scientific (Waltham, MA). Organic standards for the LC-MS/MS panel, in addition to those in *Section 3.2.1*, included: acardite II (AK II), 2-nitrodiphenyalamine (2-NDPA), and 4-nitrodiphenylamine (4-NDPA) purchased from Sigma-Aldrich (St. Louis, MO). Additional negative control stubs were collected from unfired wood and drywall. Colorimetric reagents were only used to perform testing on fabric samples. *Section 3.2.2* describes the electrode platforms and instrumentation used for electrochemical analysis.

4.2.2   Fabric Sample Preparation, Collection, Blood Application

Please refer to *Sections 3.2.3* for the preparation and collection of the clothing samples used for both distance determination and bullet hole identification. *Section 3.2.4* discusses the application of blood to five white fabrics, which were also analyzed for bullet hole identification.

4.2.3   Sample Preparation and Collection of Hard Substrates

Two hard substrate samples were investigated in this project, including wood (3/8-inch pine plywood) and drywall. The collection was performed at the West Virginia University Ballistics Laboratory under controlled conditions. The same firearm, a Springfield XD, was used to fire Winchester .40 caliber ammunition was used to shoot substrate at a single distance, 6 inches, to ensure GSR deposition onto the sample.

Each substrate was cut into 15 by 15-inch pieces which were stored in clean butcher paper to avoid contamination. The collection apparatus was a tall wooden structure, 182 cm, with a 15 by 15-inch inset to safely secure the substrate using clamps for the shooting of hard substrates. Prior to the shooting, the floor was covered with clean painters' paper to keep the range safe from any stray wood and drywall dislodged during shooting.

4.2.4   Sampling Methodology for Bullet Hole Identification

A rapid methodology for collecting IGSR and OGSR from the bullet hole was performed using commonly employed SEM aluminum stubs with carbon adhesive tape. The same bullet hole stub was used for electrochemical detection by sampling in the 12, 3, 6, and 9 o'clock positions (denoted as the red 1, 2, 3, and 4 in f**igure 4.2**). An additional GSR stub used to sample the bullet wipe by lifting in the 2, 4, 8, and 10 o'clock positions around the bullet wipe for LC-MS/MS analysis (denoted as green A, B, C, and D in **figure 4.2**).
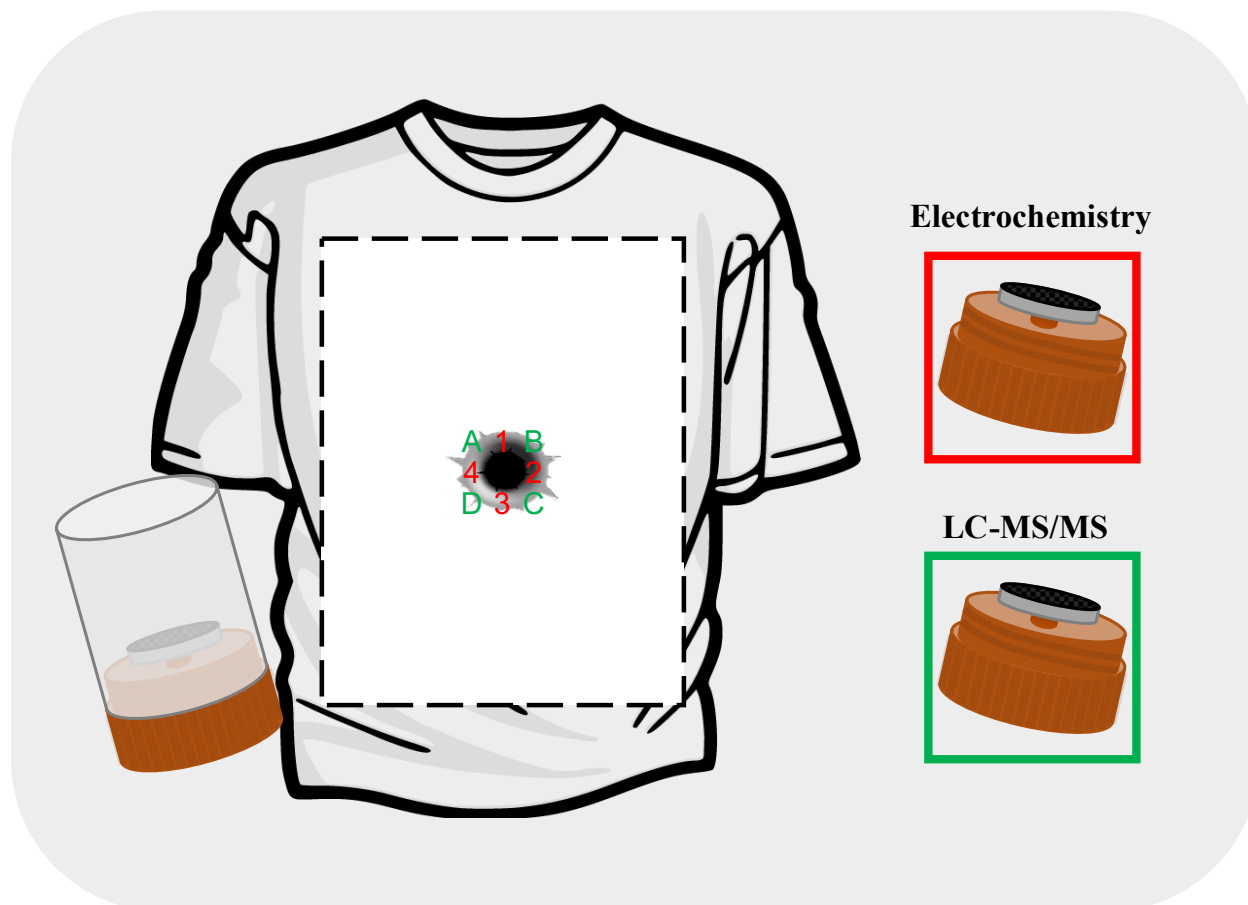
Figure 4.2. *Sampling methods used to collect GSR particles from fabric for EC and LC-MS/MS analysis.*

4.2.5   Extraction Procedure

Section 3.2.6 describes the extraction procedure of the stubs after collection from the fabric substrates. The same procedure was carried out on the additional stubs collected from the wood and drywall.

4.2.6   SWASV Technique and Data Analysis

The electrochemical technique for analysis was the same as explained in *Section 3.2.7*. Data analysis employed the same software mentioned in *Section 3.2.8*. Bullet hole data analysis explored critical thresholds as a technique for classification and positive identification of GSR.

4.2.7   Liquid Chromatography-tandem Mass Spectrometry methods

LC-MS/MS was used a confirmatory analysis method for OGSR analytes for the bullet hole identification study adapted from a validated method by Feeney et al. [98–100] The panel of the six monitored OGSR analytes included akardite II (AK II), ethyl centralite (EC), methyl centralite (MC), diphenylamine (DPA), 2-nitrodiphenylamine (2-NDPA), and 4-nitrodiphenylamine (4-NDPA).

For OGSR extraction from the stub surface, six consecutive washes of 50 μL of methanol were collected for a total of 300 μL in a 0.2 μm filtration tubes. The filtration tubes were centrifuged for 4 minutes before transferring to an LC vial. A dry down was performed under a constant stream of nitrogen for the samples in the LC vial and reconstituted to 300 μL using 291 μL of Methanol with 0.1% formic acid and 9 μL of 5 ppm working solution of D_{10}-DPA to give 150 ppb concentration as the internal standard.

Analysis by LC-MS/MS was performed on an Agilent 1290 Infinity II liquid chromatography coupled to an Agilent 6470 triple quadrupole mass spectrometer. Separation was achieved using an Agilent pentafluorophenyl (PFP) Poroshell® 120 column (2.7 μm 2.1 x 50mm) for separation. The mobile phases consisted of water with 0.1% formic acid (FA) as the aqueous phase (A) and acetonitrile with 0.1% FA as the organic phase (B). The starting column conditions were

80%A/20%B with a gradient elution over nine minutes to 5%A/95%B with a flow of 0.300mL/min (Appendix III Table S4.1). The volume of injection was 1.0 μL.

Organic GSR analytes were monitored by a Multiple Reaction Monitoring (MRM) method using quantifiers and qualifiers ions for classification of compounds created by Feeney et al.[50,98,99] Source parameters are provided in Appendix III table S4.2. The chosen quantifier and qualifier ion are provided in a summary **Table 4.1** below. Agilent MassHunter QQQ Quantitative Analysis (Version B.08.00) software was used for data analysis for peak integration and predicted concentration by the internal standard relative ratio.

Table 4.1. *Summary table of analytes and the respective precursor, product ion, fragmentor voltage, collision energy, and retention time for LC-MS/MS analysis.*

Analyte	Precursor	Product Ions (*m/z*)*	Fragmentor Voltage (V)	Collision Energy (V)	Retention Time
Akardite II	227.0	**170.0** 168.0 92.0	96.0	16.0	2.333
Ethyl Centralite	269.2	**148.0** 120.0	96.0	12.0	3.671
Methyl Centralite	241.0	**134.0** 106.0	100.0	16.0	3.053
Diphenylamine	170.0	**93.0** 66.0 65.0	120.0	32.0	3.919
2-Nitrodiphenylamine	215.0	**180.0** 198.0	100.0	16.0	4.148
4-Nitrodiphenylamine	215.0	**167.0** 198.0	90.0	50.0	3.913

*Bolded ions were used as the quantifier ion.

A number of performance checks were analyzed by the LC-MS/MS to ensure proper performance of the instrument and quality data collection. Calibration curves between 5 and 200 ppb were used as positive controls and quantitation for the 6 OGSR compounds monitored by the method. The internal standard concentration was 150 ppb. Negative controls were used to ensure no contamination or background interferences and included methanol blanks as well as stub samples

collected from the unfired substrates. Blanks were run between samples to ensure no carryover or cross-contamination.

4.3 Results and Discussion

For the purpose of bullet hole identification, electrochemistry was charged with the detection of IGSR and OGSR from multiple substrate materials and OGSR was confirmed by LC-MS/MS. The assessment of this chapter's results is divided into *electrochemical performance for bullet hole identification* and *confirmation of OGSR by LC-MS/MS*. Electrochemical data evaluated identification for the panel of IGSR and OGSR analytes, and performance measures including true positives, true negatives, and accuracy were assessed. Excellent sensitivity and specificity were achieved with 98% accuracy in the appraisal of bullet holes from the various substrate materials. Organic gunshot residues have been a recent discussion in the gunshot shot residue community and can provide critical information to shooting investigation. Electrochemistry has proven to be a reliable screening method for IGSR and OGSR, and, in this study, LC-MS/MS was used for the bullet hole application to confirm the presence of OGSR findings by electrochemistry.

4.3.1   Electrochemical performance for bullet hole identification

Bullet hole identification using electrochemical detection explored using critical threshold to make individual positive and negative analyte calls. These critical thresholds were created using the average of the integrated peak current area for the low calibrator level plus three time their standard deviation obtained from the calibration curves using IGSR and OGSR standards described in *Section 3.1.1*. **Table 4.2** provide the average lowest calibrator thresholds used to call a sample positive for a panel of IGSR or OGSR analytes. Note that while all the thresholds are provided for all analytes, not all were seen in every sample.

Table 4.2. *Average lowest calibrator peak current areas used to create thresholds for calling an analyte positive in a sample.*

Analyte	Average Lowest Calibrator (A)
Pb	8.04×10^{-08}
Sb	5.94×10^{-08}
Cu	4.27×10^{-08}
2,4-DNT	8.44×10^{-08}
DPA	5.15×10^{-08}
NG	1.84×10^{-09}
EC	6.13×10^{-08}

The calibration curves were stubbed and evaluated in the previous chapter for distance determination and heat map creation, where the positive analyte calls are shown in **Table 4.3**. From this calibration data, different trends depending on the specific analyte and distance can be seen, which is relevant to actual casework since the true firing distance will be unknown to the investigators. Lead and copper were the most prevalent at all distances, where 100% of the 30 samples were called positive for both. High copper occurrence is believed to be caused by the ammunition used, Winchester .40 caliber, which used full metal jacketed bullets that cover the soft leaded core with an alloy metal material like cupronickel, in addition to the brass cartridge case. Antimony was seen most often in the closer firing distances, with 33% of the contact samples containing the element. While nitroglycerin was the only organic residue present in the data, this is still an advantageous OGSR compound as it has been classified as a category I compound in the OSAC Standard Practice for Analysis of OGSR, which are those compounds used in the manufacturing of smokeless powder and priming compounds and uncommon from other sources. [17] Other organic compounds like DPA were seen in samples; however, in work by Ott et al., it has been demonstrated that the NG and DPA potential windows overlap. [11] Due to this challenge, DPA was noted if seen during analysis, but it is not included in data analysis since the number of samples where the compounds could be discerned was limited. A decreasing trend in positive calls for NG was demonstrated from the 12 to 36 inches shooting distance.

Table 4.3. *Positive of lead, antimony, copper, and nitroglycerin calls above the threshold for the shooting distance calibration samples by shooting distance and overall analytes in the 30 bullet hole samples.*

Calibration Distances / Analytes	Pb	Sb	Cu	NG
Contact (n=6)	6 (100%)	2 (33%)	6 (100%)	6 (100%)
6 Inches (n=6)	6 (100%)	1 (16%)	6 (100%)	6 (100%)
12 Inches (n=6)	6 (100%)	1 (16%)	6 (100%)	6 (100%)
24 Inches (n=6)	6 (100%)	0 (0%)	6 (100%)	5 (83%)
36 Inches (n=6)	6 (100%)	0 (0%)	6 (100%)	0 (0%)
Total (N=30)	30 (100%)	4 (13%)	30 (100%)	23 (76%)

Various distances were tested that were blind to the analyst for different populations of fabric substrates, including white, colored, patterned, and blood stained, which could interfere with the recognition of bullet holes during investigations. **Figure 4.3** provides examples of voltammograms from white and colored fabric that were positive for GSR compared to the substrate controls taken from the blank unfired fabric used as true negative samples. A table of the complete positive call findings for the white and colored/patterned is shown in **Table 4.4**. The white and colored fabric bullet hole results were similar, where lead and copper were found in 100% of samples. Antimony was found in 8% of the colored and patterned samples. Additionally, nitroglycerin presence was similar at 70% and 88% reported in the white and colored populations, respectively.
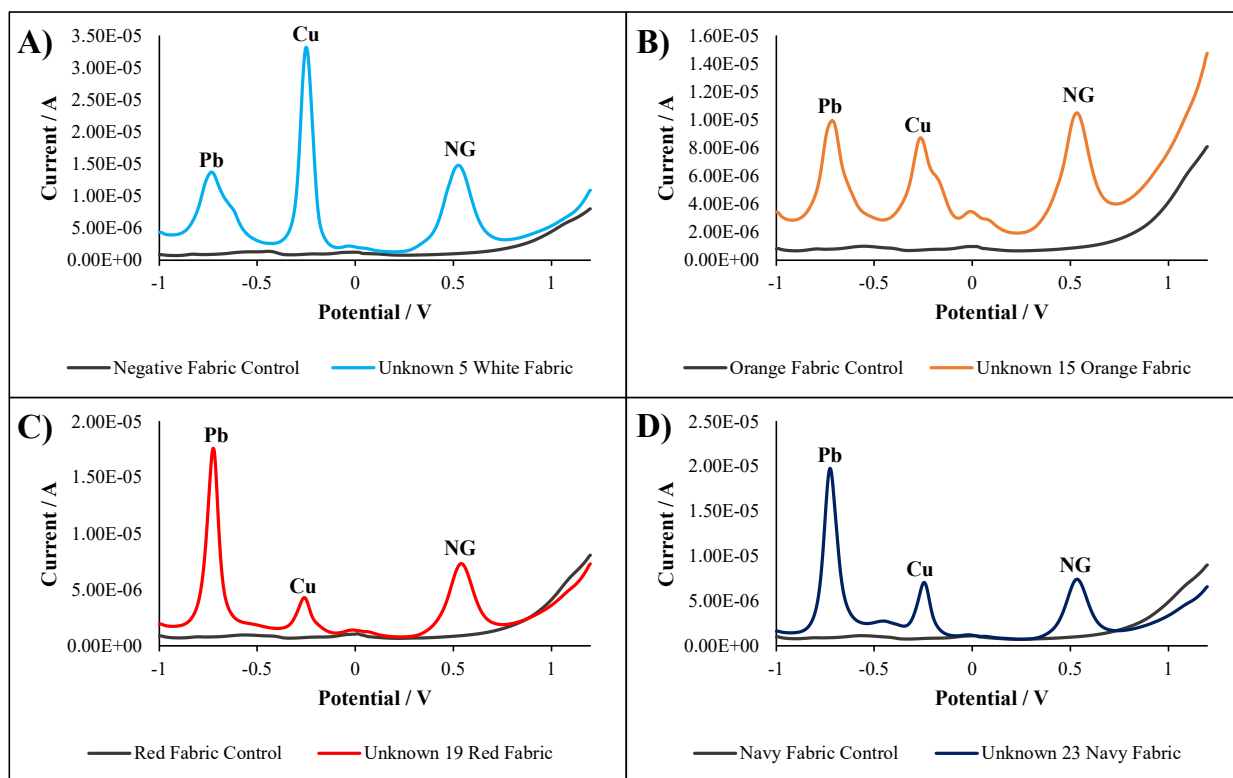
Figure 4.3. *Example voltammograms from the A) white, B) orange, C) red, and D) navy unknown bullet hole sampled fabric with positive calls for lead, copper, and nitroglycerin.*

Table 4.4. *Positive lead, antimony, copper, and nitroglycerin calls above the threshold for the white and colored bullet hole samples by electrochemical analysis.*

Positive Counts above Average Lowest Calibrator				
Populations/ Analytes	Pb	Sb	Cu	NG
White Fabric (N=10)	10 (100%)	0 (0%)	10 (100%)	7 (70%)
Colored Fabric (N=25)	25 (100%)	2 (8%)	25 (100%)	22 (88%)

Similarly, the bloodstained fabric was investigated compared to pristine white fabric bullet hole samples to assess any interferences from the biological matrix. In the bloodstained substrate control, there was a peak at approximately +0.60 V which is visible in **Figure 4.4**. Nevertheless, this did not interfere with the detection of nitroglycerin based on the peak potential and a positive identification was still accomplished in the bloodstained samples. Interestingly, 100% of the bloodstained and non-bloodstained fabrics were positive for lead. All non-bloodstained substrates were positive for copper while it was not seen in bloodstained samples subset. In regard to OGSR analytes, nitroglycerin was identified in 90% of the bloodstained and non-bloodstained fabrics.

The missed identification was within the blood-stained samples (**Table 4.5**). Overall, the blood had no interference and GSR could be characterized by electrochemistry.
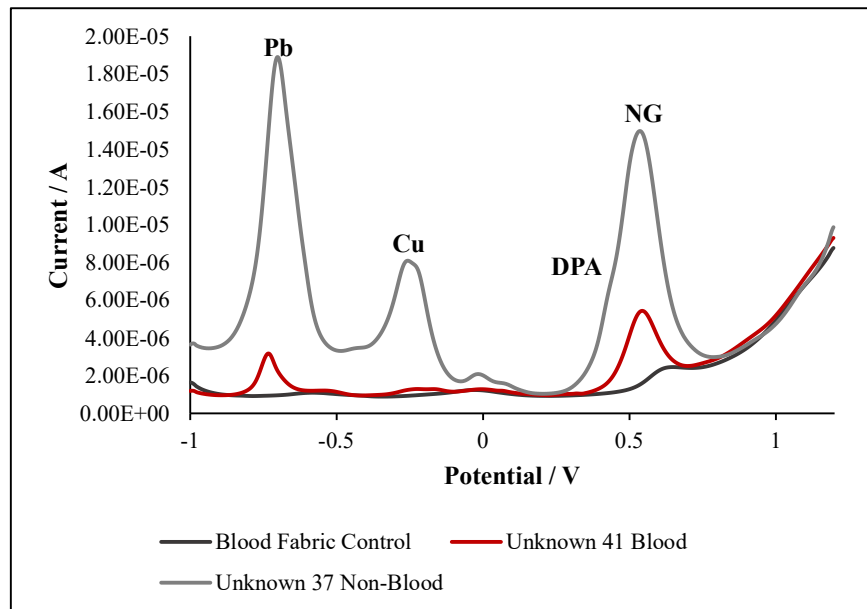
Figure 4.4. *Example voltammograms from the bloodstained (red trace) and non-bloodstained (gray trace) unknown bullet hole sampled fabric with positive calls for lead, copper, and nitroglycerin.*

Table 4.5. *Positive lead, copper, and nitroglycerin calls above the threshold for the bloodstained and non-bloodstained bullet hole samples by electrochemical analysis.*

Populations/ Analytes	Pb	Cu	NG
Non-Bloodstained (N=5)	5 (100%)	5 (100%)	5 (100%)
Bloodstained (N=5)	5 (100%)	0 (0%)	4 (80%)
Total (N=10)	10 (100%)	5 (50%)	9 (90%)

While GSR was identified via thresholds, the screening of bullet holes was not called positive unless two or more analytes were present in a single sample. A true positive sample could be a combination of two IGSR analytes or an IGSR and OGSR analyte being present above the thresholds. Negative samples tested were the unfired substrates sampled and analyzed by electrochemistry. A table of the performance measures for the unknown distance bullet hole samples is provided in **Table 4.6.** The white and colored fabrics had excellent performance with 100% accuracy. The bloodstained population resulted in 1 false-negative call; however, 95% accuracy was still achieved. Considering all 45 fabric unknowns, the electrochemical method was 98% accurate in identifying bullet holes for GSR on various fabric substrates. Completion of the

first task in this objective demonstrates how electrochemical detection is fit for the identification of bullet holes with no observed interference from complex fabric materials as a fast-screening method for this application.

Table 4.6. Performance measures of the unknown distance fabric bullet hole samples for white, colored, and bloodstained subsets.

Performance Measures			
	White Fabric (N=10)	**Colored Fabric (N=25)**	**Bloody (N=10)**
True Positives (Sensitivity)	10 (100%)	25 (100%)	9 (90%)
False Negatives	0 (0%)	0 (0%)	1 (10%)
True Negatives (Specificity)	8 (100%)		
False Positives	0 (0%)		
Accuracy	100%	100%	95%
Overall Accuracy	98%		

4.3.2   Bullet hole Identification on Hard Substrates

Evaluating the robustness of the electrochemical method would be unrealistic on fabric alone since an authentic shooting-related crime may involve other common substrates that could be questioned at a crime scene. For this proof of concept, the hard substrates tested by electrochemistry consisted of wood and drywall. These materials were chosen to represent difficult or immovable objects like walls or furniture which may present complex or untenable surfaces for administering testing for suspected bullet holes at the crime scene or laboratory settings by traditional methods.

The sampling method as described in *Section 4.2.4* was unchanged in performing GSR collection from around the bullet wipe on the substrates. Square-wave anodic stripping voltammetry resulted in the voltammograms for the 14 samples and negative controls which were taken from substrates that were not fired at. **Figure 4.5** provides examples of wood and drywall voltammograms that were positive for lead, copper, and nitroglycerin. In the wood negative control, an oxidation peak at approximately +0.37 V was observed and was thought to be from the cellulose composition of wood, which is electroactive and has been studied in the past.[104,105] While this oxidation potential from wood was close to nitroglycerin, this was not an interference where the current from the wood background was much less than for the detection of nitroglycerin.
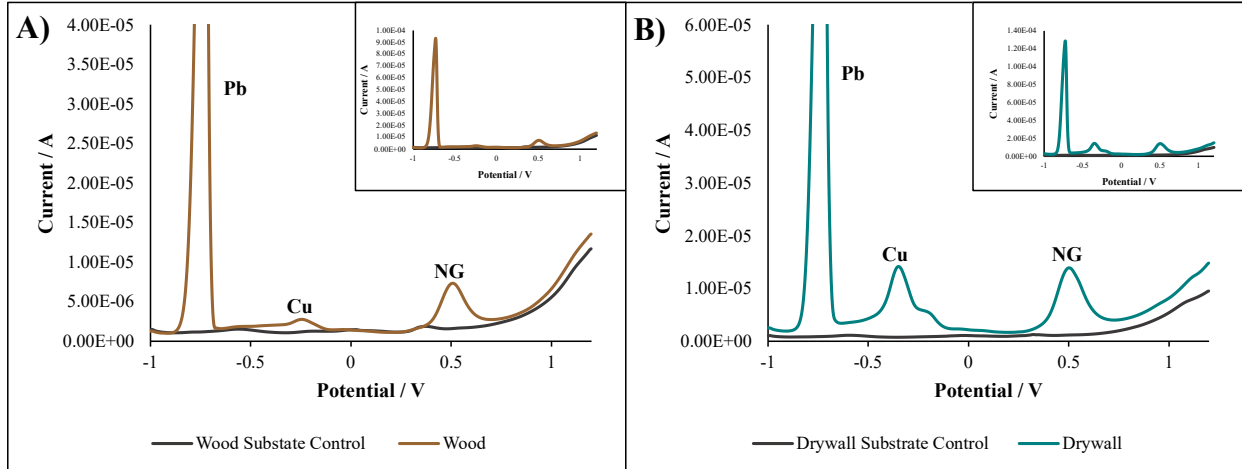
Figure 4.5. *Example voltammograms from A) wood and B) drywall bullet hole samples with positive calls for lead, copper, and nitroglycerin*

For 14 hard substrates, analyte detection above the average lowest calibrator current identified the presence of lead, antimony, copper, and nitroglycerin. Accuracy of calling positive and negative sample was defined by the presence of two or more GSR analytes. Lead and nitroglycerin were detected in all samples, with copper slightly less at 71% (**Table 4.7**). Interestingly, the 3 calls for antimony were detected only in the drywall samples. **Table 4.8** exhibits the performance measures for electrochemical detection for wood and drywall which demonstrated 100% accuracy in determining the presence of GSR.

Table 4.7. *Positive lead, antimony, copper, and nitroglycerin calls above the threshold for the wood and drywall bullet hole samples by electrochemical analysis.*

Positive Counts above Average Lowest Calibrator				
Populations/ Analytes	**Pb**	**Sb**	**Cu**	**NG**
Hard Substrates (N=14)	14 (100%)	3 (21%)	9 (64%)	14 (100%)

Table 4.8. *Performance measures of the bullet hole samples for wood and drywall substrates.*

Performance Measures for Hard Substrates	
	Hard Substrates (N=14)
True Positives (Sensitivity)	14 (100%)
False Negatives	0 (0%)
True Negatives (Specificity)	2 (100%)
False Positives	0 (0%)
Accuracy	100%

4.3.3 Confirmation of OGSR by Liquid Chromatography tandem Mass Spectrometry

As confirmation of the electrochemical technique for OGSR, LC-MS/MS was utilized to analyze all the unknown fabric and hard substrates samples. The purpose of LC-MS/MS analysis was to provide confirmatory OGSR detection and application of the previously validated method by Feeney et al to bullet hole identification.[98–100] The confirmation of OGSR offers higher confidence in the identification of bullet holes due to incorporation of a wider panel of analytes which are more specific to a firearm-related discharge event. The samples underwent the extraction and filtering protocol for OGSR analysis described in *Section 4.2.8*. Electrochemistry and LC-MS/MS techniques are complementary for OGSR detection due to instrument-specific analyte detection and different limits of detection, which are compared in **Table 4.9**. Note, that nitroglycerin can be detected by LC-MS/MS analysis in negative mode, which was not used in this research.

Table 4.9. *Comparison of limits of detection in part-per-billion for electrochemical and LC-MS/MS detection of OGSR analytes where N/A denotes non-detectable by the method.*

Analyte	Electrochemistry / ppb	LC-MS/MS / ppb
2,4-dinitrotoluene	200	N/A
Ethyl centralite	450	1.0
Methyl centralite	N/A	0.3
Nitroglycerin	147	N/A
Diphenylamine	462	3.4
2-Nitrodiphenylamine	557	2.7
4-Nitrodiphenylamine	254	3.0
Akardite II	842	0.3

By LC-MS/MS analysis, 68% of samples were positive for two or more OGSR analytes, and 78% were positive for at least one OGSR analyte. Negative controls were extracted and analyzed which demonstrated no interferences with LC-MS/MS detection. Samples not positive by LC-MS/MS analysis have various factors such as variation of GSR distribution depending on shooting distance, ammunition manufacturing variation, and natural variation in GSR distribution on samples. The nature of bullet holes indicates more IGSR being present closer to the bullet wipe than OGSR due

to coming into direct contact with the projectile. It was noticed that samples that did not identify nitroglycerin by electrochemistry saw little to no OGSR analytes by mass spectrometry analysis as well.

In combination with electrochemical detection, a comparison between all the IGSR and OGSR analytes detected between instruments is summarized in **Table 4.10**. In this table, the analytes were assessed for each instrument, positives by electrochemistry are denoted in yellow, LC-MS/MS positives are represented by blue, and positive by both methods is represented by a yellow/blue gradient. Overall, both methods demonstrated the capability of detecting OGSR from bullet holes. When taking both methods into consideration, the overall accuracy of combining analytical techniques resulted in 100% of samples being called true positives for at least two IGSR or OGSR compounds present.

4.4 Conclusions

Bullet hole identification can be difficult to ascertain at a crime scene due to a lack of knowledge of the environmental conditions beforehand. This challenge requires a rapid screening method to provide confidence on whether a suspected bullet hole is positive for gunshot residue. In addition, practices currently in use for nitrite and lead detection have high limits of detection, lack of specificity, and complicated application on large or immovable objects in the field. This study aimed at targeting these needs for the development of a fast collection and screening method which can provide simultaneous detection of IGSR and OGSR analytes with application to various materials and interferences that can be encountered in authentic casework. In addition, the confirmation of OGSR in bullet hole applications by LC-MS/MS provides complimentary OGSR information and increases the reliability of results of the electrochemical detection.

The developed sampling method utilizing SEM aluminum stubs and carbon adhesive tape affords an easily carried out collection method from the suspected bullet hole to be analyzed at the laboratory and fits current collection practices for other methods like SEM-EDS. Additionally, the collection stub offers the potential for less contamination and the ability to collect controls from the target material away from the suspected bullet hole similar to ignitable liquid analysis. The collection method provided an excellent collection of GSR in under a minute, saving crime scene investigators time when processing a shooting-related crime scene.

Little sample preparation is needed for electrochemical analysis, where a sample can be extracted and analyzed in approximately five minutes. The sample preparation is less involved than the conventional methods which require the use of hazardous chemicals and are destructive to the gunshot residue patterns if a further analysis is needed. The electrochemical method allows for minimal destruction of the sample and a faster and safer analysis method.

The electrochemical analysis offers a superior assessment of bullet hole identification to current colorimetric practices due to the increased sensitivity and specificity for simultaneous multi-IGSR and OGSR detection. The findings of this study demonstrate the fit-for-purpose of the electrochemical method, demonstrated with various materials like fabric, wood, and drywall, as well as potential interferences like bloodstained fabric. It was shown that 98% of fabric samples and 100% of hard substrates were determined to be positive for GSR by electrochemical detection. These conclusions, in addition to the confirmation of OGSR by LC-MS/MS, provide the foundation for practical use of these methods in shooting investigation to help with rapid identification of suspected bullet holes and provide leading information to investigators.

Table 4.10. *Comparison of positive analytes by electrochemical (yellow) and LC-MS/MS (blue) detection of IGSR and OGSR analytes for various fabrics and hard substrates and positive samples by both instruments (blue/yellow gradient).*

| Distance | Sample ID | Electrochemistry | | | | LC-M/MS | | | | | Positive |
		Pb	Sb	Cu	NG	DPA	EC	AK II	4-NDPA	2-NDPA	for GSR
Unknown 1	White	Y		Y	Y	B	B	B	B	B	both
Unknown 2	White	Y		Y	Y	B	B	B	B	B	both
Unknown 3	White	Y		Y	Y	B	B		B	B	both
Unknown 4	White	Y		Y	Y	B	B	B	B	B	both
Unknown 5	White	Y		Y	Y	B	B	B	B	B	both
Unknown 6	White	Y		Y		B	B	B	B	B	both
Unknown 7	White	Y		Y	Y						Y
Unknown 8	White	Y		Y							Y
Unknown 9	White	Y		Y							Y
Unknown 10	White	Y		Y		B					Y
Unknown 11	Orange	Y		Y	Y	B					Y
Unknown 12	Orange	Y		Y		B					Y
Unknown 13	Orange	Y		Y		B					Y
Unknown 14	Orange	Y		Y		B					Y
Unknown 15	Orange	Y		Y		B	B	B	B	B	both
Unknown 16	Red	Y		Y							Y
Unknown 17	Red	Y		Y							Y
Unknown 18	Red	Y		Y		B	B		B		both
Unknown 19	Red	Y		Y	Y	B	B	B	B	B	both
Unknown 20	Red	Y		Y	Y	B	B	B	B	B	both
Unknown 21	Navy	Y		Y	Y	B	B	B	B	B	both
Unknown 22	Navy	Y		Y	Y	B	B	B	B	B	both
Unknown 23	Navy	Y		Y	Y	B	B	B	B	B	both
Unknown 24	Navy	Y		Y	Y	B	B		B		both
Unknown 25	Navy	Y	Y	Y	Y	B	B	B	B	B	both
Unknown 26	Dark Pattern	Y		Y	Y	B					Y
Unknown 27	Dark Pattern	Y		Y	Y						Y
Unknown 28	Dark Pattern	Y		Y		B					Y
Unknown 29	Dark Pattern	Y		Y		B			B		both
Unknown 30	Dark Pattern	Y		Y							Y
Unknown 31	Light Pattern	Y		Y	Y	B					Y
Unknown 32	Light Pattern	Y		Y	Y						Y
Unknown 33	Light Pattern	Y		Y	Y						Y
Unknown 34	Light Pattern	Y		Y	Y		B				both
Unknown 35	Light Pattern	Y	Y	Y	Y						Y
Unknown 36	Blood	Y			Y	B	B	B	B	B	both
Unknown 37	Blood	Y			Y	B	B	B	B	B	both
Unknown 38	Blood	Y			Y	B	B	B	B	B	both
Unknown 39	Blood	Y			Y	B	B	B	B	B	both
Unknown 40	Blood	Y			Y	B	B	B	B	B	B
Unknown 41	Non-blood	Y		Y	Y	B	B	B	B	B	both
Unknown 42	Non-blood	Y		Y	Y	B	B	B	B	B	both
Unknown 43	Non-blood	Y		Y	Y	B			B	B	both
Unknown 44	Non-blood	Y		Y	Y	B	B	B	B	B	both
Unknown 45	Non-blood	Y		Y	Y						Y
Unknown 46	Wood					B	B	B		B	B
Unknown 47	Wood	Y		Y	Y	B	B	B	B	B	both
Unknown 48	Wood	Y		Y	Y	B	B	B	B	B	both
Unknown 49	Wood	Y		Y	Y	B	B	B	B		both
Unknown 50	Wood	Y		Y	Y	B	B	B	B		both
Unknown 51	Wood	Y		Y	Y	B	B	B	B	B	both
Unknown 52	Wood	Y		Y	Y	B	B	B	B		both
Unknown 53	Drywall	Y			Y	B	B	B	B	B	both
Unknown 54	Drywall	Y			Y	B	B	B	B	B	both
Unknown 55	Drywall	Y			Y	B	B	B	B	B	both
Unknown 56	Drywall	Y	Y		Y	B	B	B	B	B	both
Unknown 57	Drywall	Y	Y		Y	B	B	B	B	B	both
Unknown 58	Drywall	Y		Y	Y	B	B	B	B	B	both
Unknown 59	Drywall	Y		Y	Y	B	B	B	B	B	both

V. CHAPTER 5: COMPARISON OF BENCHTOP AND PORTABLE POTENTIOSTATS FOR GSR DETECTION

5.1 Overview

This chapter proposes the application of portable electrochemical instrumentation as a capable and reliable on-site screening method for the analysis of inorganic and organic gunshot residue detection. This study investigated a comparison between benchtop and portable potentiostats for the screening of GSR via the assessment of standards and evaluation of authentic non-shooter and shooter populations. Seven GSR analytes were monitored (lead, antimony, copper, 2,4-dinitrotoluene, diphenylamine, nitroglycerin, and ethyl centralite) using electrochemical methods in combination with screen-printed carbon electrodes as a rapid, small, and cost-efficient platform. Typical SEM aluminum stubs were used to collect from the left and right individuals followed by extraction for the IGSR and OGSR and analyzed using square-wave anodic stripping voltammetry electrochemical method. The assessment of the two potentiostat began with figures of merit including potential windows, linearity, R^2, repeatability, and limits of detection and performance of positive quality controls IGSR and OGSR mixtures. Authentic sample evaluation of the non-shooter population consisted of 200 hand samples where the shooter population was comprised of 150 hand samples split into two subsets, 100 leaded primer ammunition samples and 50 lead-free primer ammunition samples. Evaluation included percent positives, data visualization, and performance measures of the benchtop and portable instruments which resulted in accuracies of 95.7% and 96.5%, respectively (**Figure 5.1**). The findings of the study indicates that electrochemical methods provide a fast, sensitive, and selective for GSR and reliability of the portable instrument were the potentiostats resulted were comparable to the benchtop instruments. The conclusions made demonstrate a proof-of-concept for shifting the methods from research setting to implementation in forensic laboratories as a practical, inexpensive, on-site screening method to aid with backlog reduction, provide investigative leads, and workflow and decision making at the crime scene and laboratory.

The methods, results, and conclusions of this chapter are an adaptation from:

Dalzell, K. A.; Ott, C. E.; Trejos, T.; Arroyo, L. E. Comparison of Portable and Benchtop Electrochemical Instruments for Detection of Inorganic and Organic Gunshot Residues in Authentic Shooter Samples. *J. Forensic Sci.* **2022**. https://doi.org/10.1111/1556-4029.15049.

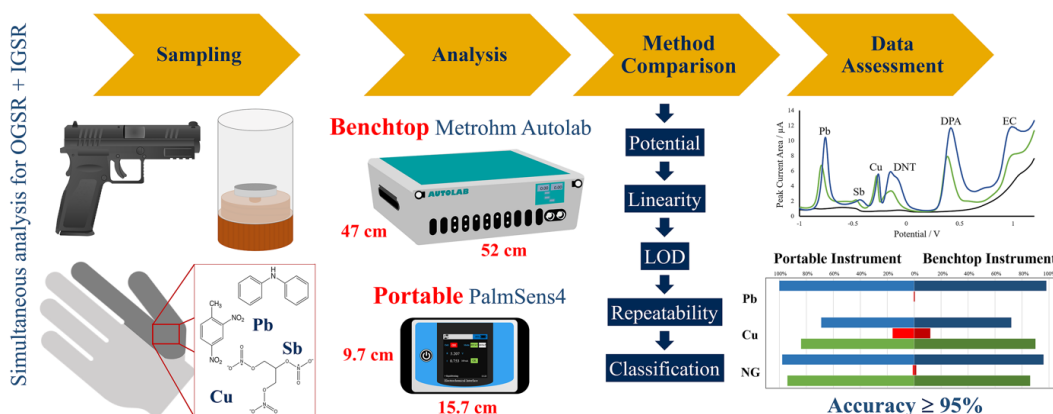The full, copyrighted article can be found in Appendix V.

Figure 5.1. *Overview of the analytical scheme applied for the collection, comparison, and assessment of portable versus benchtop electrochemical instruments for authentic GSR samples in Chapter 5.*

5.2 Materials and Methods

5.2.1 Reagents and Standards

Extractions were achieved using both acetate buffer prepared to a pH of 4.0 using sodium acetate anhydrous and glacial acetic acid (HPLC grade) and acetonitrile (Optima®) obtained from Fisher Scientific (Fair Lawn, NJ). Ultrapure water (≥18.2 MΩ) was provided by a Millipore Direct-Q® UV water purification system (Billerica, MA). Analyte standards were purchased as follows: 1,3-diethyl-1,3-diphenylurea 99% (ethyl centralite) from Sigma-Aldrich (St. Louis, MO); diphenylamine from SPEX Certiprep® (Metuchen, NJ); lead, copper, and antimony from Ultra Scientific® (Kingstown, RI); and nitroglycerin and 2,4-dinitrotoluene from AccuStandard® (New Haven, CT). Nitrogen was purchased from Matheson Tri-Gas, Inc. (Irving, TX).

Quality controls were prepared prior to authentic sample analysis using two mixtures of the IGSR and OGSR analytes in acetate buffer, where the first was a solution consisting of 2 ppm Pb, 0.2

ppm Cu, 8 ppm Sb, and 10 ppm of OGSR (2,4-DNT, DPA or NG, and EC). The second solution was the same; however, DPA was replaced with NG to evaluate their peak potential since peak resolution is difficult to achieve when DPA and NG are in solution together. These two solutions were referred to as the 10 ppm NG QC and 10 ppm DPA QC. Then 1:4 dilutions were made for both to generate a mixture of 2.5 ppm of OGSR analytes and 0.5 ppm Pb, 0.05 ppm Cu, and 2 ppm Sb for the IGSR analytes. Other controls run prior to analysis were a tailor-made pGSR standard, negative substrate control, and reagent control to ensure the quality performance of the instruments.[101]

5.2.2   Electrodes and Instrumentation

Screen-printed carbon electrodes (SPCEs) were purchased from Metrohm DropSens USA, Inc. in the DRP-110 format containing carbon working and counter electrodes and a pseudo-silver reference electrode. Control over pH was performed using a Mettler Toledo FiveEasy pH meter (Columbus, OH). The benchtop potentiostat used was an Autolab PGSTAT128N with NOVA software version 2.1.4 from Metrohm USA, Inc. (Riverview, FL). The portable potentiostat was a PalmSens4 with PSTrace software version 5.8 (Randhoeve, Netherlands).

5.2.3   Sample Collection

Samples were collected from the hands of individuals as described previously by our group and following Institutional Review Board (IRB) protocol #1506706336.[11,106] Following standard protocol for GSR collection, aluminum SEM stubs with carbon adhesive tape (Ted Pella, Inc. Redding, CA) were used as the collection substrate. Both shooter and background (non-shooter) samples were collected using a total of two stubs: one stub for the palm and back of the right hand and one stub for the palm and back of the left hand. Non-shooter background samples were collected from individuals on the West Virginia University (WVU) campus who had not fired or handled a firearm, fireworks, or participated in activities that could lead to GSR over the previous 24 hours. Shooter samples were collected from the hands of shooters after firing 5 shots in the WVU ballistics laboratory using a Springfield XD firearm with Remington Range and reloaded Specialty Winchester 9 mm ammunition for leaded samples and reloaded Fiocchi ammunition for lead-free samples. Shooters washed their hands with soap and water between firing events. A total

of 100 leaded shooter samples, 50 lead-free shooter samples, and 200 background samples were collected for analysis.

5.2.4   Sample Preparation

All measurements were carried out in 0.1 M acetate buffer pH 4.0 using SPCEs. Extraction of the sampling stub surface was achieved in two portions: extraction of IGSR and extraction of OGSR. The IGSR extraction was achieved by placing 50 µL of acetate buffer on the stub surface and using the pipette to move the drop around the entire surface and allowing it to sit for approximately 10 seconds. This drop was transferred to a microfuge tube and saved. Then, a 50 µL drop of acetonitrile was added to cover the entire surface, allowed to sit for approximately 10 seconds, and then pipetted up and down prior to transfer to a second microfuge tube. This process was repeated for the GSR stub from the other hand simultaneously and a total of 100 µL for each extraction aliquot was placed in their respective tubes. Then the organic fraction was dried down under nitrogen and reconstituted using the aqueous portion prior to electrochemical analysis. Analysis was then conducted using 50 µL of the reconstituted sample for the benchtop instrumental method and the remaining 50 µL for the portable instrumental method. **Figure 5.2** demonstrates the sample preparation process.
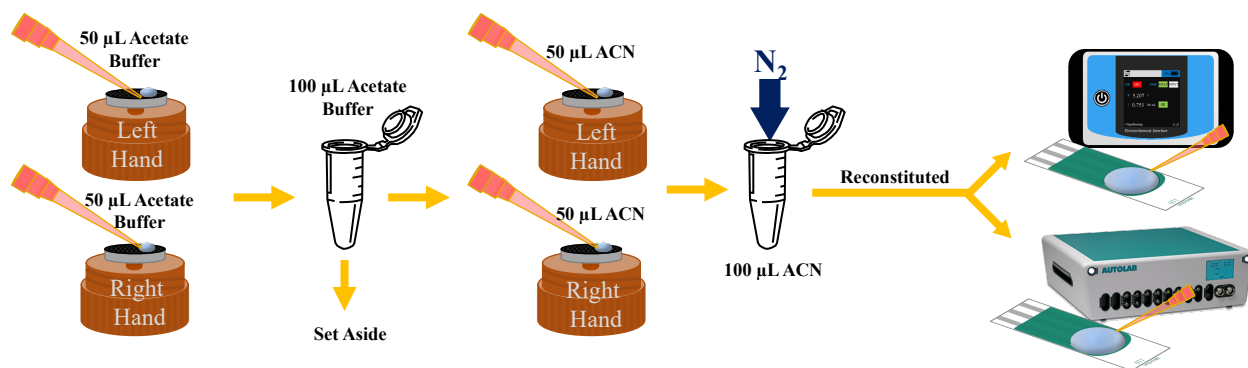
Figure 5.2. *GSR extraction procedure to assess the same samples by two methods: benchtop and portable potentiostats.*

5.2.5   Square-wave Anodic Stripping Voltammetry (SWASV) Method

Electrochemical analysis of GSR was achieved through the application of a deposition potential at -950 mV for 120 seconds. Then the potential was scanned between -1000 mV and +1200 mV using a square-wave procedure. The additional parameters of frequency, modulation amplitude, and step potential were optimized for the portable instrument using a response surface design. **Table 5.1**

provides the comparison between the parameters used for the benchtop and portable instrument. Quality control (QC) samples were also used to assess the performance of the method and included a buffer blank, negative stub control, positive stub control, and several mixtures of GSR compounds at varying concentrations.

Table 5.1. *SWASV parameters for the analysis of GSR using both a benchtop potentiostat and a field-portable potentiostat.*

Parameter	Benchtop Instrument	Portable Instrument
Deposition Time	120 s	120 s
Deposition Potential	-0.95 V	-0.95 V
Start Potential	-1.0 V	-1.0 V
End Potential	1.2 V	1.2 V
Potential Step	0.004 V	0.005 V
Amplitude	0.025 V	0.025 V
Frequency	8 Hz	11 Hz

5.2.6   Data Analysis

The Nova 2.1.4 and PSTrace 5.8 software were used for peak integration and exported for data analysis in Excel 16 (version 16.56, Microsoft Corporation). The critical threshold method, detailed in Ott et al., was used for classification and assessment of the results.[11] The critical thresholds used were the same as in Ott et al. for all samples and were Pb: 1.59×10^{-8} A×V, Cu: 3.33×10^{-8} A×V, NG: 4.28×10^{-9} A×V as assessed based on the background data sets previously collected using the same Metrohm Autolab potentiostat.

JMP Pro (version 16.0.0, SAS Institute) was used to carry out significance testing for standards and authentic samples using t-tests, where the assumption of normality and constant variance were evaluated, and the test was adjusted accordingly. Test adjustments included one-tailed versus two-tailed t-tests, unequal versus equal variance, univariate versus multivariate, and the sample sizes and power of the test (at alpha 0.05). When normality was not met, a nonparametric test was performed.

5.3 Results and Discussion

The motivation of this study was to demonstrate the reliability of electrochemical sensors as a fast and accurate screening tools with efficient and rugged portable instrumentation comparable to laboratory benchtop potentiostats. The first objective involved the application and optimization of the previously developed method for simultaneous detection of IGSR and OGSR on the portable PalmSens4 potentiostat and evaluation of the performance in comparison to the benchtop Autolab, described in the Comparison of Analytical Performance Measures section. The second objective is discussed in the Comparison of Authentic Samples section detailing an assessment of the detection capabilities of both instruments and the estimated error rates and accuracy using authentic populations of non-shooter background (n=200), leaded shooter (n=100), and lead-free shooter (n=50) samples.

5.3.1   Comparison of Analytical Performance Measures

The Metrohm Autolab potentiostat has been assessed in previous work for the electrochemical parameters, performance characteristics, and a large population of authentic samples.[11] Prior to starting the comparison study, the square-wave voltammetry method was optimized for the PalmSens4 using a Box Behnken surface response design and the JMP software. The design used 3 factors: frequency, amplitude, and step, each with 3 levels. A total of 15 experiments were analyzed using the 2.5 ppm DPA quality control. As a result of this optimization process, the potential step was increased to 0.005 V and the frequency was increased to 11 Hz for the portable device. The square-wave anodic stripping voltammetry method (SWASV) demonstrated no other differences between optimal parameters for the portable or benchtop instruments (Table 5.1).

Following method optimization, the individual GSR analytes were tested to demonstrate any variations between oxidation potentials, peak shape, and peak resolution, which are critical for the correct identification of IGSR elements and OGSR compounds of interest. The comparison of performance characteristics obtained for our portable instrument was completed for the GSR analyte panel including lead (Pb), copper (Cu), antimony (Sb), 2,4-dinitrotoluene (2,4-DNT), diphenylamine (DPA), nitroglycerin (NG), and ethyl centralite (EC). The performance characteristics of interest for individual analytes were oxidation potential, linear range, coefficient of correlation (R2), repeatability, and limit of detection (LOD). Calibration curves were prepared

via serial dilution to measure the electrochemical response and repeated in triplicate. The extracted current measurements for analysis used peak current area or peak current height depending on the analyte of interest. Limits of detection were calculated using 3 times the standard deviation of the lowest calibrator divided by the average slope of the calibration curves.[107,108] The results of the analytical performance tests can be seen in **Table 5.2** for the benchtop Metrohm Autolab and in **Table 5.3** for the portable PalmSens4.

Peak potential windows showed significant differences between potentiostats, although some potential windows overlapped. The differences in square-wave parameters or conditions affected analyte oxidation potentials, although copper's potential showed no significant difference between the portable and benchtop potentiostats (two–tailed t-test, p=0.0918). All other GSR analytes demonstrated differences between the benchtop and portable potential windows using two tailed t-tests with p-values less than 0.0418. It is important to note; however, that these differences were generally small and ranged between approximately 10 mV and 70 mV. Slight differences were demonstrated in the sensitivity of the two instruments for the GSR analysis and can be seen in the remaining parameters. The linear range of several analytes was changed as a result; however, the linearity of the constructed calibration curves was excellent using both instruments with adequate residual plots and R^2 values over 0.98 for the benchtop and 0.99 for the portable potentiostat, with the exception of ethyl centralite (0.92) due to oxidation of the analyte near the edge of the electrode potential window.

The largest difference between the two instruments was the repeatability. For the benchtop potentiostat, repeatability for all analytes was below 10%. However, the portable instrument demonstrated values under 16% for IGSR, with lead and copper below 5%, but for the OGSR analytes, repeatability ranged from 14 to 33%, significantly higher than observed for the benchtop instrument. This difference is attributed to the different specifications of the instruments or variation in the SWASV parameters between instruments.[109,110] It is important to note that since quantitative measurements are not performed in this qualitative screening, the effect is not as critical.

The final difference noted was within the limit of detection for the analytes. Although generally comparable, various differences across the two instruments can be observed. Overall, there was no

trend related to IGSR or OGSR in terms of improvements or decreases to the calculated LOD values. For example, the LODs for DNT, DPA, Cu, and Sb demonstrated improvements with the portable instrument (one sided t-test where Prob < t, p-values of 0.0005, <0.0001, 0.0007, and 0.0109, respectively). The alternative can be said for Pb and NG, which demonstrated inferior sensitivity than the benchtop unit where the one-sided t-test (Prob > t) resulted in p-values <0.001 and 0.0074, respectively. The only analyte with a comparable LOD value was EC with a p-value of 0.1314 (Prob > t). Overall, the LODs were in the sub/low part-per-million range with a majority of analyte LOD values less than 0.300 µg/mL and all under 0.600 µg/mL. While various trends and differences were seen in the analytical performance measures, the detection limit windows for lead, copper, and nitroglycerin were within ranges typically observed in authentic shooter samples, while the other analytes are typically detected at levels below the LOD values for these electrochemical methods, although some instances of DNT were observed.[11,99] However, the true measure of the performance of each instrument relies on the assessment and comparison of authentic samples in order to screen for GSR analytes, as well as the assessment of quality controls.

Table 5.2. *Performance characteristics calculated based on the Metrohm Autolab benchtop instrument.*[11]

IGSR	Potential (V)	Linear Range (µg/mL)	R²	Repeatability (%RSD, n=3)	LOD (µg/mL)
Lead	-0.784 ± 0.035	0.10 to 2.0	0.999	4.4	0.055 ± 0.01
Antimony	-0.401 ± 0.027	0.75 to 7.5	0.986	10	0.183 ± 0.07
Copper	-0.292 ± 0.053	0.05 to 1.0	0.990	2.3	0.012 ± 0.001
OGSR	Potential (V)	Linear Range (µg/mL)	R²	Repeatability (%RSD, n=3)	LOD (µg/mL)
2,4-Dinitrotoluene*	−0.132 ± 0.032	1.0 to 20	0.982	5.6	0.200 ± 0.03
Diphenylamine	0.406 ± 0.018	1.0 to 8.0	0.987	6.2	0.462 ± 0.06
Nitroglycerin	0.509 ± 0.010	0.50 to 8.0	0.998	10	0.147 ± 0.08
Ethyl centralite	1.03 ± 0.045	0.50 to 8.0	0.998	8.0	0.450 ± 0.09

* 2,4-DNT was assessed as peak current height, whereas all other analytes were assessed as peak current area.

Table 5.3. *Performance characteristics calculated based on the PalmSens4 portable instrument.*

IGSR	Potential (V)	Linear Range (µg/mL)	R^2	Repeatability (%RSD, n=3)	LOD (µg/mL)
Lead	-0.790 ± 0.017	0.10 to 2.0	0.995	4.6	0.278 ± 0.13
Antimony*	-0.391 ± 0.017	0.1 to 2	0.992	16	0.235 ± 0.39
Copper	-0.317 ± 0.021	0.05 to 1.0	0.999	4.2	0.009 ± 0.004

OGSR	Potential (V)	Linear Range (µg/mL)	R^2	Repeatability (%RSD, n=3)	LOD (µg/mL)
2,4-Dinitrotoluene*	−0.148 ± 0.025	1.0 to 10	0.998	14	0.061 ± 0.09
Diphenylamine	0.417 ± 0.008	1.0 to 8.0	0.999	29	0.152 ± 0.44
Nitroglycerin	0.523 ± 0.007	0.50 to 8.0	0.995	33	0.438 ± 1.46
Ethyl centralite	0.945 ± 0.004	2.0 to 10	0.926	30	0.566 ± 1.67

* Antimony and 2,4-DNT were assessed as peak current height, whereas all other analytes were assessed as peak current area.

Quality controls were run with these screening methods to ensure the proper functioning of the instrument and that there was no contamination present within any steps of the analysis process. The electrochemical quality controls were analyzed on both instruments and overlaid for comparison purposes. **Figure 5.3** demonstrates the voltammogram comparison of the four quality control mixtures. As suggested by the analytical metrics, the mixture voltammograms were comparable to those obtained using the benchtop potentiostat, with the only differences being in terms of sensitivity and repeatability. In general, peak currents were similar for the majority of analytes; however, one important note is that the method for the portable potentiostat resulted in larger antimony signals for the standards. Based on previous work, it has been shown by our research group that this method is capable of correctly identifying GSR based on lead, copper, and nitroglycerin.
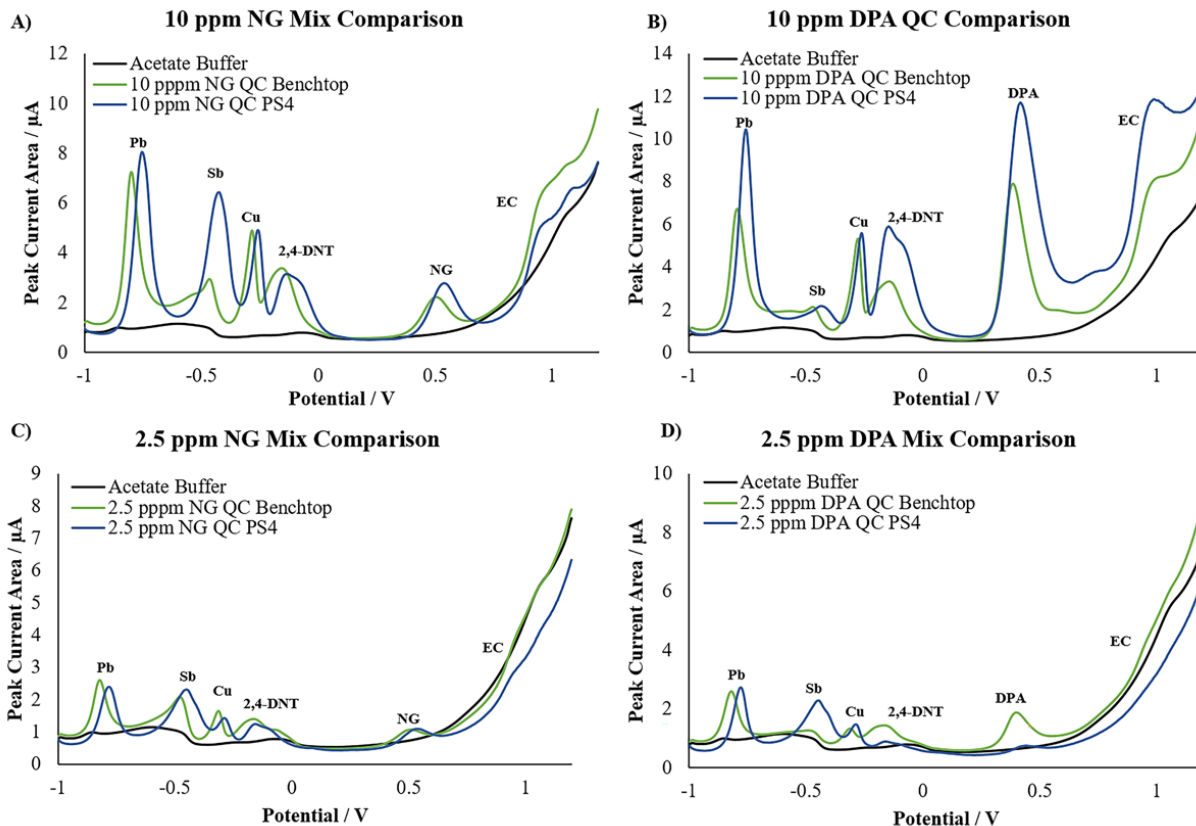
Figure 5.3. *Comparison voltammograms of the quality control mixtures for the A) 10 ppm NG QC, B) 10 ppm DPA QC, C) 2.5 ppm NG QC, and D) 2.5 ppm DPA QC for the portable and benchtop instruments.*

5.3.2 Comparison of Authentic Samples

In this study, a dataset of 350 samples was collected to represent background samples (non-shooter, 200 samples) and authentic shooters (150 samples) consisting of 100 leaded samples and 50 lead-free samples. Each of these samples was analyzed by both the portable and benchtop instruments for direct comparison, which was performed by first assessing the current signals obtained in the voltammogram against the critical threshold values. Critical threshold values were obtained from our previous study using 350 background non-shooter set [11]. The prevalence of each of the three most detected analytes (lead, copper, and nitroglycerin) above the critical threshold values was assessed and can be seen graphically in **Figure 5.4**. As expected, very low instances of lead and nitroglycerin were observed in the background population, with copper levels being the most identified analyte in the samples, at an average of 14% of the background non-shooter samples for both the benchtop and portable instruments. Lead and nitroglycerin were rare in the

background population at averages of 1% and 2.5% for the two instruments. Clearly, the electrochemical profile for background samples is generally absent of GSR markers.

This was in contrast to the leaded shooter samples, where approximately 70% of the samples contained copper. More significantly, an average of 97% of the leaded shooter samples contained nitroglycerin and 99% contained lead. The high prevalence of nitroglycerin demonstrates the significance of detecting OGSR when many other GSR detection methods focus solely on IGSR. In relation to the comparison of the two instruments, it is important to observe that the largest difference in analyte identifications on leaded datasets between the benchtop and portable potentiostats was 3%, where lead and nitroglycerin were separated by 2% or less. **Figure 5.4** shows the direct comparison between both instruments and both populations.
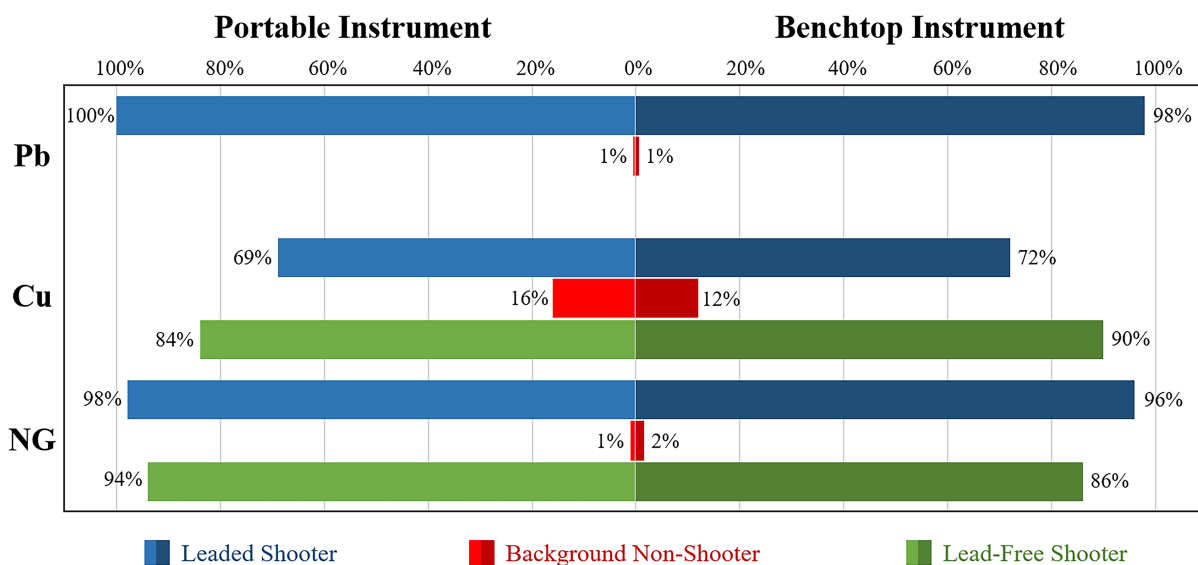

Figure 5.4. *Graphical comparison between the positive analyte identifications from the leaded and lead-free shooter and background populations for both the portable PalmSens4 instrument and benchtop Autolab instrument.*

Additionally, the lead-free population can be seen in green in **Figure 5.4**. Due to the ammunitions being considered as lead-free, lead was not plotted in this figure but can be seen in Appendix IV Figure S5.1. The lead-free ammunition demonstrated difficulty in the proper cycling of the firearm, resulting in problems with the ejection of the cartridge cases, causing the shooters to handle the slide of the firearm and to sometimes reload cartridges that have fallen on the floor of the shooting range. Additionally, the ammunition used was reloaded in-house with lead-free primers; however, the projectiles available were lead bullets that were copper plated. Therefore, it is reasonable to

assume that low-level lead contamination may have arisen from the high heat and pressure needed to propel these projectiles from the firearm in combination with contamination from the range floor itself. This was believed to result in possible lead contamination from the range environment, where an average of 77% of the lead-free samples were positive for lead. However, it is of importance to note that the lead signal size (peak current area) was significantly smaller for the lead-free ammunition than the leaded ammunition, as can be seen in **Figure 5.5** (one-sided t-test, Prob < t, p-value <0.0001 and 0.0005 for the benchtop and portable instruments, respectively). The signals for lead resulting from the lead-free ammunition were significantly smaller and closer to the critical threshold cut-off than the leaded ammunition, providing evidence for possible firearm handling contamination rather than the presence of lead in the lead-free formulation. Memory effect from the barrel is not considered the major contributor, as the firearm barrel and mechanism was cleaned between ammunition types; however, as mentioned previously, low levels of lead may have been introduced during safety procedures during misfires, the range environment, or the projectile. Appendix IV Figures S5.2 and S5.3 provide the box plots for the comparison of copper and nitroglycerin signals between the leaded and lead-free populations, where no significant difference was found (t-test, p-values >0.05). The lead-free shooter samples demonstrated positive copper results in 84% and 90% of samples for the portable and benchtop instruments, respectively. This is in comparison to the leaded samples at an average of 70% positive for copper, demonstrating similar response for leaded and lead-free ammunition with a slight increase in positive copper signal. Interestingly, the mean and median signals were similar between the two populations (Appendix IV Figure S5.2). However, a different trend was noted for nitroglycerin, where 94% and 86% of lead-free samples were above critical threshold with the portable and benchtop instruments, respectively, which was lower than what was observed in the leaded samples. Additionally, the mean and median signals for the lead-free samples were visually slightly lower than the leaded samples for nitroglycerin, although this difference was not statistically significant (Appendix IV Figure S5.3).
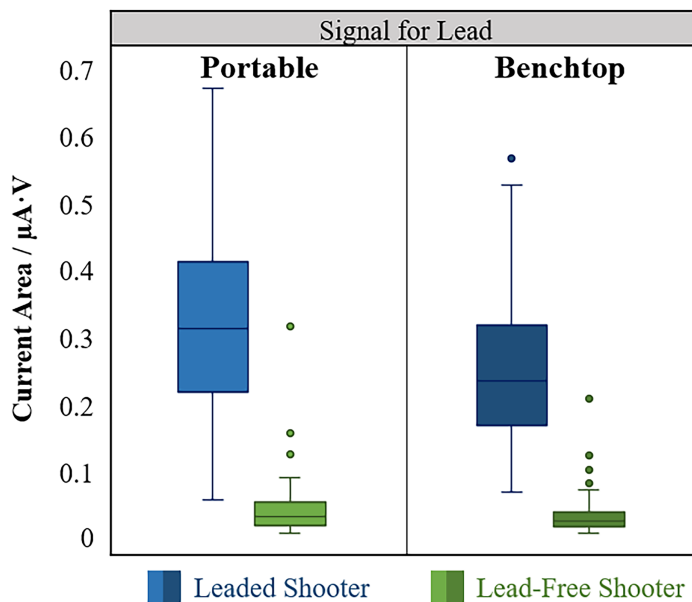
Figure 5.5. *Box plot comparison of the lead peak current area signal between leaded and lead-free populations for the benchtop and portable potentiostats.*

These results support the utility of portable instrumentation for GSR detection, strengthening our previous evidence showing the importance of electrochemistry for the analysis of GSR and demonstrating that the portable potentiostat is capable of accurate and reliable screening as an alternative for on-site testing.

During the collection of the background non-shooter samples, volunteers were asked a series of questions to ensure they did not handle or discharge a firearm in the past 24 hours or participate in activities considered to be high-risk for detection of GSR-type residues. Additionally, a note was taken if the participant had any pen ink, tattoos, or other residues, or if the individual was wearing any rings or nail polish as those could lead to potential interferences or false positive calls in the background population. Of the 38 samples which demonstrated one IGSR or OGSR analyte, 45% had an additional comment during the collection. An interesting finding regarding these comments showed that of those 69% and 72% calls (Appendix IV Table S5.1) for copper by the benchtop and portable instruments, respectively, 38% of calls had the note of the individual wearing a ring during collection.

More importantly, a single analyte does not represent a positive identification of GSR. For the electrochemical screening, we defined the criteria that at least two different analytes (one IGSR, and one OGSR) must be present for positive identification of GSR. In this study, lead, copper, and

nitroglycerin were the GSR identifiers used due to their prevalence in the sampled populations. While additional OGSR indicators would increase the reliability, nitroglycerin is a category one compound as defined by the OSAC classification of OGSR, increasing the value when present in a sample. Additionally, these methods are meant for screening, where laboratories could perform further confirmation of other OGSR analytes by methods like mass spectrometry.[99,100]

When assessing the leaded shooter samples, an average of 70% of samples were positive for all three analytes as depicted in **Figure 5.6.** The next two most common calls were for lead and nitroglycerin at 25% of samples for the benchtop potentiostat and 30% of samples for the portable potentiostat. Furthermore, just 1% of samples contained only the IGSR combination of lead and copper being present with no OGSR. This is a significant finding since the majority of positive samples contained a mixture of IGSR and OGSR analytes (>96%), a fact that improves the reliability in the identification of GSR in a sample.
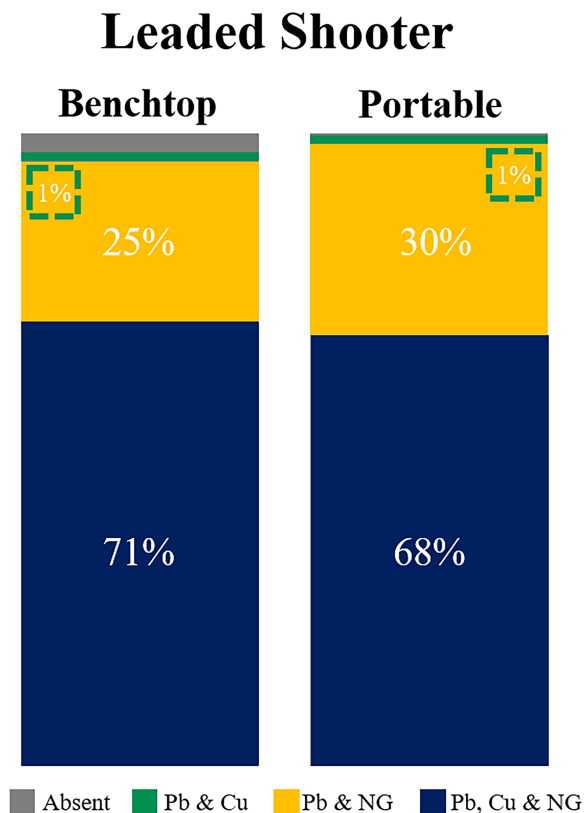

Figure 5.6. Comparison between the benchtop and portable potentiostats for positive call combinations of Pb+Cu (navy), Pb+NG (yellow), and Pb+Cu+NG (green) in the leaded shooter population.

Following the identification of analytes above the critical threshold, performance measures were calculated based on the presence of two or more analytes as described above. Performance measures demonstrate the true positive, true negative, false positive, false negative, and accuracy calculated for each population analyzed by both electrochemical methods. **Table 5.4** demonstrates the performance measures for the background and leaded shooter samples with a direct comparison between the benchtop and portable instrument. Both instruments were able to accurately assess all 200 background samples as not having the presence of GSR compounds, resulting in a 100% true negative rate. In the case of the leaded shooter samples, a small difference was seen between the benchtop and portable instruments; however, this difference may be attributed to the loss of two samples due to an electrical failure within the instrument cable of the benchtop potentiostat. Due to this error, two samples were unable to be analyzed properly and were therefore considered negative for this comparison. Despite this, the true positive results for the leaded shooter samples were 97% for the benchtop and 99% for the portable instrument. Additionally, lead signals were not considered for the lead-free population in order to assess the strength of the method in the absence of lead and to account for the possible contamination as described previously. Therefore, the lead-free samples were considered positive if both copper and nitroglycerin were present above the critical threshold. Appendix IV Figure S5.4 provides the percentage of samples called with copper and nitroglycerin, as well as samples which were false negatives for only copper or only nitroglycerin identified in the sample. By these criteria, the true positive results were 78% for the portable instrument and 76% for the benchtop instrument for the lead-free sample population.

High true positive rates and low false negative rates were seen for both instruments for all populations, giving an average true positive rate of 88.5% and 86.5% for the portable and benchtop instruments when the different ammunition types were considered, respectively. The overall accuracy of the method was 96.5% for the portable instrument and 95.7% for the benchtop method, demonstrating the strength of electrochemistry for the screening of GSR and the ability of the portable instrument to produce results that were as accurate as the benchtop model. Further, excellent reproducibility between portable methods and benchtop instruments was demonstrated, along with high accuracy for a screening method for the correct classification of the samples. Moreover, most instances of false negatives occurred on the same samples when analyzed by both methods.

Table 5.4. *Comparison of performance measures for the three populations between the benchtop and portable instrumentation.*

	Metrohm Benchtop Instrument			PalmSens4 Portable Instrument		
Background and Shooter Samples Performance Rates by Critical Threshold						
	Background	**Leaded Shooter**	**Lead Free Shooter**	**Background**	**Leaded Shooter**	**Lead Free Shooter**
Number of Sets	200	100	50	200	100	50
True Positive (Sensitivity)	N/A	97* (97%)	38 (76%)	N/A	99 (99%)	39 (78%)
False Negative	N/A	3 (3%)	12 (24%)	N/A	1 (1%)	11 (22%)
True Negative (Specificity)	200 (100%)	N/A	N/A	200 (100%)	N/A	N/A
False Positive	0 (0%)	N/A	N/A	0 (0%)	N/A	N/A
Accuracy	95.7%			96.5%		

*Electrical issue caused the loss of two samples

5.4 Conclusions

The fast-paced innovation of technology has emphasized the need for testing portable devices to ensure the quality of results from analysis to identification and interpretation of evidence. The purpose of this study was to compare the sensitivity, reliability, and selectivity of a field-portable potentiostat to a laboratory benchtop instrument for electrochemical screening of GSR. The results demonstrate equivalent identification of GSR between the two instruments, which provides a foundation for further implementation for preliminary testing of suspected GSR at forensic laboratories and at the crime scene.

The sample preparation method provided the ability to analyze the same specimens on both instruments with ease of analysis taking under 10 minutes per sample and resulting in data directly comparable between instruments for the authentic samples.

Electrochemical performance characteristics demonstrated the comparable specificity and sensitivity between the benchtop and portable potentiostats for simultaneous IGSR and OGSR detection with limits of detection below 0.6 μg/mL for both instruments. The most significant difference was that the benchtop potentiostat demonstrated better repeatability.

Most importantly, both instruments provided GSR identification for lead, copper, and nitroglycerin using critical threshold approaches with accuracies over 95% for classification of samples as shooter or non-shooter based on combined IGSR/OGSR profiles. This demonstrates the scientific reliability of the portable electrochemical method for casework-like samples. Assessing the application of the portable potentiostat lays a groundwork for this screening approach as a future tool for forensic laboratories. The advantage of this portable system is that it provides a rapid and sensitive GSR field-screening method to minimize the disconnect of decisions between crime scene and laboratory analysis within the discipline. Additionally, portable devices help in triage, both at crime scenes and laboratories, to provide a cost-efficient screening method that can decrease backlogs and allow for further confirmatory testing when needed. Most importantly, fast decision making at crime scenes can significantly aid the collection of relevant information. This application contributes to the necessary developments in forensic technology with dual IGSR and OGSR detection in addition to low sensitivity with the reliability comparable to laboratory instrumentation. The main findings of this work demonstrate not only the speed and convenience of simultaneous IGSR and OGSR detection, but also the effectiveness of the portable technology.

This study furthers the information needed for forensic laboratories to implement electrochemical screening methods as a portable detection instrument for GSR. Continued research in portable electrochemical potentiostats by our research group will include demonstrating the convenience of the method at mock crime scenes and testing with authentic casework samples and collaboration with practicing forensic laboratories to showcase the importance and efficiency of on-site GSR screening.

VI.   CHAPTER 6: CONCLUSIONS AND FUTURE WORK

6.1 Overall Conclusions

Nationally, the increasing trend in gun violence-related death over the past decade provides relevance to why GSR analysis is still performed by forensic laboratories. In the state of West Virginia, a life is lost on average 305 lives per year, and 1.6 billion dollars are spent toward gun violence-related deaths from suicides, homicides, and accidental firearm situations. The objectives set at the beginning of this thesis were to aid in the effort to provide a faster sampling method to complement current methodologies and increase the reliability of GSR detection for onsite screening to aid in the effort to improve workflow for the surmounting increasing gun violence related crime in America. The goals were achieved by this research by combining approved GSR collection techniques, electrochemical analysis, and statistical methods.

Electrochemical methods for distance determination found that integrated voltammetric data could be used to visualize spatial GSR patterns as well as perform discriminant analysis classification of shooting distance. Bar graphs and macro-spatial heat maps afford a permanent visualization of GSR pattern from the clothing substrates. Discriminant analysis of electrochemical method had comparative performance to physical measurements at 82% and color test at 88% accuracy for light-colored fabric with an accuracy of 94%. Electrochemical detection offered greater success for complex material at 85% for dark and patterned fabric, and 68% for bloody clothing over observations by the naked eye or interpretation of colorimetric test. The overall performance demonstrates 74% accuracy for the 45 unknown distance samples on various fabric materials.

Development of a simple collection approach combined with electrochemical testing afforded a straightforward, quick analysis method of bullet holes to identify GSR analytes with the capability for simultaneous IGSR and OGSR detection. The developed methodology was assessed by various substrates commonly found at crime scenes like light and dark fabric, blood-stained fabric, wood, and drywall. Electrochemical GSR detection resulted in 98% accuracy for fabric and 100% for hard substrates having two or more IGSR or OGSR analytes present. To confirm the OGSR presence, the samples were additionally analyzed using a previously validated LC-MS/MS method. This work offers good proof of concept of how sampling and electrochemical detection

can provide chemical information rapidly for ease of collection and testing of suspected bullet holes from various materials.

Finally, the comparison of benchtop and portable potentiostat defined the performance characteristics and authentic population assessment by both instrumentations. Statistic comparison of potential windows and LOD found slight differences depending on analytes, however, detection limits were below 600 ug/mL for both potentiostats. Overall accuracies from evaluation of non-shooter, leaded shooter, and lead-free shooter populations resulted in 95.7% and 96.5% for the benchtop and portable potentiostat, respectively. The findings of this work increase the reliability of portable electrochemical instrumentation for its capabilities of portability, aid with triage, and use for onsite testing.

6.2 Future Work

Expansion of this work has the potential for improvement from the sample collection, addition mediums, and statistical methods for electrochemical detection for distance determination, bullet hole identification, and GSR applications. Based on the finding of this work, the recommendation for future work is described below.

Regarding sampling methodology for distance determination, the use of smaller aluminum stubs to allow for more discrete collection intervals to potentially gain more information from electrochemical data for macro-spatial mapping and statistical classification. Larger stubs collected many GSR particles visual to the naked eye which may have a skewed concentration of IGSR and OGSR intensities for classification. An expansion of electrochemical assessment of distance determination by changing variables which were controlled in this work such as textile compositions, ammunition, type of firearm, and various volumes of blood to soak samples. Additional interference and ruggedness testing for bullet hole identification by expanding the materials to include more complex substrates like glass, painted wood or drywall, automobile doors or plastics. Increasing sample size to explore more statistical models for classification like multiple logistic regression, or even neutral networks. To continue transition from research to portable electrochemical implementation, future work will include developing housing and workflow to prevent contamination during analysis on crime scenes like analysis location, disposable bags to protect the potentiostats wires and electrodes from environment of a shooting

related event. These developments can additionally be achieved by application of the methods in mock crime scenes scenarios or inter-laboratory studies to work on the transition from research to industry use of techniques.

VII. REFERENCES

(1)   Archive, G. V. Gun Violence Archive https://www.gunviolencearchive.org/ (accessed 2022 -06 -02).

(2)   Center, G. L. Giffords Law Center To Prevent Gun Violence https://giffords.org/lawcenter/gun-violence-statistics/.

(3)   Dalby, O.; Butler, D.; Birkett, J. W. Analysis of Gunshot Residue and Associated Materials - A Review. *J. Forensic Sci.* **2010**, *55* (4), 924–943. https://doi.org/10.1111/j.1556-4029.2010.01370.x.

(4)   ASTM-American Standards and Testing Materials. *Standard Guide for Gunshot Residue Analysis by Scanning Electron Microscopy / Energy Dispersive X-Ray Spectrometry*; Conshohoken, PA, 2020. https://doi.org/10.1520/E1588-20.2.

(5)   Harris, A. Analysis of Primer Residue from CCI Blazer® Lead Free Ammunition by Scanning Electron Microscopy/Energy Dispersive X-Ray. *J. Forensic Sci.* **1995**, *40* (1), 13755J. https://doi.org/10.1520/jfs13755j.

(6)   Schwoelble, A. J.; Exline, D. L. *Current Methods in Forensic Gunshot Residue Analysis*; CRC Press: Boca Raton, 2000. https://doi.org/10.1201/9781420038712.ch8.

(7)   SWGGUN. Guidelines for Gunshot Residue Distance Determinations. **2013**, 1–8.

(8)   Mosher, P. V.; McVicar, M. J.; Randall, E. D.; Sild, E. H. Gunshot Residue-Similar Particles Produced by Fireworks. *J. Can. Soc. Forensic Sci.* **1998**, *31* (3), 157–168. https://doi.org/10.1080/00085030.1998.10757115.

(9)   Tucker, W.; Lucas, N.; Seyfang, K. E.; Kirkbride, K. P.; Popelka-Filcoff, R. S. Gunshot Residue and Brakepads: Compositional and Morphological Considerations for Forensic Casework. *Forensic Sci. Int.* **2017**, *270*, 76–82. https://doi.org/10.1016/j.forsciint.2016.11.024.

(10)   Sharma, S. P.; Lahiri, S. C. A Preliminary Investigation into the Use of FTIR Microscopy as a Probe for the Identification of Bullet Entrance Holes and the Distance of Firing. *Sci. Justice* **2009**, *49* (3), 197–204. https://doi.org/10.1016/j.scijus.2008.07.002.

(11)   Ott, C. E.; Dalzell, K. A.; Calderón-Arce, P. J.; Alvarado-Gámez, A. L.; Trejos, T.; Arroyo, L. E. Evaluation of the Simultaneous Analysis of Organic and Inorganic Gunshot Residues Within a Large Population Data Set Using Electrochemical Sensors*,†. *J. Forensic Sci.* **2020**, *65* (6), 1935–1944. https://doi.org/10.1111/1556-4029.14548.

(12)   Vander Pyl, C.; Morris, K.; Arroyo, L.; Trejos, T. Assessing the Utility of LIBS in the Reconstruction of Firearm Related Incidents. *Forensic Chem.* **2020**, *19* (March). https://doi.org/10.1016/j.forc.2020.100251.

(13)   Trejos, T.; Vander Pyl, C.; Menking-Hoggatt, K.; Alvarado, A. L.; Arroyo, L. E. Fast Identification of Inorganic and Organic Gunshot Residues by LIBS and Electrochemical Methods. *Forensic Chem.* **2018**, *8* (October), 146–156. https://doi.org/10.1016/j.forc.2018.02.006.

(14) Menking-Hoggatt, K.; Arroyo, L.; Curran, J.; Trejos, T. Novel LIBS Method for Micro-Spatial Chemical Analysis of Inorganic Gunshot Residues. *J. Chemom.* **2021**, *35* (1). https://doi.org/10.1002/cem.3208.

(15) Calhoun, R. B.; Dunson, C.; Johnson, M. L.; Lamkin, S. R.; Lewis, W. R.; Showen, R. L.; Sompel, M. A.; Wollman, L. P. Precision and Accuracy of Acoustic Gunshot Location in an Urban Environment. **2020**, No. January, 1–18.

(16) Blakey, L. S.; Sharples, G. P.; Chana, K.; Birkett, J. W. Fate and Behavior of Gunshot Residue—A Review. *J. Forensic Sci.* **2018**, *63* (1), 9–19. https://doi.org/10.1111/1556-4029.13555.

(17) OSAC. Standard Practice for the Collection, Preservation, and Analysis of Organic Gunshot Residues. **2020**, 1–14.

(18) ASTM International. *E1588-20 Standard Guide for Gunshot Residue Analysis by Scanning Electron Microscopy/Energy Dispersive X-Ray Spectrometry*; 1991. https://doi.org/10.1520/E1588-20.2.

(19) ASTM-American Standards and Testing Materials. Standard Practice for Characterization and Classification of Smokeless Powder. **2016**, *i*, 1–7. https://doi.org/10.1520/E2998-16.2.

(20) Meng, H.; Caddy, B. Gunshot Residue Analysis A Review. **2020**, *42* (4), 553–570.

(21) Feeney, W.; Vander Pyl, C.; Bell, S.; Trejos, T. Trends in Composition, Collection, Persistence, and Analysis of IGSR and OGSR: A Review. *Forensic Chem.* **2020**, *19* (March), 11–16. https://doi.org/10.1016/j.forc.2020.100250.

(22) Goudsmits, E.; Sharples, G. P.; Birkett, J. W. Recent Trends in Organic Gunshot Residue Analysis. *TrAC - Trends Anal. Chem.* **2015**, *74*, 46–57. https://doi.org/10.1016/j.trac.2015.05.010.

(23) Yeager, B.; Bustin, K.; Stewart, J.; Dross, R.; Bell, S. Evaluation and Validation of Ion Mobility Spectrometry for Presumptive Testing Targeting the Organic Constituents of Firearms Discharge Residue. *Anal. Methods* **2015**, *7* (22), 9683–9691. https://doi.org/10.1039/c5ay02417j.

(24) Stevens, B.; Bell, S.; Adams, K. Initial Evaluation of Inlet Thermal Desorption GC–MS Analysis for Organic Gunshot Residue Collected from the Hands of Known Shooters. *Forensic Chem.* **2016**, *2*, 55–62. https://doi.org/10.1016/j.forc.2016.10.001.

(25) Laza, D.; Nys, B.; Kinder, J. De; Kirsch-De Mesmaeker, A.; Moucheron, C. Development of a Quantitative LC-MS/MS Method for the Analysis of Common Propellant Powder Stabilizers in Gunshot Residue. *J. Forensic Sci.* **2007**, *52* (4), 842–850. https://doi.org/10.1111/j.1556-4029.2007.00490.x.

(26) Hofstetter, C.; Maitre, M.; Beavis, A.; Roux, C.; Weyermann, C.; Gassner, A. A Study of Transfer and Prevalence of Organic Gunshot Residues. *Forensic Sci. Int.* **2017**, No. 48, 241–251.

(27) Lopez-Lopez, M.; De La Ossa, M. A. F.; Garcia-Ruiz, C. Fast Analysis of Complete Macroscopic Gunshot Residues on Substrates Using Raman Imaging. *Appl. Spectrosc.*

2015, *69* (7), 889–893. https://doi.org/10.1366/14-07816.

(28)   López-López, M.; Delgado, J. J.; García-Ruiz, C. Ammunition Identification by Means of the Organic Analysis of Gunshot Residues Using Raman Spectroscopy. *Anal. Chem.* **2012**, *84* (8), 3581–3585. https://doi.org/10.1021/ac203237w.

(29)   MacCrehan, W. A.; Ricketts, K. M.; Baltzersen, R. A.; Rowe, W. F. Detecting Organic Gunpowder Residues from Handgun Use. *Investig. Forensic Sci. Technol.* **1999**, *3576* (February 1999), 116–124. https://doi.org/10.1117/12.334522.

(30)   Mahoney, C.; Gillen, G.; Fahey, A. Characterization of Gunpowder Samples Using Time-of-Flight Secondary Ion Mass Spectrometry (TOF-SIMS). *Forensic Sci. Int.* **2006**, No. 158, 39–51.

(31)   Moran, J.; Bell, S. Analysis of Organic Gunshot Residue Permeation through a Model Skin Membrane Using Ion Mobility Spectrometry. *Int. J. Ion Mobil. Spectrom.* **2013**, *16* (4), 247–258. https://doi.org/10.1007/s12127-013-0138-0.

(32)   Morelato, M.; Beavis, A.; Ogle, A.; Doble, P.; Kirkbride, K. P.; Roux, C. Screening of Gunshot Residues Using Desorptive Electrospray Ionization-Mass Spectrometry (DESI-MS). *Forensic Sci. Int.* **2012**, No. 217, 101–106. https://doi.org/10.1016.

(33)   Olson, E. J.; Isley, W. C.; Brennan, J. E.; Cramer, C. J.; Bu, P. Electrochemical Reduction of 2 , 4-Dinitrotoluene in Aprotic and PH- Bu Ff Ered Media. **2015**. https://doi.org/10.1021/acs.jpcc.5b02840.

(34)   Redouté Minzière, V.; Werner, D.; Schneider, D.; Manganelli, M.; Jung, B.; Weyermann, C.; Gassner, A. L. Combined Collection and Analysis of Inorganic and Organic Gunshot Residues. *J. Forensic Sci.* **2020**, *65* (4), 1102–1113. https://doi.org/10.1111/1556-4029.14314.

(35)   Salles, M. O.; Bertotti, M.; Paixão, T. R. L. C. Use of a Gold Microelectrode for Discrimination of Gunshot Residues. *Sensors Actuators, B Chem.* **2012**, *166–167*, 848–852. https://doi.org/10.1016/j.snb.2012.02.097.

(36)   Tarifa, A.; Almirall, J. R. Fast Detection and Characterization of Organic and Inorganic Gunshto Residues on the Hands of Suspects by CMV-GC-MS and LIBS. *Sci. Justice* **2015**, No. 55, 168–175. https://doi.org/10.1016.

(37)   Zeichner, A.; Eldar, B. A Novel Method for Extraction and Analysis of Gunpowder Residues on Double-Side Adhesive Coated Stubs. *J. Forensic Sci.* **2004**, *49* (6), 1–13. https://doi.org/10.1520/jfs2004022.

(38)   Zeichner, A.; Eldar, B.; Glattstein, B.; Koffman, A.; Tamiri, T.; Muller, D. Vacuum Collection of Gunpowder Residues from Clothing Worn by Shooting Suspects, and Their Analysis by GC/TEA, IMS, and GC/MS. *J. Forensic Sci.* **2003**, *48* (5), 2002390. https://doi.org/10.1520/jfs2002390.

(39)   Zhao, M.; Zhang, S.; Yang, C.; Xu, Y.; Wen, Y.; Sun, L.; Zhang, X. Desorption Electrospray Tandem MS (DESI-MSMS) Anlaysis of Methyl Centralite and Ethyl Centralite as Gunshot Residue on Skin and Other Surfaces. *J. Forensic Sci.* **2008**, No. 53, 807–811.

(40) Maitre, M.; Kirkbride, K. P.; Horder, M.; Roux, C.; Beavis, A. Thinking beyond the Lab: Organic Gunshot Residues in an Investigative Perspective. *Aust. J. Forensic Sci.* **2018**, *50* (6), 659–665. https://doi.org/10.1080/00450618.2018.1457718.

(41) Mach, M. H.; Pallos, A.; Jones, P. F. Feasibility of Gunshot Residue Detection Via Its Organic Constituents. Part II: A Gas Chromatography-Mass Spectrometry Method. *J. Forensic Sci.* **1978**, *23* (3), 10691J. https://doi.org/10.1520/jfs10691j.

(42) Joshi, M.; Rigsby, K.; Almirall, J. R. Analysis of the Headspace Composition of Smokeless Powders Using GC-MS, GC-MECD and Ion Mobility Spectrometry. *Forensic Sci. Int.* **2011**, *208* (1–3), 29–36. https://doi.org/10.1016/j.forsciint.2010.10.024.

(43) Gassner, A. L.; Weyermann, C. Prevalence of Organic Gunshot Residues in Police Vehicles. *Sci. Justice* **2020**, *60* (2), 136–144. https://doi.org/10.1016/j.scijus.2019.09.009.

(44) Gandy, L.; Najjar, K.; Terry, M.; Bridge, C. A Novel Protocol for the Combined Detection of Organic, Inorganic Gunshot Residue. *Forensic Chem.* **2018**, *8*, 1–10. https://doi.org/10.1016/j.forc.2017.12.009.

(45) Vuki, M.; Shiu, K. K.; Galik, M.; O'Mahony, A. M.; Wang, J. Simultaneous Electrochemical Measurement of Metal and Organic Propellant Constituents of Gunshot Residues. *Analyst* **2012**, *137* (14), 3265–3270. https://doi.org/10.1039/c2an35379b.

(46) Tong, Y.; Wu, Z.; Yang, C.; Yu, J.; Zhang, X.; Yang, S.; Deng, X.; Xu, Y.; Wen, Y. Determination of Diphenylamine Stabilizer and Its Nitrated Derivatives in Smokeless Gunpowder Using a Tandem MS Method. *Analyst* **2001**, *126* (4), 480–484. https://doi.org/10.1039/b010183o.

(47) Abrego, Z.; Grijabla, N.; Unceta, N.; Maguregui, M.; Sanchez, A.; Ferandez-Isla, A.; Giocolea, M.; Barrio, R. A Novel Method for the Identification of Inorganic and Organic Gunshot Reside Particles of Lead-Free Ammunitions from the Hands of Shooters Using Scanning Laser Ablation-ICPMS and Raman Micro-Spectroscopy. *Analyst* **2014**, No. 139, 6232–6241. https://doi.org/10.1039.

(48) Ali, L.; Brown, K.; Castellano, H.; Wetzel, S. A Study Fo the Presence of Gunshot Residue in Pittsburgh Police Stations Using SEM/EDS and LC-MS/MS. *Forensic Sci.* **2016**, No. 61, 928–938. https://doi.org/10.1111.

(49) Arndt, J.; Bell, S.; Crookshanks, L.; Lovejoy, M.; Oleska, C.; Tulley, T.; Wolfe, D. Preliminary Evaluation of the Persistence of Organic Gunshot Residue. *Forensic Sci. Int.* 137–145.

(50) Bell, S.; Feeney, W. Single Shot, Single Sample, Single Instrument Detection of IGSR and OGSR Using LC/MS/MS. *Forensic Sci. Int.* **2019**, *299* (2019), 215–222. https://doi.org/10.1016/j.forsciint.2019.04.002.

(51) White, R. S.; Owens, A. D. Automation of Gunshot Residue Detection and Analysis by Scanning Electron Microscopy/Energy Dispersive X-Ray Analysis (SEM/EDX). *J. Forensic Sci.* **1987**, *32* (6), 11219J. https://doi.org/10.1520/jfs11219j.

(52) Kara, llker; Sarikavak, Y.; Lisesivdin, S. B.; Kasap, M. Evaluation of Morphological and Chemical Differences of Gunshot Residues in Different Ammunitions Using SEM/EDS

107

Technique. *Environ. Forensics* **2016**, *17* (1), 68–79.
https://doi.org/10.1080/15275922.2015.1133729.

(53)   Charpentier, B.; Desrochers, C. Analysis of Primer Residue from Lead Free Ammunition by X-Ray Microfluorescence. *J. Forensic Sci.* **2000**, *45* (2), 14705J.
https://doi.org/10.1520/jfs14705j.

(54)   ENFSI. Best Practice Manual for Chemographic Methods in Gunshot Residue Analysis.
2015, *1* (November), 1–16.

(55)   Dillon, J. The Modified Griess Test: A Chemically Specific Chromophoric Test for Nitrite Compounds in Gunshot Residues. *AFTE J.* **1990**, *22* (3), 52–55.

(56)   Dillon, J. H. Chemistry of the Sodium Rhodizonate Test. *AFTE J.* **1990**, *22* (3), 58–62.

(57)   Bailey, J. A. Analysis of Bullet Wipe Patterns on Cloth Targets. *J. Forensic Identif.* **2005**, *55* (4), 448–460.

(58)   Halim, M. I. A.; Ahmas, U. K.; Yew, C.-H.; Abdullah, M. K. Analysis of Gunshot Residue Deposited on Cotton Cloth Target at Close Range Shooting Distances. *Malayisan J. Forensic Sci.* **2010**, *1* (1), 48–53.

(59)   Hepp, N. C.; Mindak, W. R.; Gasper, J. W.; Thompson, C. B.; Barrows, J. N. Survey of Cosmetics for Arsenic, Cadmium, Chromium, Cobalt, Lead, Mercury, and Nickel Content. *J. Cosmet. Sci.* **2014**, *65*, 125–145.

(60)   Laflèche, D. J. N.; Brière, S. J. J.; Faragher, N. F.; Hearns, N. G. R. Gunshot Residue and Airbags: Part I. Assessing the Risk of Deployed Automotive Airbags to Produce Particles Similar to Gunshot Residue. *J. Can. Soc. Forensic Sci.* **2018**, *51* (2), 48–57.
https://doi.org/10.1080/00085030.2018.1463202.

(61)   Berger, J.; Upton, C.; Springer, E. Evaluation of Total Nitrite Pattern Visualization as an Improved Method for Gunshot Residue Detection and Its Application to Casework Samples. *J. Forensic Sci.* **2019**, *64* (1), 218–222. https://doi.org/10.1111/1556-4029.13802.

(62)   Bartsch, M. R.; Kobus, H. J.; Wainwright, K. P. An Update on the Use of the Sodium Rhodizonate Test for the Detection of Lead Originating from Firearm Discharges. *J. Forensic Sci.* **1996**, *41* (6), 14047J. https://doi.org/10.1520/jfs14047j.

(63)   Andreola, S.; Gentile, G.; Battistini, A.; Cattaneo, C.; Zoja, R. Forensic Applications of Sodium Rhodizonate and Hydrochloric Acid: A New Histological Technique for Detection of Gunshot Residues. *J. Forensic Sci.* **2011**, *56* (3), 771–774.
https://doi.org/10.1111/j.1556-4029.2010.01689.x.

(64)   Wongpakdee, T.; Buking, S.; Ratanawimarnwong, N.; Saetear, P.; Uraisin, K.; Wilairat, P.; Tiyapongpattana, W.; Nacapricha, D. Simple Gunshot Residue Analyses for Estimating Firing Distance: Investigation with Four Types of Fabrics. *Forensic Sci. Int.* **2021**, *329* (2021), 111084. https://doi.org/10.1016/j.forsciint.2021.111084.

(65)   Berendes, A.; Neimke, D.; Schumacher, R.; Barth, M. A Versatile Technique for the Investigation of Gunshot Residue Patterns on Fabrics and Other Surfaces: M-XRF. *J.*

Forensic Sci. **2006**, *51* (5), 1085–1090. https://doi.org/10.1111/j.1556-4029.2006.00225.x.

(66)   Vander Pyl, C.; Ovide, O.; Ho, M.; Yuksel, B.; Trejos, T. Chemical Analysis of Firearm Discharge Residues Using Laser Chemical Analysis of Firearm Discharge Residues Using Laser Induced Breakdown Spectroscopy Induced Breakdown Spectroscopy Recommended Citation Recommended Citation. *Spectrochim. Acta Part B* **2019**, *152*, 93–101.

(67)   Gagliano-Candela, R.; Colucci, A. P.; Napoli, S. Determination of Firing Distance. Lead Analysis on the Target by Atomic Absorption Spectroscopy (AAS). *J. Forensic Sci.* **2008**, *53* (2), 321–324. https://doi.org/10.1111/j.1556-4029.2008.00668.x.

(68)   Kersh, K. L.; Childers, J. M.; Justice, D.; Karim, G. Detection of Gunshot Residue on Dark-Colored Clothing Prior to Chemical Analysis. *J. Forensic Sci.* **2014**, *59* (3), 754–762. https://doi.org/10.1111/1556-4029.12409.

(69)   Zapata, F.; López-López, M.; Amigo, J. M.; García-Ruiz, C. Multi-Spectral Imaging for the Estimation of Shooting Distances. *Forensic Sci. Int.* **2018**, *282* (2018), 80–85. https://doi.org/10.1016/j.forsciint.2017.11.025.

(70)   Brożek-Mucha, Z. A Study of Gunshot Residue Distribution for Close-Range Shots with a Silenced Gun Using Optical and Scanning Electron Microscopy, X-Ray Microanalysis and Infrared Spectroscopy. *Sci. Justice* **2017**, *57* (2), 87–94. https://doi.org/10.1016/j.scijus.2016.11.004.

(71)   Trejos, T.; Vander Pyl, C.; Menking-Hoggatt, K.; Alvarado, A. L.; Arroyo, L. E. Fast Identification of Inorganic and Organic Gunshot Residues by LIBS and Electrochemical Methods. *Forensic Chem.* **2018**, *8*, 146–156. https://doi.org/10.1016/j.forc.2018.02.006.

(72)   Heineman, W. R.; Strobel, H. A. *Chemical Instrumention: A Systematic Approach*, Third.; John Wiley & Sons, 1989.

(73)   Luong, J. H. T.; Male, K. B.; Glennon, J. D. Boron-Doped Diamond Electrode: Synthesis, Characterization, Functionalization and Analytical Applications. *Analyst* **2009**, *134* (10), 1965–1979. https://doi.org/10.1039/b910206j.

(74)   Lai, B. C.; Wu, J. G.; Luo, S. C. Revisiting Background Signals and the Electrochemical Windows of Au, Pt, and GC Electrodes in Biological Buffers. *ACS Appl. Energy Mater.* **2019**, *2* (9), 6808–6816. https://doi.org/10.1021/acsaem.9b01249.

(75)   Elgrishi, N.; Rountree, K. J.; McCarthy, B. D.; Rountree, E. S.; Eisenhart, T. T.; Dempsey, J. L. A Practical Beginner's Guide to Cyclic Voltammetry. *J. Chem. Educ.* **2018**, *95* (2), 197–206. https://doi.org/10.1021/acs.jchemed.7b00361.

(76)   Wang, J. *Analytical Electrochemistry*, Second Edi.; John Wiley & Sons, 2001. https://doi.org/10.1016/0003-2670(95)90287-2.

(77)   Barfidokht, A.; Mishra, R. K.; Seenivasan, R.; Liu, S.; Hubble, L. J.; Wang, J.; Hall, D. A. Wearable Electrochemical Glove-Based Sensor for Rapid and on-Site Detection of Fentanyl. *Sensors Actuators, B Chem.* **2019**, *296*, 1–16. https://doi.org/10.1016/j.snb.2019.04.053.

(78) de Araujo, W. R.; Cardoso, T. M. G.; da Rocha, R. G.; Santana, M. H. P.; Muñoz, R. A. A.; Richter, E. M.; Paixão, T. R. L. C.; Coltro, W. K. T. Portable Analytical Platforms for Forensic Chemistry: A Review. *Anal. Chim. Acta* **2018**, *1034*, 1–21. https://doi.org/10.1016/j.aca.2018.06.014.

(79) Konanur, N. K.; Van Loon, G. W. Determination of Lead and Antimony in Firearm Discharge Residues on Hands by Anodic Stripping Volatmmetry. *Talanta* **1977**, *23* (3), 184–187.

(80) Woolever, C. A.; Dewald, H. D. Differential Pulse Anodic Stripping Voltammetry of Barium and Lead in Gunshot Residues. *Forensic Sci. Int.* **2001**, *117* (3), 185–190. https://doi.org/10.1016/S0379-0738(00)00402-3.

(81) Karl Bratin; Kissinger, P. T.; Briner, R. C.; Bruntlett, C. S. Determination of Nitro Aromatic, Nitramine, and Nitrate Ester Explosive Compounds in Explosive Mixtures and Gunshot Residue by Liquid Chromatgraphy and Reductive Electrochemical Detection. *Anal. Chim. Acta* **1981**, *130* (2), 295–311.

(82) Briner, R. C.; Chouchoiy, S.; Webster, R. W. Anodic Stripping Voltammetric Determination of Antimony in Gunshot Residue. *Anal. Chim. Acta* **1985**, *172*, 31–37.

(83) Wang, J.; Tian, B.; Wang, J.; Lu, J.; Olsen, C.; Yarnitzky, C.; Olsen, K.; Hammerstrom, D.; Bennett, W. Stripping Analysis into the 21st Century: Faster, Smaller, Cheaper, Simpler and Better. *Anal. Chim. Acta* **1999**, *385* (1–3), 429–435. https://doi.org/10.1016/S0003-2670(98)00664-3.

(84) Liu, J. H.; Lin, W.-F.; Nicol, J. D. The Application of Anodic Stripping Voltammetry to Forensic Science. II Anodic Stripping Voltemmatric Analysis of Gunshot Residue. *Forensic Sci. Int.* **1980**, *16*, 53–62.

(85) De Donato, A.; Gutz, I. G. R. Fast Mapping of Gunshot Residues by Batch Injection Analysis with Anodic Stripping Voltammetry of Lead at the Hanging Mercury Drop Electrode. *Electroanalysis* **2005**, *17* (2), 105–112. https://doi.org/10.1002/elan.200303048.

(86) Arduini, F.; Calvo, J. Q.; Palleschi, G.; Moscone, D.; Amine, A. Bismuth-Modified Electrodes for Lead Detection. *TrAC - Trends Anal. Chem.* **2010**, *29* (11), 1295–1304. https://doi.org/10.1016/j.trac.2010.08.003.

(87) Salles, M. O.; Naozuka, J.; Bertotti, M. A Forensic Study: Lead Determination in Gunshot Residues. *Microchem. J.* **2012**, *101*, 49–53. https://doi.org/10.1016/j.microc.2011.10.004.

(88) O'Mahony, A. M.; Wang, J. Electrochemical Detection of Gunshot Residue for Forensic Analysis: A Review. *Electroanalysis* **2013**, *25* (6), 1341–1358. https://doi.org/10.1002/elan.201300054.

(89) O'Mahony, A. M.; Windmiller, J. R.; Samek, I. A.; Bandodkar, A. J.; Wang, J. Swipe and Scan: Integration of Sampling and Analysis of Gunshot Metal Residues at Screen-Printed Electrodes. *Electrochem. commun.* **2012**, *23* (1), 52–55. https://doi.org/10.1016/j.elecom.2012.07.004.

(90) Harshey, A.; Srivastava, A.; Das, T.; Nigam, K.; Shrivastava, R.; Yadav, V. K. Trends in Gunshot Residue Detection by Electrochemical Methods for Forensic Purpose. *J. Anal.*

Test. **2021**, 12. https://doi.org/10.1007/s41664-020-00152-x.

(91) Erden, S.; Durmus, Z.; Kiliç, E. Simultaneous Determination of Antimony and Lead in Gunshot Residue by Cathodic Adsorptive Stripping Voltammetric Methods. *Electroanalysis* **2011**, *23* (8), 1967–1974. https://doi.org/10.1002/elan.201000612.

(92) O'Mahony, A. M.; Windmiller, J. R.; Samek, I. A.; Bandodkar, A. J.; Wang, J. Swipe and Scan: Integration of Sampling and Analysis of Gunshot Metal Residues at Screen-Printed Electrodes. *Electrochem. commun.* **2012**, *23* (1), 52–55. https://doi.org/10.1016/j.elecom.2012.07.004.

(93) Vuki, M.; Shiu, K. K.; Galik, M.; O'Mahony, A. M.; Wang, J. Simultaneous Electrochemical Measurement of Metal and Organic Propellant Constituents of Gunshot Residues. *Analyst* **2012**, *137* (14), 3265–3270. https://doi.org/10.1039/c2an35379b.

(94) Omahony, A. M.; Samek, I. A.; Sattayasamitsathit, S.; Wang, J. Orthogonal Identification of Gunshot Residue with Complementary Detection Principles of Voltammetry, Scanning Electron Microscopy, and Energy-Dispersive X-Ray Spectroscopy: Sample, Screen, and Confirm. *Anal. Chem.* **2014**, *86* (16), 8031–8036. https://doi.org/10.1021/ac5016112.

(95) Promsuwan, K.; Kanatharana, P.; Thavarungkul, P.; Limbut, W. Nitrite Amperometric Sensor for Gunshot Residue Screening. *Electrochim. Acta* **2020**, *331*. https://doi.org/10.1016/j.electacta.2019.135309.

(96) Skoog, D. A.; Holler, F. J.; Crouch, S. R. *Principals of Instrumental Analysis*, 6th ed.; Cengage Learning, 2007.

(97) Harris, D. C. *Quantitative Chemical Analysis*, 8th ed.; Fiorillo, J., Quinn, D., Szczepanski, T., Byrd, M. L., Eds.; Clancy Marshall: New York, 2010.

(98) Feeney, W. J. Modified Firearm Discharge Residue Analysis Utilizing Advanced Analytical Techniques , Complexing Agents , and Quantum Chemical Calculations Modified Firearm Discharge Residue Analysis Utilizing Advanced Analytical Techniques , Complexing Agents , and Qua, West Virginia University, 2021.

(99) Feeney, W.; Menking Hoggatt, K.; Vander Pyl, C.; Ott, C. E.; Bell, S.; Arroyo, L.; Trejos, T. Detection of Organic and Inorganic Gunshot Residues from Hands Using Complexing Agents and LC-MS/MS. *Anal. Methods* **2021**, No. June. https://doi.org/10.1039/d1ay00778e.

(100) Feeney, W.; Menking-Hoggatt, K.; Arroyo, L. E.; Curran, J.; Bell, S.; Trejos, T. Evaluation of Organic and Inorganic Gunshot Residues in Various Populations Using LC-MS/MS. *SSRN Electron. J.* **2021**, *27* (October 2021). https://doi.org/10.2139/ssrn.3945297.

(101) Menking-Hoggatt, K.; Martinez, C.; Vander Pyl, C.; Heller, E.; Pollock, E. "Chip"; Arroyo, L.; Trejos, T. Development of Tailor-Made Inorganic Gunshot Residue (IGSR) Microparticle Standards and Characterization with a Multi-Technique Approach. *Talanta* **2021**, *225*, 13. https://doi.org/10.1016/j.talanta.2020.121984.

(102) Dalzell, K. A.; Ott, C. E.; Trejos, T.; Arroyo, L. E. Comparison of Portable and Benchtop Electrochemical Instruments for Detection of Inorganic and Organic Gunshot Residues in

Authentic Shooter Samples. *J. Forensic Sci.* **2022**. https://doi.org/10.1111/1556-4029.15049.

(103) Sauzier, G.; Van Bronswijk, W.; Lewis, S. W. Chemometrics in Forensic Science: Approaches and Applications. *Analyst* **2021**, *146* (8), 2415–2448. https://doi.org/10.1039/d1an00082a.

(104) Sugano, Y.; Latonen, R. M.; Akieh-Pirkanniemi, M.; Bobacka, J.; Ivaska, A. Electrocatalytic Oxidation of Cellulose at a Gold Electrode. *ChemSusChem* **2014**, *7* (8), 2240–2247. https://doi.org/10.1002/cssc.201402139.

(105) Liu, Q.; Chen, Z.; Jing, S.; Zhuo, H.; Hu, Y.; Liu, J.; Zhong, L.; Peng, X.; Liu, C. A Foldable Composite Electrode with Excellent Electrochemical Performance Using Microfibrillated Cellulose Fibers as a Framework. *J. Mater. Chem. A* **2018**, *6* (41), 20338–20346. https://doi.org/10.1039/c8ta06635c.

(106) WVU IRB Protocol 1506706336. West Virginia University: Morgantown 2018.

(107) Mocák, J.; Janiga, I.; Rábarová, E. Evaluation of IUPAC Limit of Detection and ISO Minimum Detectable Value - Electrochemical Determination of Lead. *Nov. Biotechnol. Chim.* **2021**, *9* (1), 91–100. https://doi.org/10.36547/nbc.1291.

(108) Lavagnini, I.; Antiochia, R.; Magno, F. A Calibration-Base Method for the Evaluation of the Detection Limit of an Electrochemical Biosensor. *Electroanalysis* **2007**, *19* (11), 1227–1230. https://doi.org/10.1002/elan.200703847.

(109) Gamry Instruments. Understanding the Specifications of Your Potentiostat. *Tech. Note* **2016**, 1–6.

(110) Colburn, A. W.; Levey, K. J.; O'Hare, D.; Macpherson, J. V. Lifting the Lid on the Potentiostat: A Beginner's Guide to Understanding Electrochemical Circuitry and Practical Operation. *Phys. Chem. Chem. Phys.* **2021**, *23* (14), 8100–8117. https://doi.org/10.1039/d1cp00661d.

APPENDICES

APPENDIX I. LITERATURE REVIEW

Table S1.1. *Common IGSR and OGSR elements and compounds, CAS Numbers, molecular formulas, structures, and molecular weights.*
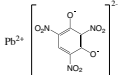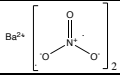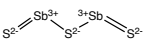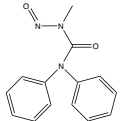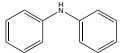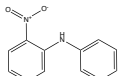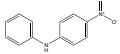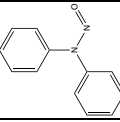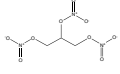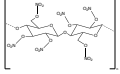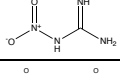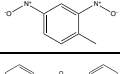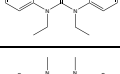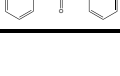
Analyte	Molecular Formula	Structure	Molecular Weight
IGSR			
Lead Styphnate CAS: 15245-44-0	$C_6HN_3O_8Pb$		450.9
Copper CAS: 4770-50-8	Cu	Cu	63.5
Barium Nitrate CAS: 10022-31-8	$Ba(NO_3)_2$		261.3
Antimony Sulfide CAS: 12627-52-0	Sb_2S_3		153.8
OGSR			
Akardite II CAS: 13114-72-2	$C_{14}H_{14}N_2O$		226.2
Diphenylamine CAS: 122-39-4	$C_{12}H_{11}N$		169.2
2-nitrodiphenylamine CAS: 119-75-5	$C_{12}H_{10}N_2O_2$		214.2
4-nitrodiphenylamine CAS: 836-30-6	$C_{12}H_{10}N_2O_2$		214.2
N-nitrosodiphenylamine CAS: 86-30-6	$C_{12}H_{10}N_2O$		198.2
Nitroglycerin CAS: 55-63-0	$C_3H_5N_3O_9$		227.0
Nitrocellulose CAS: 9004-70-0	$(C_{18}H_{21}N_{11}O_{38})_n$		999.4
Nitroguanidine CAS: 556-88-7	$CH_4N_4O_2$		104.0
2,4-Dinitrotoluene CAS: 121-14-2	$C_7H_6N_2O_4$		182.1
Ethyl Centralite CAS: 85-98-3	$C_{17}H_{20}N_2O$		268.3
Methyl Centralite CAS: 611-92-7	$C_{15}H_{16}N_2O$		240.3

Table S1.2. *Summary of 34 manuscripts for OGSR frequency reported in literature from section 1.1.2.*

Author	Year	Sampling	Collection Media	Instrumentation	IGSR/ OGSR Analytes	Concentration/Particle Counts
Mach et al.	1978	Hands, Clothing	Swab, Flakes	GCMS	NG, 2,4-DNT, DPA, DBP, EC, 2,6-DNT, 2-NDPA, 4-NDPA	20 pg for DPA
Bratin et al.	1981	Explosives/Propellants	N/A	LC, Electrochemistry (CV)	HMX, Picric acid, RDX, Tetryl, TNT, NG, 2,4-DNT, 2,6-DNT, PETN	DPA & derivatives by EC 0.039-0.082 ng
Bergens et al.	1985	Propellants	N/A	Electrochemistry (DPV)	AKII, EC, DPA	1-100μM
Wu et al.	1999	Hands	Swab	MS-MS	MC	60 pg
MacCrehan et al.	1999	Nasal Mucus	Nylon Mesh	CE	NG, EC, MC, DPA, 2,4-DNT, 2,6-DNT	NR
Tong et al.	2001	Propellants	N/A	MS-MS	DPA, 4-NPDA, N-NDPA	0.5-2.5 ng/mL
Zeichner et al.	2003	Clothing	Vacuum Filter	GC-TEA, IMS, GCMS	NG, 2,4-DNT, 2,6-DNT, DPA, EC, dinitro-DPA, nitroso-DPA	IMS: 0.3 ng GC-TEA: 0.05-1 ng GCMS: low ng levels
Zeichner et al.	2004	Hands/Hair	Double Sided Tape	GC-TEA, IMS	NG, 2,4-DNT, 2,6-DNT, DPA, EC, dinitro-DPA, nitroso-DPA	GC: 0.1-1 ng IMS: NR
West et al.	2006	Propellants		IMS	DPA & derivatives, EC, TNT, NG, 2,4-DNT, 2,6-DNT	
Laza et al.	2007	Hands	Swab	LC-MS/MS	DPA, AKII, 2-NDPA, 4-NDPA, EC, MC, N-NDPA	low ng levels
Zhao et al.	2008	Hands/Hair	NR	DESI-MS/MS	EC, MC	8-70 pg/cm^3
Sharma et al.	2009	Clothing	KBr pellet	micro-FTIR	NG	
Joshi et al.	2011	Propellants		GCMS, GC-μED, IMS	DPA, EC, MC, 2,4-DNT, DBP, DEP, 2-NDPA, 4-NDPA	NR
Salles et al.	2012	Hands	Swab	Electrochemistry (CV)	2,4-DNT	NR
Morelato et al.	2012	Hands	Carbon Adhesive	DESI-MS, SEM-EDS	IGSR: Pb, Ba, Sb, Cu, Al, Ca, Sr, Ti, Zn Pb, Sb, Cu, OGSR: MC, EC, DPA	DESI-MS: NR
Cetó et al.	2012		Abrasive	Electrochemistry (SWV)	DPB, DPA, NG	NR
O'Mahony et al.	2012	Hands	Carbon Sensor Strips	Electrochemistry (AbrSV)	Pb, Sb, Cu	NR
López-López et al.	2012	Propellants	N/A	Raman microscope	DPA, N-NDPA, 2-NDPA, 4-NDPA, EC	NR
Bueno et al.	2012	Clothing	N/A	NIR-Raman micro spectroscopy	IGSR: Ba, Pb, OGSR: 2,4-DNT, nitrate ester	NR
Arndt et al.	2012	Hands	Cloth Acetone	IMS	DMP, DPA, N-NDPA, 2,2-DNDPA, 4,4-DNDPA	10 ng
Moran et al.	2013	Hands	PDMS Membrane	IMS	DPA, 2-NDPA, EC, N-NDPA	NR
López-López et al.	2013	Paper Targets	N/A	Raman microscope	DPA, N-NDPA, 2-NDPA, 4-NDPA, EC	NR
Abrego et al.	2014	Hands	Carbon Adhesive	LA-ICP-MS, micro-Raman	IGSR: Cu, Al, Sn, Zr, Ti, Sr OGSR: MC, EC, DPA and derivates,	NR
Bueno et al.	2014	Clothing	Tape Lift	μATR-FTIR	IGSR & OGSR	NR
Yeager et al.	2015	Hands	Swab	IMS	EC, MC, DMT, DPA	1-100 ng
López-López et al.	2015	Clothing	Carbon Adhesive	Raman microscope	OGSR	
Tarifa et al.	2015	Hands	Carbon Adhesive	CMV GC-MS, LIBS, ICP-OES	IGSR: Pb, Ba, Sb, Al, Ca, Cu, Cr, Fe, K, Li, Mg, Mn, Ni, P, S, Si, Sn, Sr, Ti, Zn OGSR: NG- 2,4-DNT, DPA	3.1-8.2 ng, 65-782 ng, 21-9767 ng

|						
Stevens et al.	2016	Hands	Cotton Swab	TD-GCMS	DMP, 2,4-DNT, DPA, MC, Carbazole, EC, DBP, 2-NDPA, 4-NDPA	0.05-0.5 ng
Ali et al	2016	Vehicles	Carbon Adhesive	LC-MS/MS, SEM-EDS	IGSR: Pb, Ba, Sb, Zn OGSR: AK II, EC, DPA, N-NDPA, 2-NDPA, 4-NDPA, NG, 2,4-DNT	1.16E-4-4.65E-4 µg/mL
Gandy et al.	2018	Ammunition	N/A	Color Tests: 4-Nitrosophenol, Nitric Acid, Sodium borohydride, LIBS, Electrochemistry (SWV)	DPA, Resorcinol, MC, EC, TNT, Carbazole	0.1-5 ng
Trejos et al.	2018	Hands	Carbon Adhesive		IGSR: Pb, Ba, Sb, Cu, Al, Ca, Sr, Ti, Zn Pb, Sb, Cu OGSR: 2,4-DNT, NG, DPA, EC	0.1-440 ng, 0.1-1.0 mg/µL
Carneiro et al.	2019		N/A			
Bell et al.	2019	Hands	Tesa Tack	LC-MS/MS	IGSR: Pb, Ba, Fe, Ca OGSR: DPA, EC, MC, N-NDPA, 4-NDPA,	0.02-12 µg
Khandasammy et al.	2019	Clothing	Tape	Raman Microscope	OGSR particles	NR
Ott et al.	2020	Hands	Carbon Adhesive	Electrochemistry (SWV)	IGSR: Pb, Sb, Cu, OGSR: 2,4-DNT, NG, DPA, EC	0.012-0.462 µg/mL (MDL)
Gassner et al.	2020	Vehicles	Carbon Adhesive	UHPLC-MS	EC, MC, DPA, N-NDPA, 2-NDPA, 4-NDPA, AKII	0.005-0.2 ng/mL
Minzière et al.	2020	Hands	Carbon Adhesive	UHPLC-MS/MS SEM-EDX	AK II, EC, DPA, N-NDPA, 2-NDPA, 4-NDPA, NG, 2,4-DNT IGSR: Pb, Ba, Sb	0.005-10 ng/mL
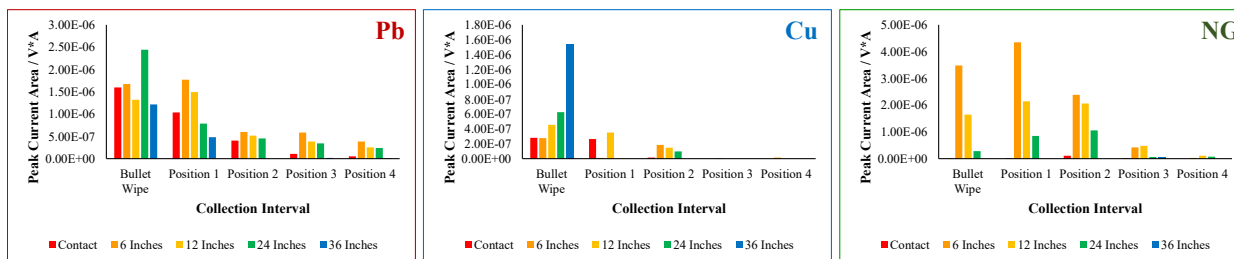
Figure S3.1. *Example bar graphs of lead (red), copper (blue), and nitroglycerin (green) peak current areas observed in a shooting distance calibration curve set 1 5 exhibiting the collection interval for the bullet wipe, position 1 (bullet wipe-2cm), position 2 (2-4cm), position 3 (4-6), and position 4 (6-8cm) on the x axis and the peak current area on the y axis where the shooting distance are color: contact (red), 6 (orange), 12 (yellow), 24 (green), and 36 (blue) inches.*
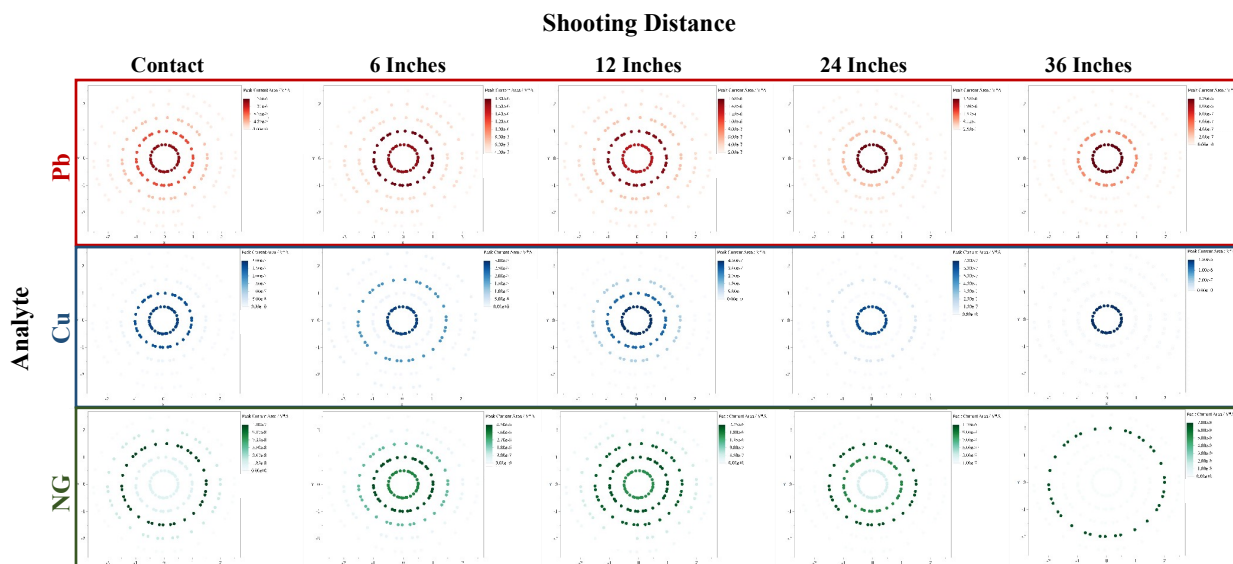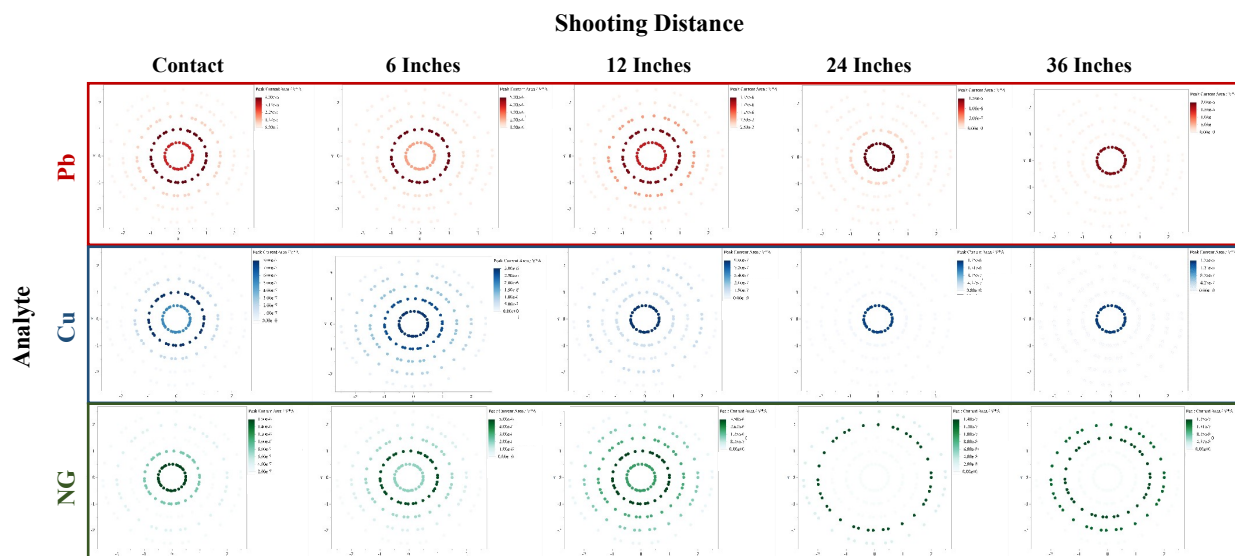

Figure S3.2. *Heat maps obtained for lead, copper, and nitroglycerin from calibration set 1 on white fabric, from left to right, contact, 6-, 12-, 24-, and 36-inch shooting distances.*
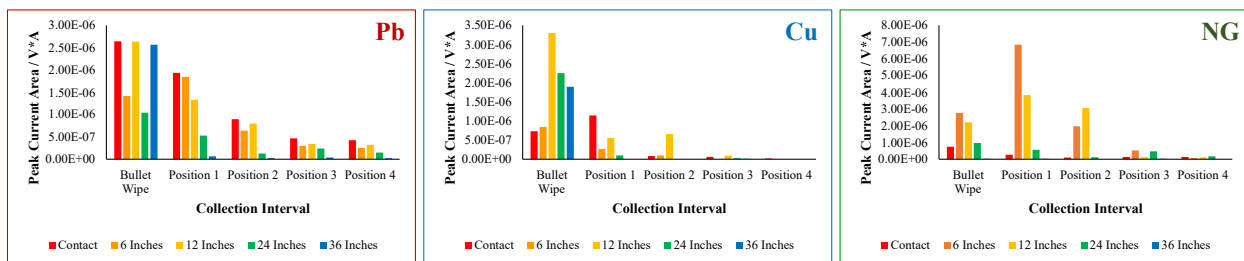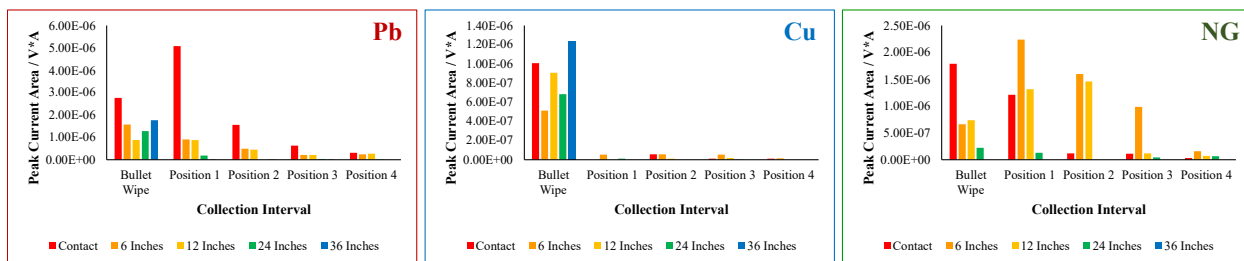
Figure S3.3. *Example bar graph of lead (red), copper (blue), and nitroglycerin (green) peak current areas observed in a shooting distance calibration curve set 2 5 exhibiting the collection interval for the bullet wipe, position 1 (bullet wipe-2cm), position 2 (2-4cm), position 3 (4-6), and position 4 (6-8cm) on the x axis and the peak current area on the y axis where the shooting distance are color: contact (red), 6 (orange), 12 (yellow), 24 (green), and 36 (blue) inches.*
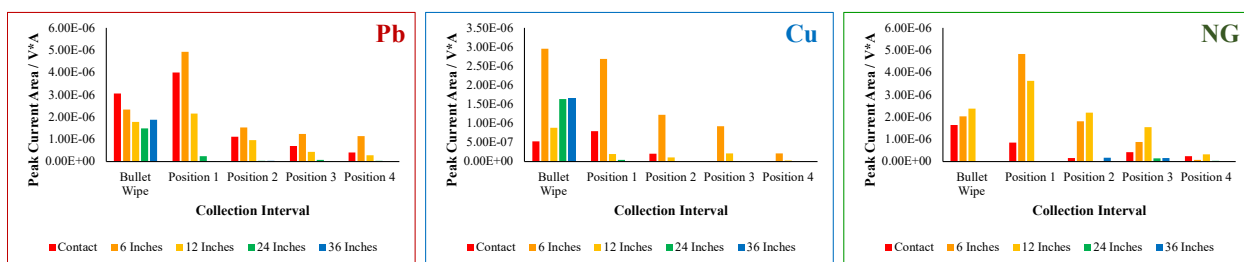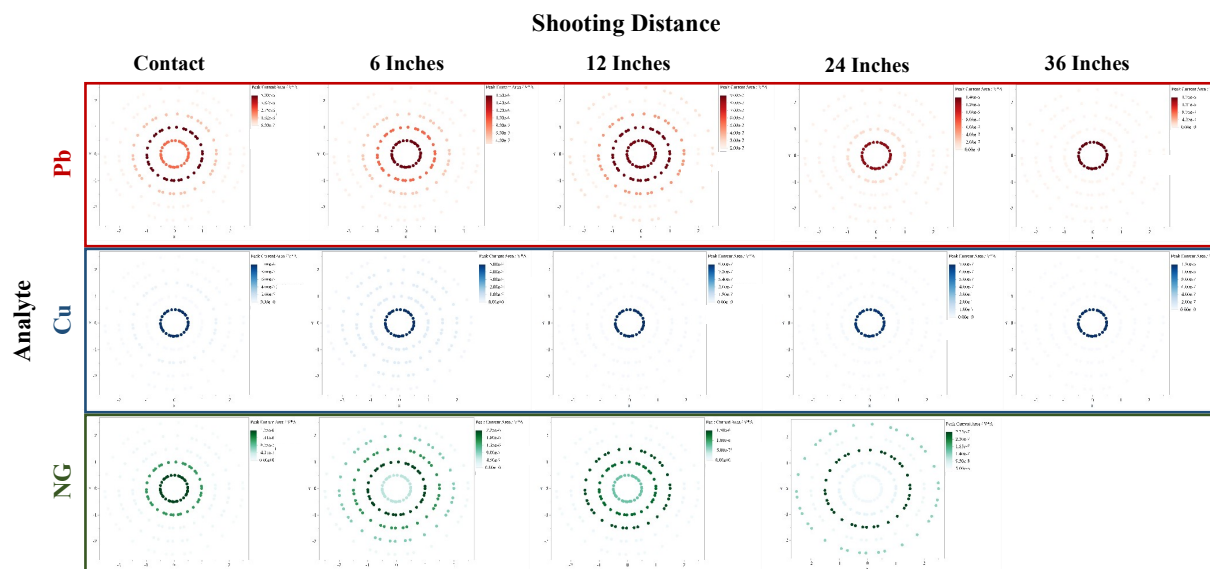

Figure S3.4. *Example bar graph of lead (red), copper (blue), and nitroglycerin (green) peak current areas observed in a shooting distance calibration curve set 3 5 exhibiting the collection interval for the bullet wipe, position 1 (bullet wipe-2cm), position 2 (2-4cm), position 3 (4-6), and position 4 (6-8cm) on the x axis and the peak current area on the y axis where the shooting distance are color: contact (red), 6 (orange), 12 (yellow), 24 (green), and 36 (blue) inches.*

Figure S3.5. *Heat maps obtained for lead, copper, and nitroglycerin from calibration set 3 on white fabric, from left to right, contact, 6-, 12-, 24-, and 36-inch shooting distances.*
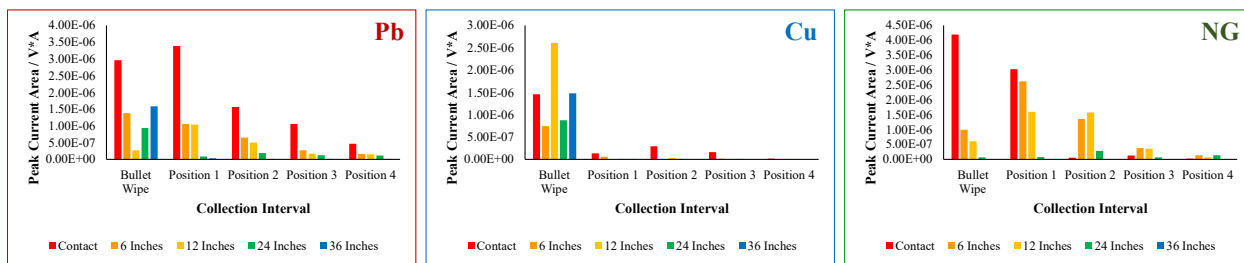
117

Figure S3.6. *Example bar graph of lead (red), copper (blue), and nitroglycerin (green) peak current areas observed in a shooting distance calibration curve set 4 5 exhibiting the collection interval for the bullet wipe, position 1 (bullet wipe-2cm), position 2 (2-4cm), position 3 (4-6), and position 4 (6-8cm) on the x axis and the peak current area on the y axis where the shooting distance are color: contact (red), 6 (orange), 12 (yellow), 24 (green), and 36 (blue) inches.*
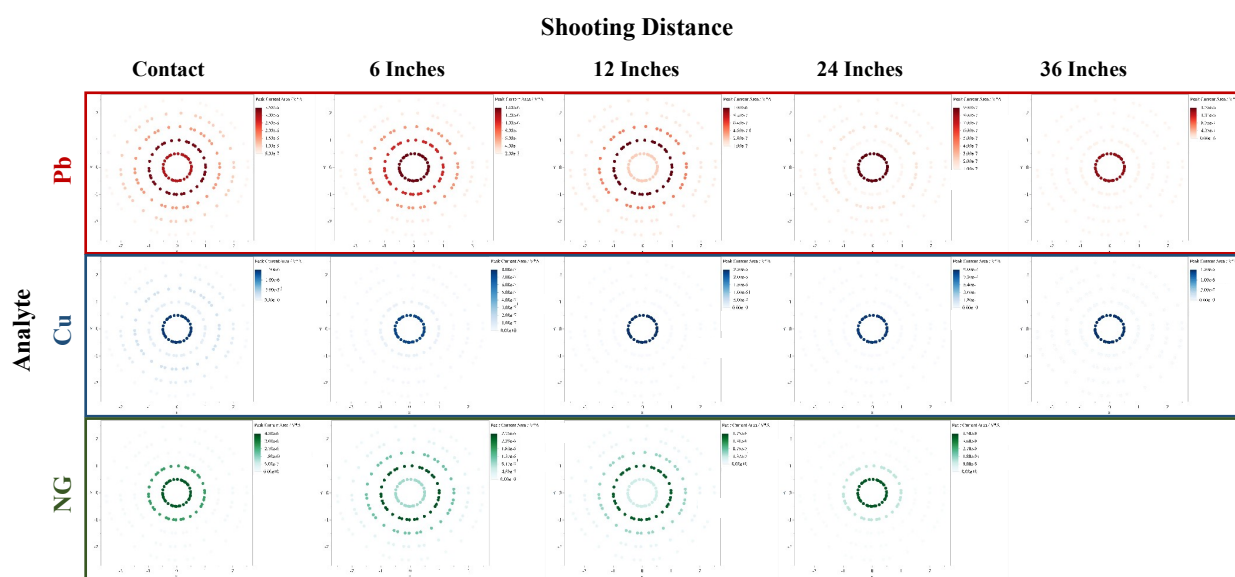

Figure S3.7. *Heat maps obtained for lead, copper, and nitroglycerin from calibration set 4 on white fabric, from left to right, contact, 6-, 12-, 24-, and 36-inch shooting distances.*
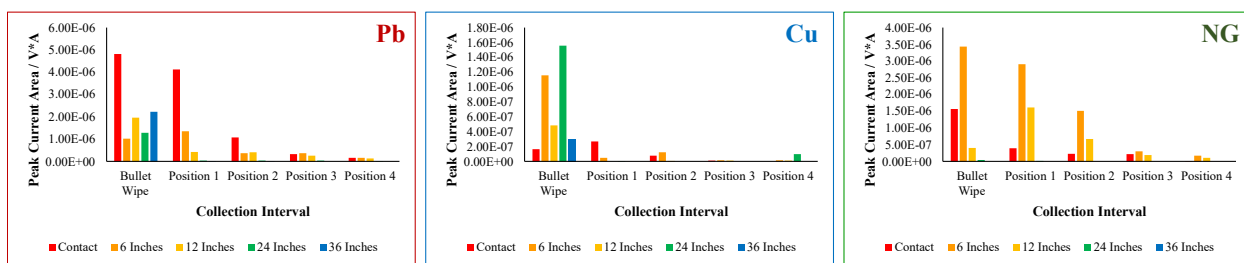
118

Figure S3.8. *Example bar graph of lead (red), copper (blue), and nitroglycerin (green) peak current areas observed in a shooting distance calibration curve set 5 exhibiting the collection interval for the bullet wipe, position 1 (bullet wipe-2cm), position 2 (2-4cm), position 3 (4-6), and position 4 (6-8cm) on the x axis and the peak current area on the y axis where the shooting distance are color: contact (red), 6 (orange), 12 (yellow), 24 (green), and 36 (blue) inches.*
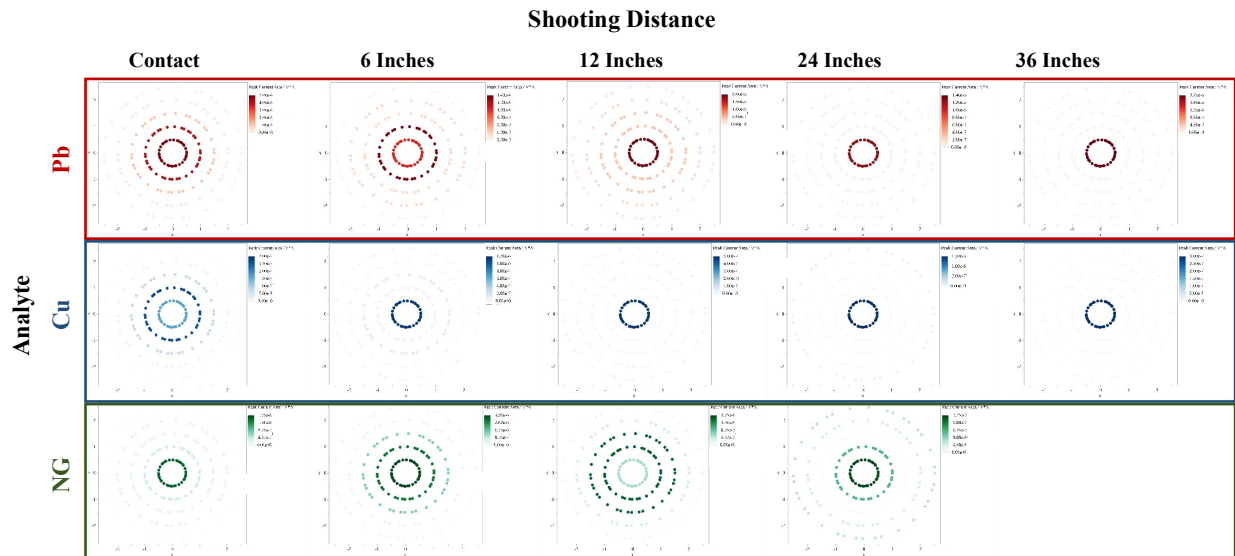

Figure S3.9. *Heat maps obtained for lead, copper, and nitroglycerin from calibration set 5 on white fabric, from left to right, contact, 6-, 12-, 24-, and 36-inch shooting distances.*
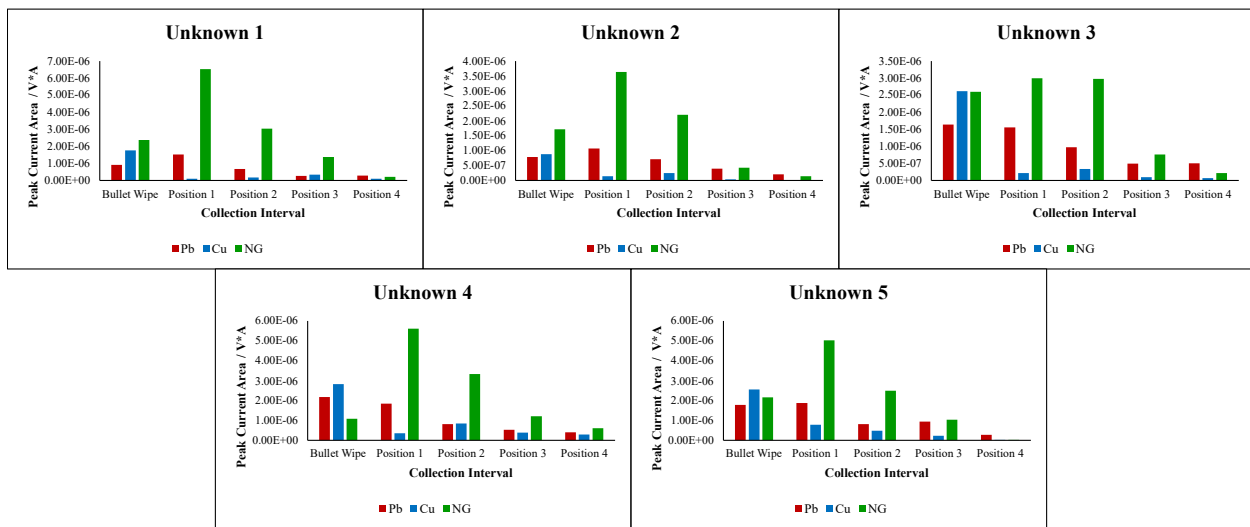

Figure S3.10. *Example bar graph of lead (red), copper (blue), and nitroglycerin (green) peak current areas observed in a shooting distance calibration curve set 6 exhibiting the collection interval for the bullet wipe, position 1 (bullet wipe-2cm), position 2 (2-4cm), position 3 (4-6), and position 4 (6-8cm) on the x axis and the peak current area on the y axis where the shooting distance are color: contact (red), 6 (orange), 12 (yellow), 24 (green), and 36 (blue) inches.*

119

Figure S3.11. *Heat maps obtained for lead, copper, and nitroglycerin from calibration set 6 on white fabric, from left to right, contact, 6-, 12-, 24-, and 36-inch shooting distances.*

Figure S3.12. *Example bar graph of lead (red), copper (blue), and nitroglycerin (green) peak current areas observed in a white unknown 1-5 exhibiting the collection interval for the bullet wipe, position 1 (bullet wipe-2cm), position 2 (2-4cm), position 3 (4-6), and position 4 (6-8cm) on the x axis and the peak current area on the y axis.*
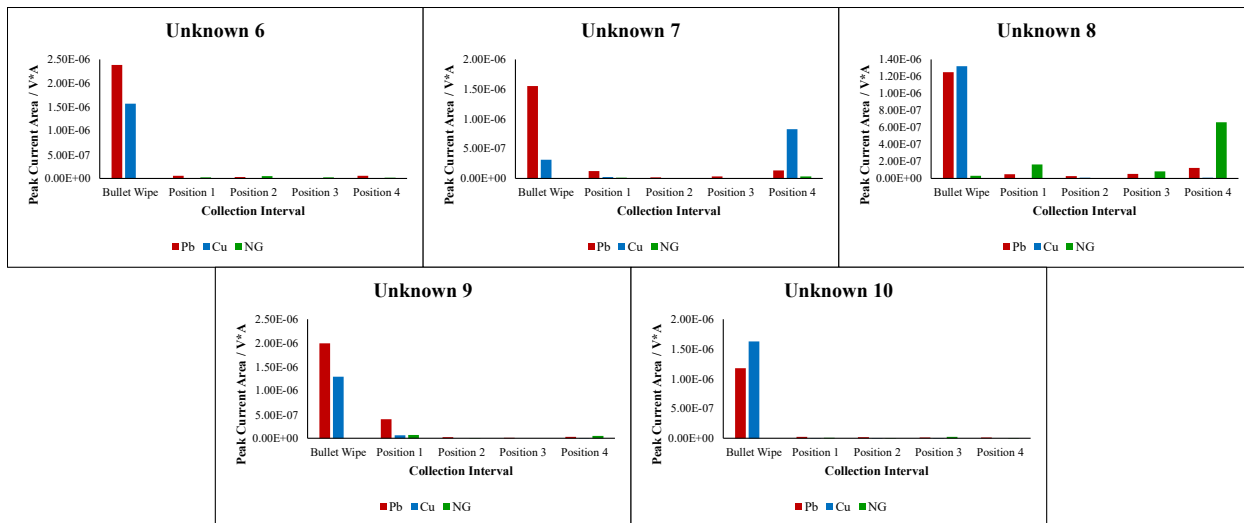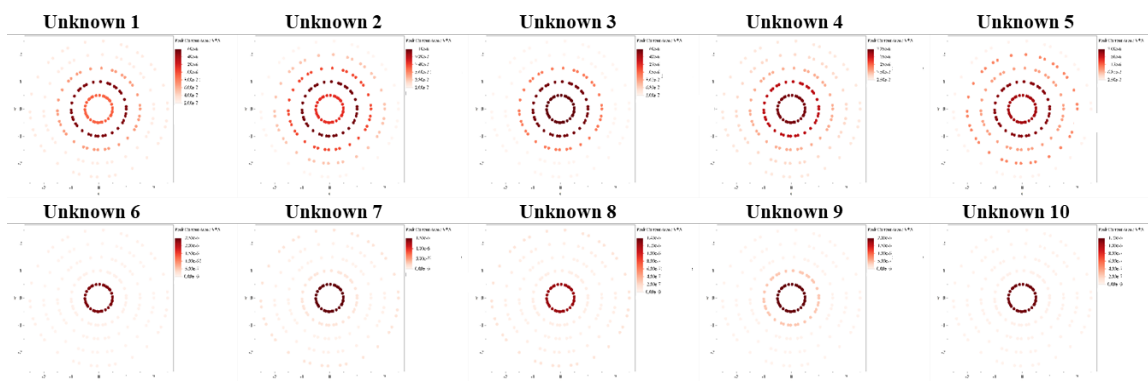
Figure S3.13. *Example bar graph of lead (red), copper (blue), and nitroglycerin (green) peak current areas observed in a white unknown 6-10 exhibiting the collection interval for the bullet wipe, position 1 (bullet wipe-2cm), position 2 (2-4cm), position 3 (4-6), and position 4 (6-8cm) on the x axis and the peak current area on the y axis.*

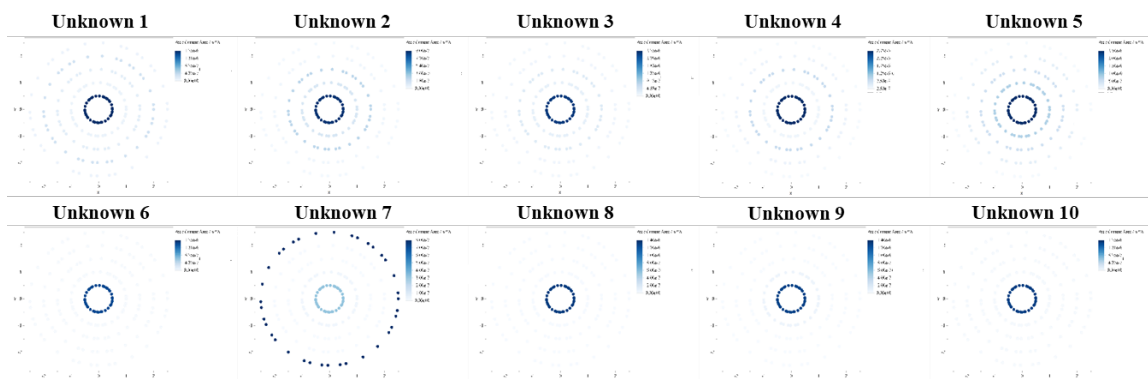***Figure S3.14.*** *Heat maps obtained from lead peak current area for white unknowns 1-10.*

Figure S3.15. *Heat maps obtained from copper peak current area for white unknowns 1-10.*
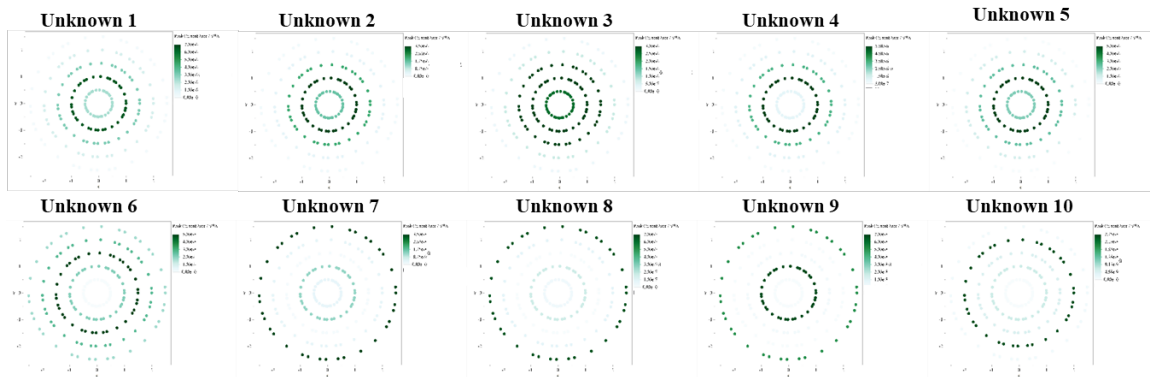
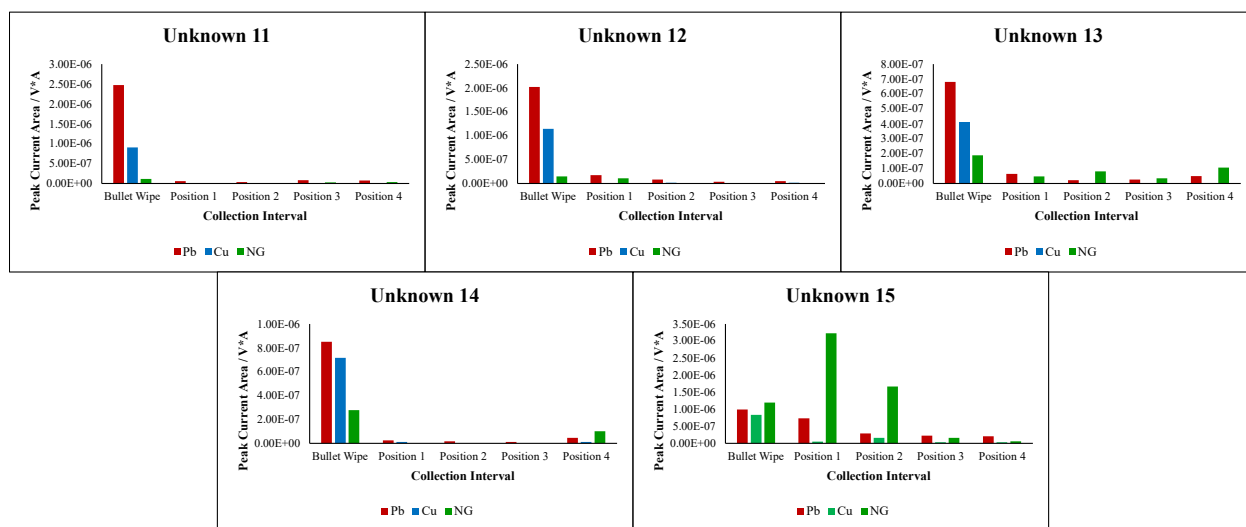***Figure S3.16.*** *Heat maps obtained from nitroglycerin peak current area for white unknowns 1-10.*

Figure S3.17. *Example bar graph of lead (red), copper (blue), and nitroglycerin (green) peak current areas observed in an orange unknown 11-15 exhibiting the collection interval for the bullet wipe, position 1 (bullet wipe-2cm), position 2 (2-4cm), position 3 (4-6), and position 4 (6-8cm) on the x axis and the peak current area on the y axis.*

Figure S3.18. *Heat maps obtained from lead (top), copper (middle) and nitroglycerin (bottom) peak current areas for orange unknowns 11-15.*

Figure S3.19. *Example bar graph of lead (red), copper (blue), and nitroglycerin (green) peak current areas observed in red unknown 16-20 exhibiting the collection interval for the bullet wipe, position 1 (bullet wipe-2cm), position 2 (2-4cm), position 3 (4-6), and position 4 (6-8cm) on the x axis and the peak current area on the y axis.*
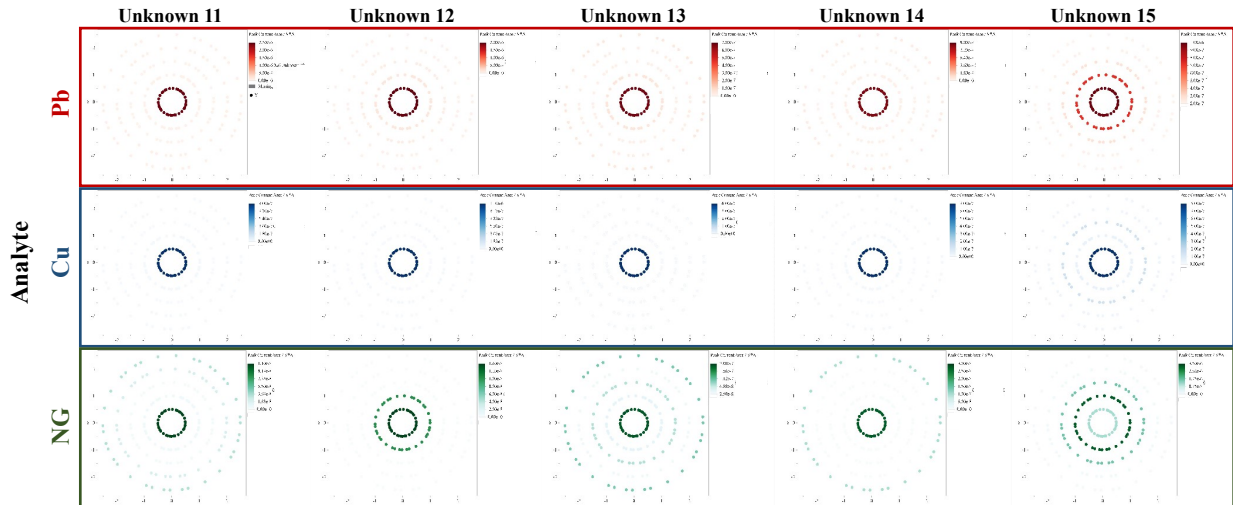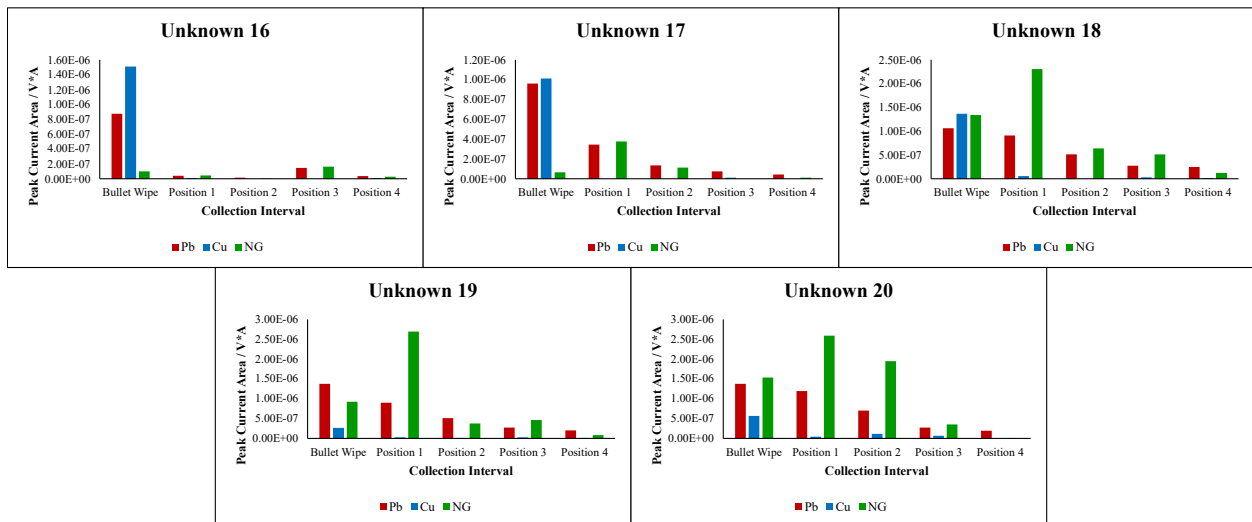
Figure S3.20. *Heat maps obtained from lead (top), copper (middle) and nitroglycerin (bottom) peak current areas for red unknowns 16-20.*

Figure 3.21. *Example bar graph of lead (red), copper (blue), and nitroglycerin (green) peak current areas observed in navy unknown 21-25 exhibiting exhibiting the collection interval for the bullet wipe, position 1 (bullet wipe-2cm), position 2 (2-4cm), position 3 (4-6), and position 4 (6-8cm) on the x axis and the peak current area on the y axis.*
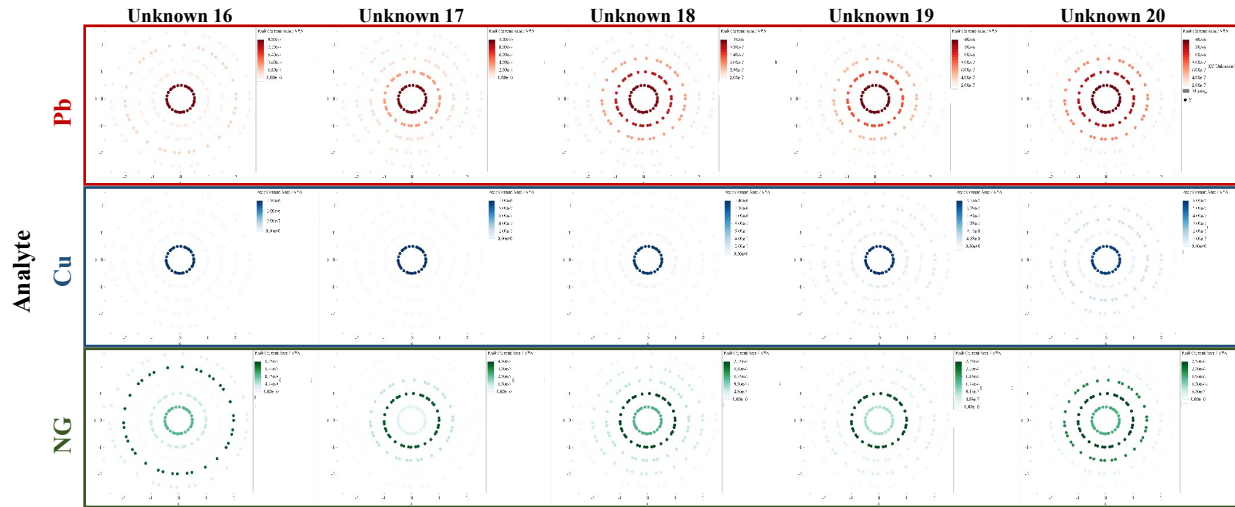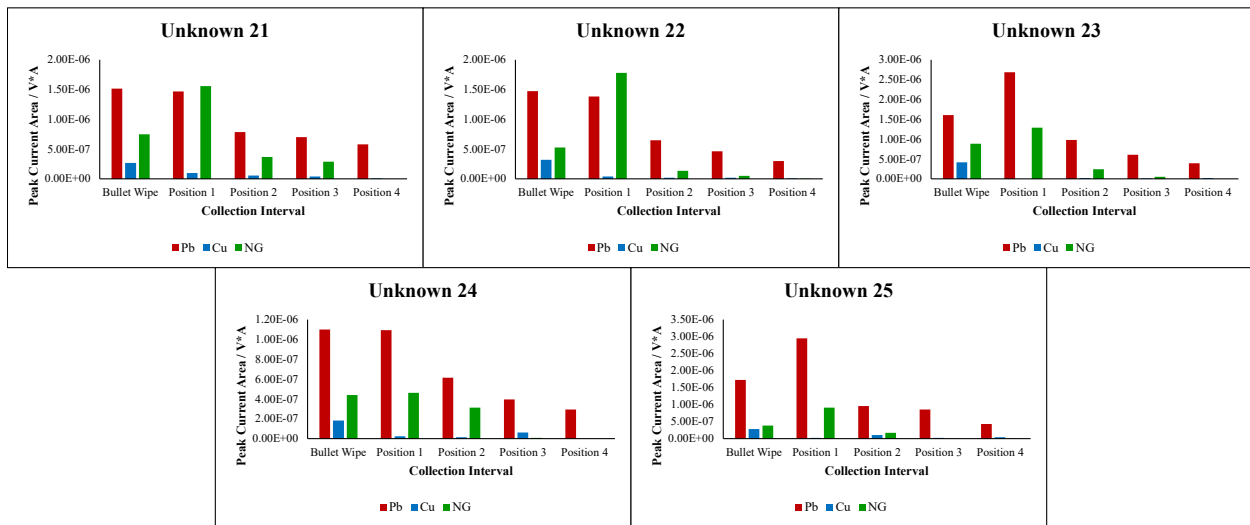
Figure S3.22. *Heat maps obtained from lead (top), copper (middle) and nitroglycerin (bottom) peak current areas for navy unknowns 21-25.*

Figure S3.23. *Example bar graph of lead (red), copper (blue), and nitroglycerin (green) peak current areas observed in dark pattern unknown 26-30 exhibiting the collection interval for the bullet wipe, position 1 (bullet wipe-2cm), position 2 (2-4cm), position 3 (4-6), and position 4 (6-8cm) on the x axis and the peak current area on the y axis.*

Figure S3.24. Heat maps obtained from lead (top), copper (middle) and nitroglycerin (bottom) peak current areas for dark pattern unknowns 26-30.

Figure S3.25. Example bar graph of lead (red), copper (blue), and nitroglycerin (green) peak current areas observed in light pattern unknown 31-35 exhibiting the collection interval for the bullet wipe, position 1 (bullet wipe-2cm), position 2 (2-4cm), position 3 (4-6), and position 4 (6-8cm) on the x axis and the peak current area on the y axis.
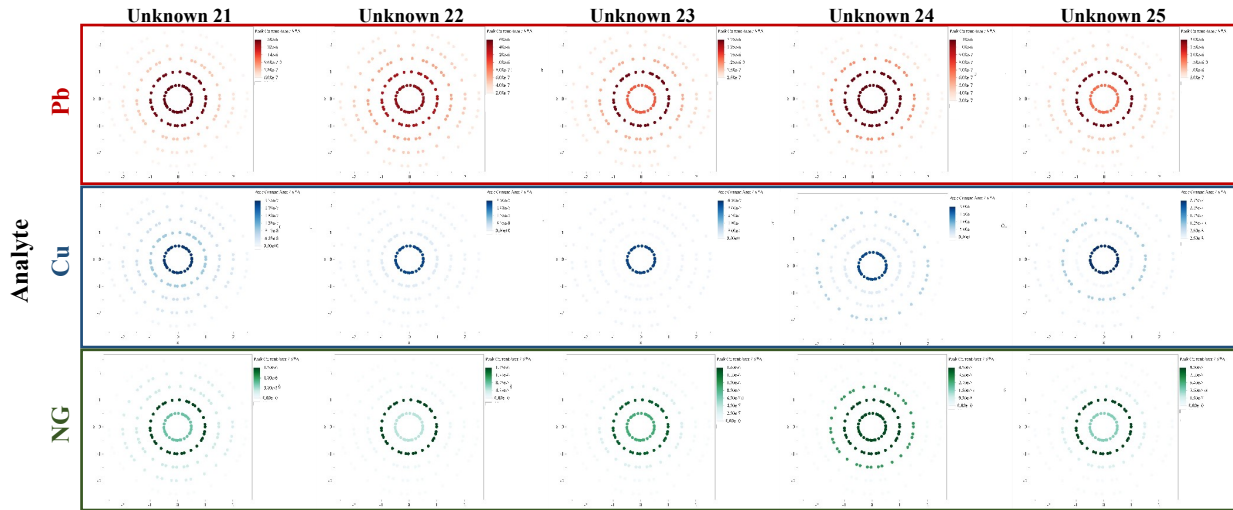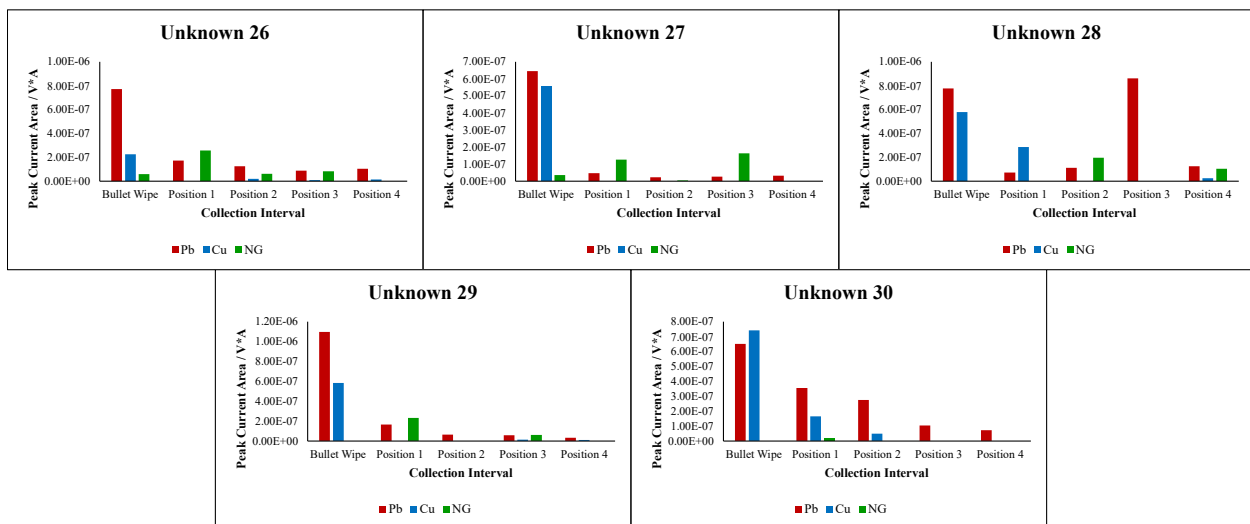
Figure S3.26. *Heat maps obtained from lead (top), copper (middle) and nitroglycerin (bottom) peak current areas for light pattern unknowns 31-35.*

Figure S3.27. *Example bar graph of lead (red), copper (blue), and nitroglycerin (green) peak current areas observed in blood-stained white unknown 36-40 exhibiting the collection interval for the bullet wipe, position 1 (bullet wipe-2cm), position 2 (2-4cm), position 3 (4-6), and position 4 (6-8cm) on the x axis and the peak current area on the y axis.*
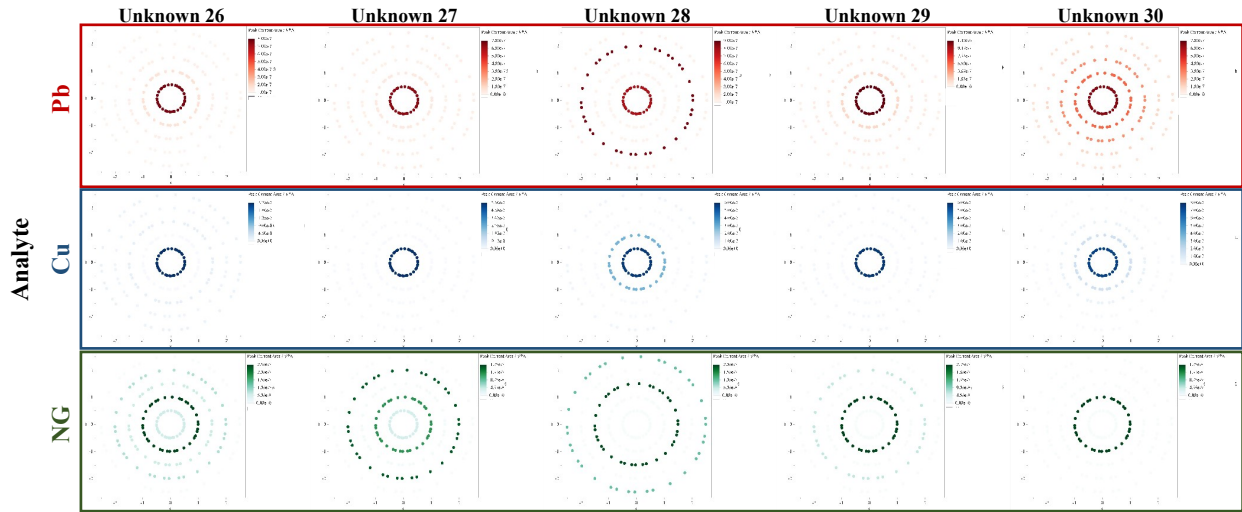
Figure S3.28. *Heat maps obtained from lead (top), copper (middle) and nitroglycerin (bottom) peak current areas for blood-stained white unknowns 36-40.*
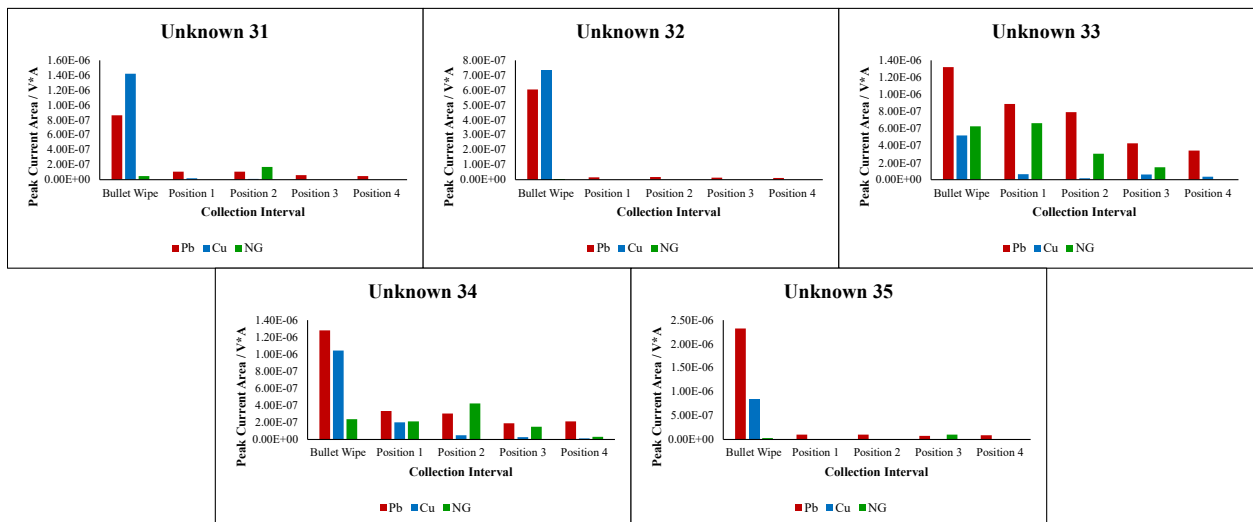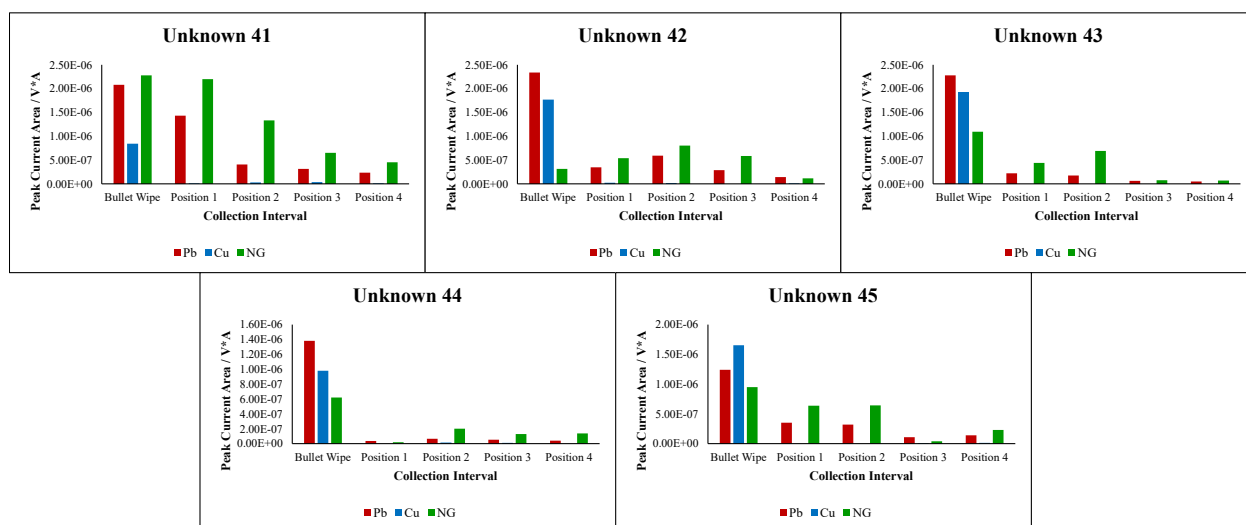

Figure S3.29. *Example bar graph of lead (red), copper (blue), and nitroglycerin (green) peak current areas observed in blood-stained white unknown 41-45 exhibiting the collection interval for the bullet wipe, position 1 (bullet wipe-2cm), position 2 (2-4cm), position 3 (4-6), and position 4 (6-8cm) on the x axis and the peak current area on the y axis.*
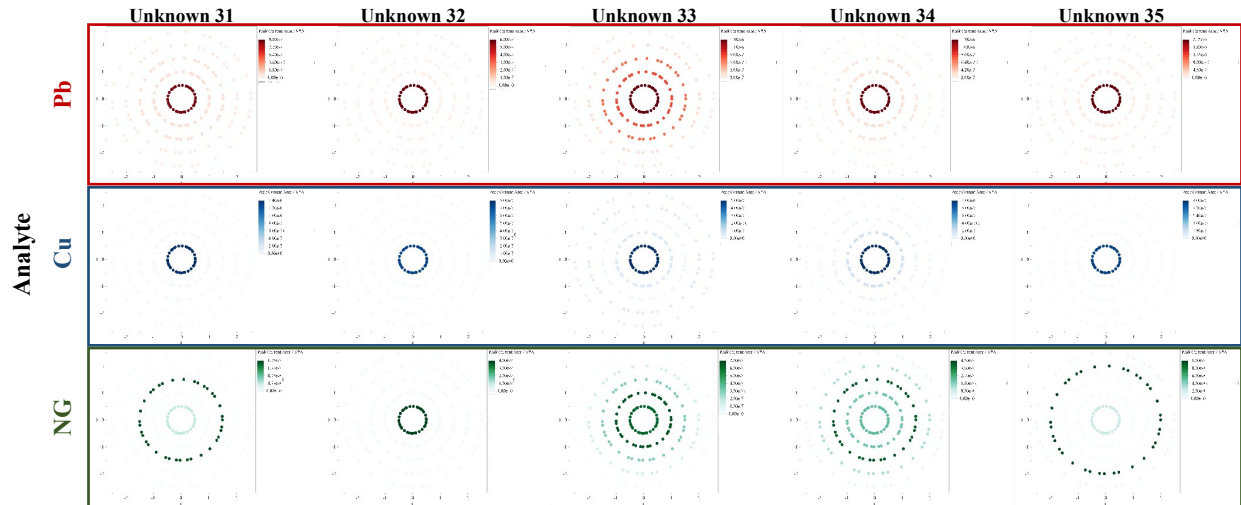
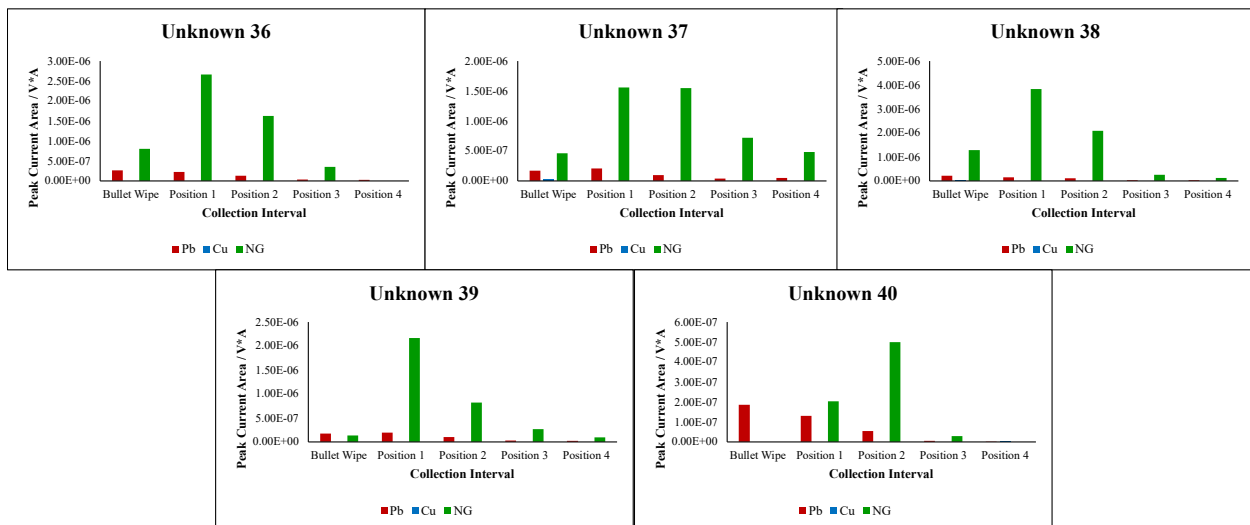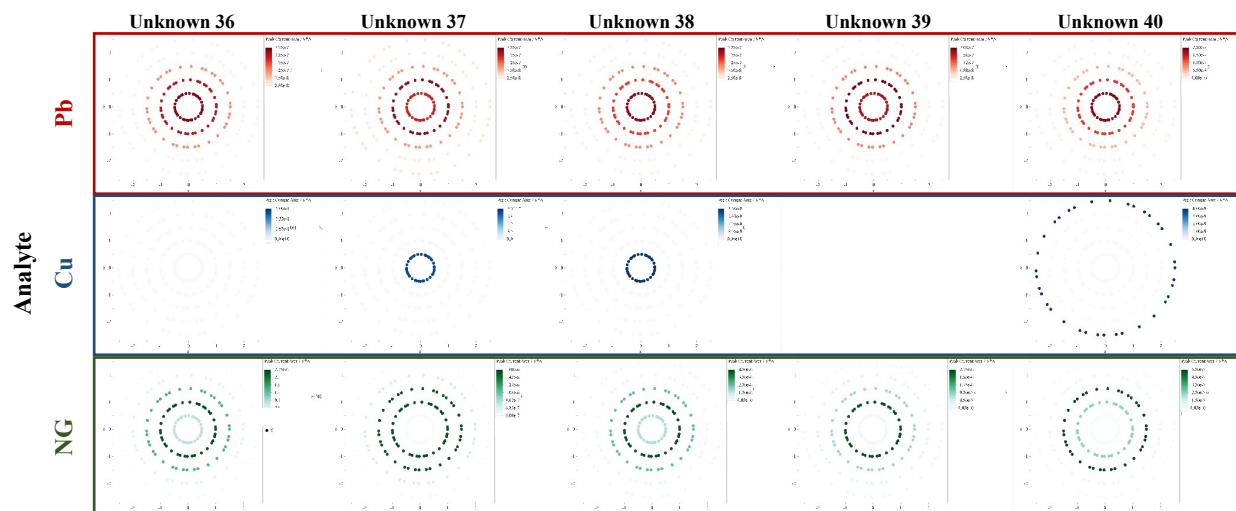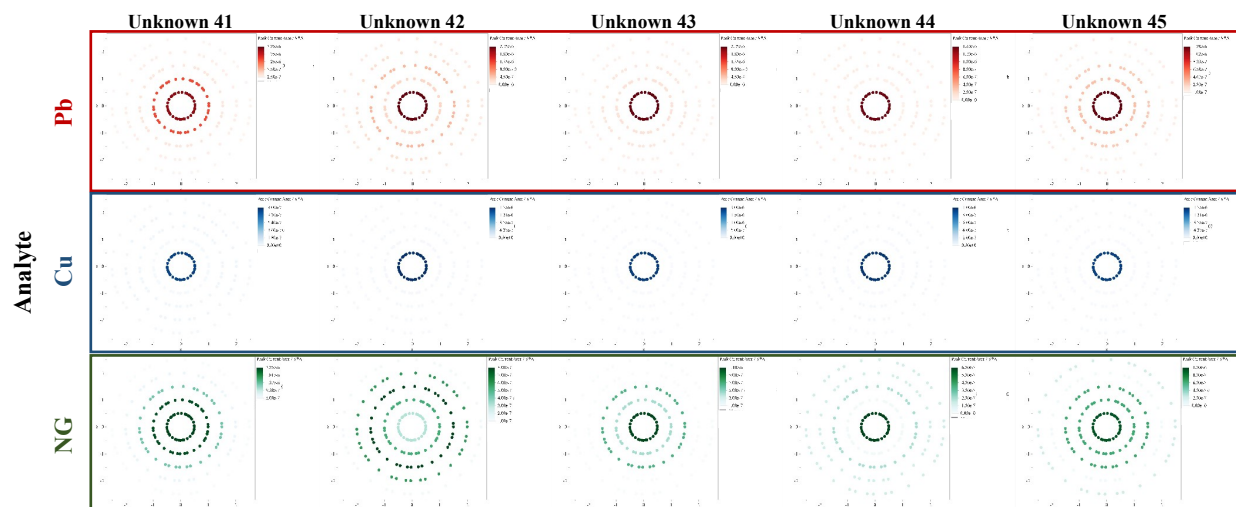***Figure S3.30.*** *Heat maps obtained from lead (top), copper (middle) and nitroglycerin (bottom) peak current areas for non-blood-stained white unknowns 41-45.*

APPENDIX III. CHAPTER 4: ELECTROCHEMICAL AND MASS SPECTROMETRY METHODS FOR BULLET HOLE IDENTIFICATION

Table S4.1. *Mobile phase gradient elution for the chromatograph of organic gunshot residues adapted from Feeney et al.*[98]

Time	Water w/ 0.1% FA (A%)	Acetonitrile w/ 0.1% FA (B%)
0.00	80	20
1.30	55	45
2.00	50	50
2.40	45	55
3.30	35	65
4.20	32	68
4.50	30	70
5.30	28	72
6.50	25	75
8.00	5	95
9.00	90	10

Table S4.2. *Mass spectrometry source parameters for detecting organic GSR adapted from Feeney et al.*[98]

Source Parameters	
Gas Temperature	300°C
Gas Flow	10.0 l/min
Nebulizer	20 psi
Sheath Gas Temperature	250°C
Sheath Gas Flow	7.0 l/min
Capillary	Positive: 4500 Negative: 2500
Nozzle	Positive/Negative: 2000
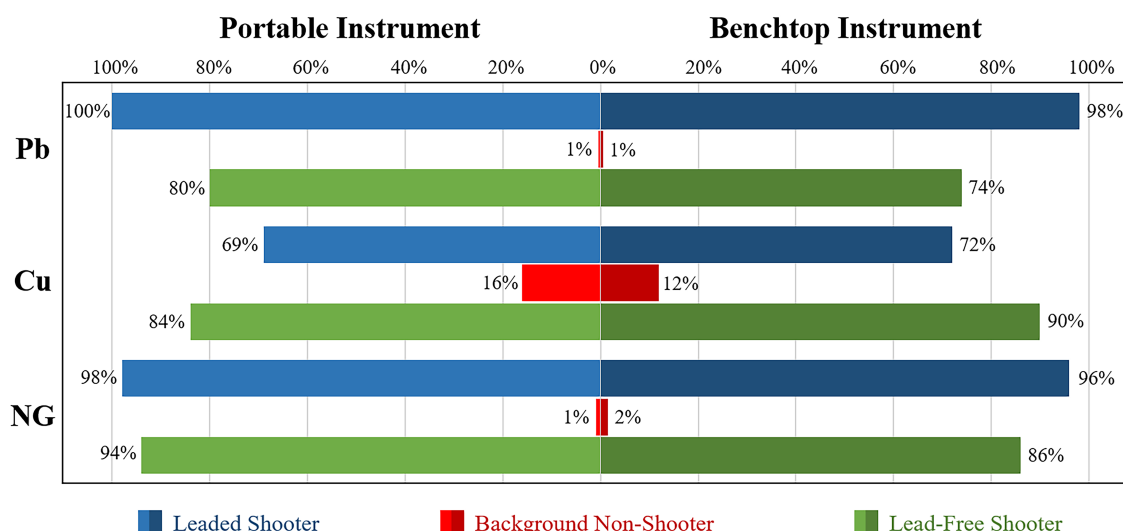
Figure S5.1. *Graphical comparison between the positive analyte identifications from the leaded and lead-free shooter and low-risk background populations for both the portable PalmSens4 instrument and benchtop Autolab instrument with the inclusion of the lead signals for the lead-free ammunition.*
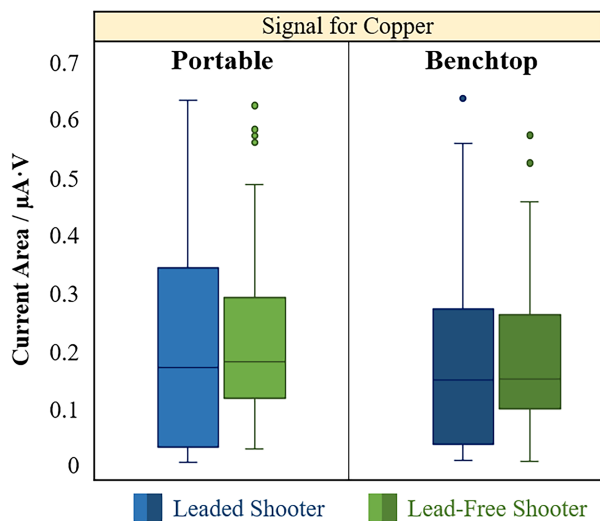
Figure S5.2. *Box plot comparison of the copper peak current area signal between leaded and lead-free populations for the benchtop and portable potentiostats.*
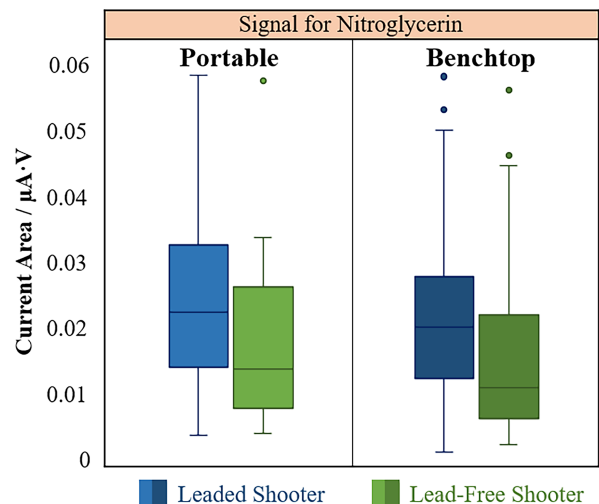
Figure S5.3. *Box plot comparison of the nitroglycerin peak current area signal between leaded and lead-free populations for the benchtop and portable potentiostats.*
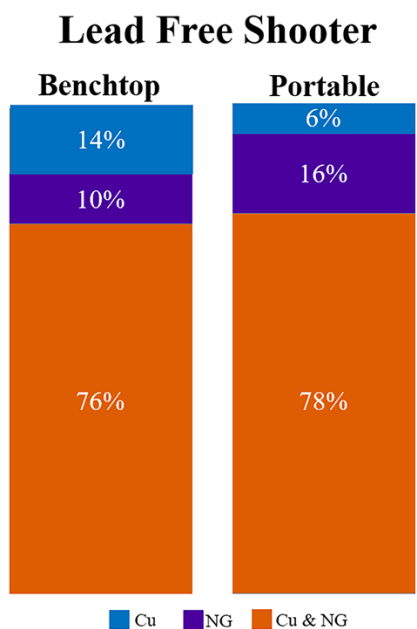
Figure S5.4. *Comparison between the benchtop and portable potentiostats for positive call combination of Cu+NG (orange) and for samples demonstrating only a single analyte Cu (blue) and NG (purple) in the lead-free shooter population.*

Table S5.1. *Comparison of positive GSR calls above critical threshold for Pb, Cu, and NG for the low-risk background and leaded shooter populations between the benchtop (green) and portable (blue) instrumentation.*

Background and Shooter Samples Positive Peak Calls Summary						
	Metrohm Benchtop Instrument			PalmSens4 Portable Instrument		
Overall	**Background Non-shooter**	**Leaded Shooter**	**Lead Free Shooter**	**Background Non-shooter**	**Leaded Shooter**	**Lead Free Shooter**
Sets	200	100	50	200	100	50
Pb Above Threshold	1 (1%)	98 (98%)	37 (74%)	1 (1%)	100 (100%)	40 (80%)
Cu Above Threshold	24 (12%)	72 (72%)	45 (90%)	32 (16%)	69 (69%)	42 (84%)
NG Above Threshold	3 (2%)	96 (96%)	43 (86%)	2 (1%)	98 (98%)	47 (94%)

APPENDIX V. COMPARISON OF PORTABLE AND BENCHTOP ELECTROCHEMICAL INSTRUMENTS FOR DETECTION OF INORGANIC AND ORGANIC GUNSHOT RESIDUES IN AUTHENTIC SHOOTER SAMPLES

The following appendix is the full, copyrighted version of the article referenced in Section 5.1.

JOURNAL OF
FORENSIC SCIENCES ⬡ AAFS

Comparison of portable and benchtop electrochemical instruments for detection of inorganic and organic gunshot residues in authentic shooter samples

Kourtney A. Dalzell BS ⬤ | **Colby E. Ott MS** ⬤ | **Tatiana Trejos PhD** ⬤ |
Luis E. Arroyo PhD ⬤

Department of Forensic and Investigative Science, West Virginia University, Morgantown, West Virginia, USA

Correspondence
Luis E. Arroyo, PhD, Department of Forensic and Investigative Science, West Virginia University, Morgantown, WV, 26506, USA.
Email: luis.arroyo@mail.wvu.edu

Abstract

Analysis of gunshot residue currently lacks effective screening methods that can be implemented in real time at the crime scene. Historically, SEM-EDS has been the standard for analysis; however, advances in technology have brought portable instrumentation to the forefront of forensic science disciplines, including the screening of GSR. This study proposes electrochemical methods with disposable screen-printed carbon electrodes for GSR screening at the laboratory and points of care due to their rapid, cost-efficient, and compact platform. GSR residues were extracted from typical aluminum/carbon adhesive collection stubs and analyzed via square-wave anodic stripping voltammetry. Benchtop and portable electrochemical instruments were compared for the assessment and classification of authentic shooter samples by monitoring a panel of inorganic and organic GSR elements and compounds including lead, antimony, copper, 2,4-dinitrotoluene, diphenylamine, nitroglycerin, and ethyl centralite. The evaluation included the assessment of figures of merit and performance measures from quality controls, nonshooter, and shooter data sets. Samples collected from the hands of 200 background individuals (nonshooters), and shooters who fired leaded ammunition (100) and lead-free ammunition (50) were analyzed by the benchtop and portable systems with accuracies of 95.7% and 96.5%, respectively. The findings indicate that electrochemical methods are fast, sensitive, and specific for the identification of inorganic and organic gunshot residues. The portable potentiostat provided results comparable with the benchtop system, serving as a proof-of-concept to transition this methodology to crime scenes for a practical and inexpensive GSR screening that could reduce backlogs, improve investigative leads, and increase the impact of gunshot residues in forensic science.

KEYWORDS
authentic shooter samples, comparisons, electrochemistry, inorganic gunshot residue, organic gunshot residue, portable instruments, screen-printed carbon electrodes

Highlights

- Comparison of field-portable potentiostats versus benchtop instruments for GSR screening.
- Results showcase the ability of portable potentiostats for GSR screening at crime scenes.

- Disposable electrodes for GSR analysis on authentic nonshooter and shooter populations.
- Simultaneous IGSR and OGSR detection with both instruments, limits of detection below 600 μg/ml.
- Over 95% accuracy for both instruments, increasing the reliability of GSR identification.

1 | INTRODUCTION

The rapid expansion in the development and application of portable instruments represents a paradigm shift in forensic science concerning the analysis of crime-related evidence. As the body of scientific knowledge advances, work concerning the miniaturization of instruments and field-ready methods are at the forefront of investigations. However, the assessment of the analytical performance of such instruments must first be tested and compared with the standard method to ensure fit-for-purpose and quality of data. The assessment of gunshot residue (GSR) on the hands of a person of interest (POI) is currently confined to laboratory testing. The standard method for GSR is scanning electron microscopy/energy dispersive X-ray spectrometry (SEM-EDS), which has a large footprint and specialized equipment. According to the ASTM E1588-20 [1], this instrument is considered the gold standard for analysis due to its capacity to offer single-particle morphology and elemental composition. However, there are currently no consensus-based standard screening methods for GSR detection from a suspected shooter's hands, whether in the laboratory or the field.

While the majority of other forensic disciplines regularly perform presumptive tests, the lack of screening for GSR presents analytical and intelligence challenges mainly related to analysis time, loss of investigative leads, time spent analyzing negative samples, and the negative perception of the evidential value of GSR [2]. SEM-EDS analysis of GSR can take 2–8 h per sample, imposing unintentional restrictions on the speed of analytical results and the number of samples collected at the scene. Also, SEM-EDS provides elemental analysis only (IGSR), missing the rich information gained by organic gunshot residue (OGSR) as it has been suggested in recent works [3–11].

Gunshot residues are formed during the discharge of a firearm and deposited on nearby surfaces such as the hands of a shooter through the gaseous cloud emitted from the openings of the firearm [12–14]. The common inorganic constituents result from primer formulations (Pb, Ba, and Sb) and elements from the projectile and casing (Cu and Al), and others [5–7,14]. However, organic compounds and their combustion products also arise from gunpowder formulations, including nitroglycerin (NG), diphenylamine (DPA), 2,4-dinitrotoluene (DNT), and ethyl centralite (EC) to name a few [5–7,14]. While ASTM E1588-20 only outlines data analysis and classification of IGSR, the Organization of Scientific Area Committees for Forensic Science Gunshot Residue Subcommittee has proposed recommendations for classification

based on OGSR, as has Goudsmits et al. [8,10]. Similar to IGSR, the typical methods applied for the assessment of OGSR utilize laboratory-based instrumentation including GC–MS and LC–MS that may benefit from orthogonal screening tools to triage the samples that require confirmation [7,9,11]. Organic gunshot residue can lead to additional information about the presence of explosives and other common propellant ingredients; however, the persistence of these compounds is still a target in many studies, including where Gassner et al. found that OGSR compounds were lost faster from the hands of shooters than from clothing [4]. For this reason, an interest in the development of new and rapid analytical methods for gunshot residue has been ongoing since the 1970s [15].

With the growth in technological developments, the forensic community began investigating the applicability and versatility of portable instrumentation for the analysis of evidence at the scene of a crime in the early 2000s. The development of fast and reliable screening methods for on-site detection remains necessary in both the GSR discipline and other areas of forensic science ranging from seized drugs to explosives detection. While forensic laboratories can take weeks to months to process and report GSR evidence [16], portable instruments provide opportunities for fast triage and decrease the time between collection and analysis, reducing the extent of sample degradation and assisting with informed decisions. Forensic researchers have explored portable instruments like microchip electrophoresis, Raman, and mass spectrometry to speed up investigative processes [2]. Recently, electrochemical, LIBS, and LC–MS/MS methods have shown promise in detecting either IGSR, OGSR, or both [3,12-25]. Electrochemistry has been demonstrated by our research group and others to provide simultaneous identification of IGSR and OGSR through rapid and cost-efficient methods in less than 5–10 min per sample [14,17,26-31]. Electrochemical methods provide a cheap, practical, and portable platform that can be utilized in laboratories or crime scenes due to the small size and weight of the apparatus.

Our research group has demonstrated the capabilities of electrochemistry for differentiation between shooter and nonshooter samples in an authentic population composed of over 700 samples based on their IGSR and OGSR profiles [17]. However, these results were obtained using a benchtop potentiostat. Herein, we demonstrate the use of a portable potentiostat that fits in the user's hand for the assessment of 150 authentic shooter samples (100 leaded and 50 lead-free) and 200 authentic background (nonshooter) samples and compare the results to the validated benchtop method. Evaluation of the performance and comparison between the portable and
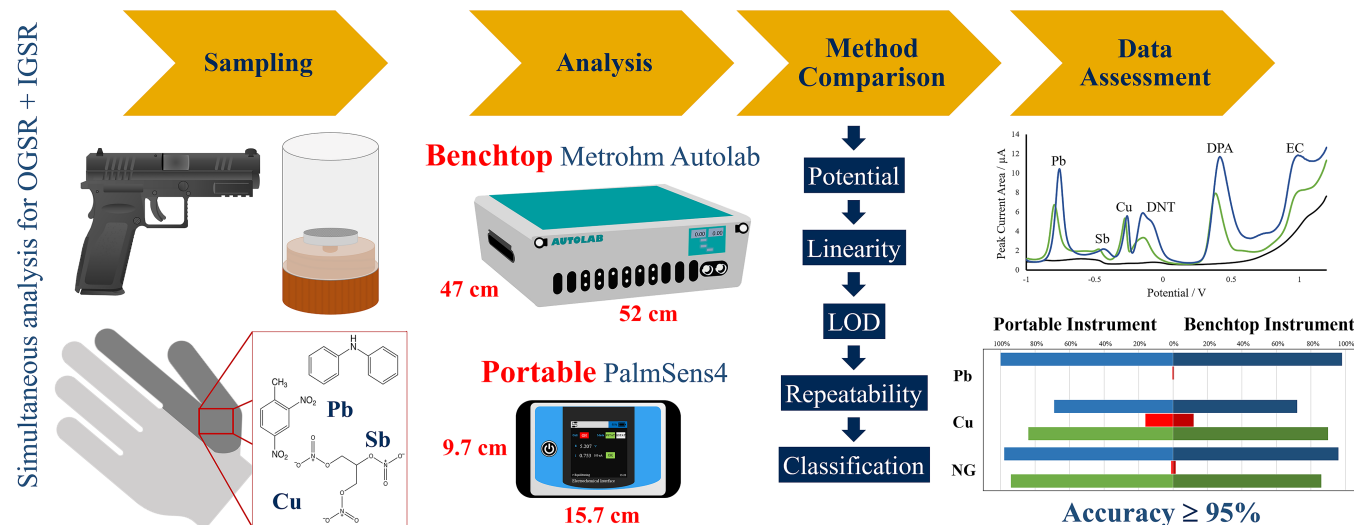
FIGURE 1 Overview of the analytical scheme applied for the collection, comparison, and assessment of portable versus benchtop electrochemical instruments for authentic GSR samples

benchtop technologies are presented to demonstrate the ability to incorporate this technology at the crime scene (Figure 1).

2 | MATERIALS AND METHODS

2.1 | Reagents and standards

Extractions were achieved using both acetate buffer prepared to a pH of 4.0 using sodium acetate anhydrous and glacial acetic acid (HPLC grade) and acetonitrile (Optima®) obtained from Fisher Scientific (Fair Lawn, NJ). Ultrapure water (≥18.2 MΩ) was provided by a Millipore Direct-Q® UV water purification system (Billerica, MA). Analyte standards were purchased as follows: 1,3-diethyl-1,3-diphenylurea 99% (ethyl centralite) from Sigma-Aldrich (St. Louis, MO); diphenylamine from SPEX Certiprep® (Metuchen, NJ); lead, copper, and antimony from Ultra Scientific® (Kingstown, RI); and nitroglycerin and 2,4-dinitrotoluene from AccuStandard® (New Haven, CT). Nitrogen was purchased from Matheson Tri-Gas, Inc. (Irving, TX).

Quality controls were prepared prior to authentic sample analysis using two mixtures of the IGSR and OGSR analytes in acetate buffer, where the first was a solution consisting of 2 ppm Pb, 0.2 ppm Cu, 8 ppm Sb, and 10 ppm of OGSR (2,4-DNT, DPA or NG, and EC). The second solution was the same; however, DPA was replaced with NG to evaluate their peak potential since peak resolution is difficult to achieve when DPA and NG are in solution together. These two solutions were referred to as the 10 ppm NG QC and 10 ppm DPA QC. Then 1:4 dilutions were made for both to generate a mixture of 2.5 ppm of OGSR analytes and 0.5 ppm Pb, 0.05 ppm Cu, and 2 ppm Sb for the IGSR analytes. Other controls run prior to analysis were a tailor-made pGSR standard [32], negative substrate control, and reagent control to ensure the quality performance of the instruments.

2.2 | Electrodes and instrumentation

Screen-printed carbon electrodes (SPCEs) were purchased from Metrohm DropSens USA, Inc. in the DRP-110 format containing carbon working and counter electrodes and a pseudo-silver reference electrode. Control over pH was performed using a Mettler Toledo FiveEasy pH meter (Columbus, OH). The benchtop potentiostat used was an Autolab PGSTAT128N with NOVA software version 2.1.4 from Metrohm USA, Inc. (Riverview, FL). The portable potentiostat was a PalmSens4 with PSTrace software version 5.8 (Randhoeve, Netherlands).

2.3 | Sample collection

Samples were collected from the hands of individuals as described previously by our group [17] and following Institutional Review Board (IRB) protocol # 1506706336. Following standard protocol for GSR collection, aluminum SEM stubs with carbon adhesive tape (Ted Pella, Inc. Redding, CA) were used as the collection substrate. Both shooter and background (nonshooter) samples were collected using a total of two stubs: one stub for the palm and back of the right hand and one stub for the palm and back of the left hand. Nonshooter background samples were collected from individuals on the West Virginia University (WVU) campus who had not fired or handled a firearm, fireworks, or participated in activities that could lead to GSR over the previous 24 h. Shooter samples were collected from the hands of shooters after firing 5 shots in the WVU ballistics laboratory using a Springfield XD firearm with Remington Range and reloaded Specialty Winchester 9 mm ammunition for leaded samples and reloaded Fiocchi ammunition for lead-free samples. Shooters washed their hands with soap and water between firing events. A total of 100 leaded shooter

samples, 50 lead-free shooter samples, and 200 background samples were collected for analysis.

2.4 | Sample preparation

All measurements were carried out in 0.1 M acetate buffer pH 4.0 using SPCEs. Extraction of the sampling stub surface was achieved in two portions: extraction of IGSR and extraction of OGSR. The IGSR extraction was achieved by placing 50 μl of acetate buffer on the stub surface and using the pipette to move the drop around the entire surface and allowing it to sit for approximately 10 s. This drop was transferred to a microfuge tube and saved. Then, a 50 μl drop of acetonitrile was added to cover the entire surface, allowed to sit for approximately 10 s, and then pipetted up and down prior to transfer to a second microfuge tube. This process was repeated for the GSR stub from the other hand simultaneously and a total of 100 μl for each extraction aliquot was placed in their respective tubes. Then the organic fraction was dried down under nitrogen and reconstituted using the aqueous portion prior to electrochemical analysis. Analysis was then conducted using 50 μl of the reconstituted sample for the benchtop instrumental method and the remaining 50 μl for the portable instrumental method. Figure 2 demonstrates the sample preparation process.

2.5 | Square-wave anodic stripping voltammetry (SWASV) method

Electrochemical analysis of GSR was achieved through the application of a deposition potential at −950 mV for 120 s. Then the potential was scanned between −1000 mV and +1200 mV using a square-wave procedure. The additional parameters of frequency, modulation amplitude, and step potential were optimized for the portable instrument using a response surface design. Table 1 provides the comparison between the parameters

used for the benchtop and portable instrument. Quality control (QC) samples were also used to assess the performance of the method and included a buffer blank, negative stub control, positive stub control, and several mixtures of GSR compounds at varying concentrations.

2.6 | Data analysis

The Nova 2.1.4 and PSTrace 5.8 software were used for peak integration and exported for data analysis in Excel 16 (version 16.56, Microsoft Corporation). The critical threshold method, detailed in Ott et al., was used for the classification and assessment of the results [17]. The critical thresholds used were the same as in Ott et al. for all samples and were Pb: 1.59×10^{-8} A×V, Cu: 3.33×10^{-8} A×V, NG: 4.28×10^{-9} A×V as assessed based on the background data sets previously collected using the same Metrohm Autolab potentiostat.

JMP Pro (version 16.0.0, SAS Institute) was used to carry out significance testing for standards and authentic samples using t-tests, where the assumption of normality and constant variance were evaluated, and the test was adjusted accordingly. Test adjustments included one-tailed versus two-tailed t-tests, unequal versus equal

TABLE 1 SWASV parameters for the analysis of GSR using both a benchtop potentiostat and a field-portable potentiostat

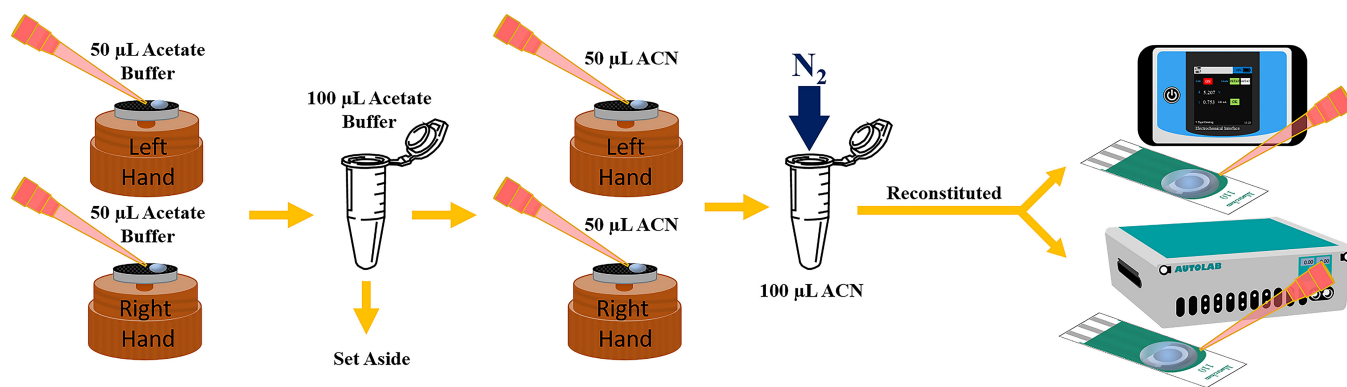| Parameter	Benchtop instrument	Portable instrument
Deposition time	120 s	120 s
Deposition potential	−0.95 V	−0.95 V
Start potential	−1.0 V	−1.0 V
End potential	1.2 V	1.2 V
Potential step	0.004 V	0.005 V
Amplitude	0.025 V	0.025 V
Frequency	8 Hz	11 Hz

FIGURE 2 GSR extraction procedure to assess the same samples by two methods: benchtop and portable potentiostats

variance, univariate versus multivariate, and the sample sizes and power of the test (at alpha 0.05). When normality was not met, a nonparametric test was performed.

3 | RESULTS AND DISCUSSION

The motivation of this study was to demonstrate the reliability of electrochemical sensors as a fast and accurate screening tool with efficient and rugged portable instrumentation comparable with laboratory benchtop potentiostats. The first objective involved the application and optimization of the previously developed method for simultaneous detection of IGSR and OGSR on the portable PalmSens4 potentiostat and evaluation of the performance in comparison to the benchtop Autolab, described in the *Comparison of Analytical Performance Measures section*. The second objective is discussed in the *Comparison of Authentic Samples* section detailing an assessment of the detection capabilities of both instruments and the estimated error rates and accuracy using authentic populations of nonshooter background ($n = 200$), leaded shooter ($n = 100$), and lead-free shooter ($n = 50$) samples.

3.1 | Comparison of analytical performance measures

The Metrohm Autolab potentiostat has been assessed in previous work for the electrochemical parameters, performance characteristics, and a large population of authentic samples [17]. Prior to starting the comparison study, the square-wave voltammetry method was optimized for the PalmSens4 using a Box Behnken surface response design and the JMP software. The design used 3 factors: frequency, amplitude, and step, each with 3 levels. A total of 15 experiments were analyzed using the 2.5 ppm DPA quality control. As a result of this optimization process, the potential step was increased to 0.005 V and the frequency was increased to 11 Hz for the portable device. The square-wave anodic stripping voltammetry

method (SWASV) demonstrated no other differences between optimal parameters for the portable or benchtop instruments.

Following method optimization, the individual GSR analytes were tested to demonstrate any variations between oxidation potentials, peak shape, and peak resolution, which are critical for the correct identification of IGSR elements and OGSR compounds of interest. The comparison of performance characteristics obtained for our portable instrument was completed for the GSR analyte panel including lead (Pb), copper (Cu), antimony (Sb), 2,4-dinitrotoluene (2,4-DNT), diphenylamine (DPA), nitroglycerin (NG), and ethyl centralite (EC). The performance characteristics of interest for individual analytes were oxidation potential, linear range, coefficient of correlation (R^2), repeatability, and limit of detection (LOD). Calibration curves were prepared via serial dilution to measure the electrochemical response and repeated in triplicate. The extracted current measurements for analysis used peak current area or peak current height depending on the analyte of interest. Limits of detection were calculated using 3 times the standard deviation of the lowest calibrator divided by the average slope of the calibration curves [33,34]. The results of the analytical performance tests can be seen in Table 2 for the benchtop Metrohm Autolab and in Table 3 for the portable PalmSens4.

Peak potential windows showed significant differences between potentiostats, although some potential windows overlapped. The differences in square-wave parameters or conditions affected analyte oxidation potentials, although copper's potential showed no significant difference between the portable and benchtop potentiostats (two-tailed t-test, $p = 0.0918$). All other GSR analytes demonstrated differences between the benchtop and portable potential windows using two-tailed t-tests with p-values less than 0.0418. It is important to note; however, that these differences were generally small and ranged between approximately 10 mV and 70 mV. Slight differences were demonstrated in the sensitivity of the two instruments for the GSR analysis and can be seen in the remaining parameters. The linear range of several analytes was changed as a result; however, the linearity of the constructed calibration curves was excellent using both instruments with adequate residual plots and R^2 values over 0.98 for the benchtop and 0.99 for the portable

TABLE 2 Performance characteristics calculated based on the Metrohm Autolab benchtop instrument [17]

	Potential (V)	Linear range (µg/ml)	R^2	Repeatability (%RSD, $n = 3$)	LOD (µg/ml)
IGSR					
Lead	-0.784 ± 0.035	0.10–2.0	0.999	4.4	0.055 ± 0.01
Antimony	-0.401 ± 0.027	0.75–7.5	0.986	10	0.183 ± 0.07
Copper	-0.292 ± 0.053	0.05–1.0	0.990	2.3	0.012 ± 0.001
OGSR					
2,4-Dinitrotoluene[a]	-0.132 ± 0.032	1.0–20	0.982	5.6	0.200 ± 0.03
Diphenylamine	0.406 ± 0.018	1.0–8.0	0.987	6.2	0.462 ± 0.06
Nitroglycerin	0.509 ± 0.010	0.50–8.0	0.998	10	0.147 ± 0.08
Ethyl centralite	1.03 ± 0.045	0.50–8.0	0.998	8.0	0.450 ± 0.09

[a]2,4-DNT was assessed as peak current height, whereas all other analytes were assessed as peak current area.

TABLE 3 Performance characteristics calculated based on the PalmSens4 portable instrument

	Potential (V)	Linear RANGE (µg/ml)	R^2	Repeatability (%RSD, $n = 3$)	LOD (µg/ml)
IGSR					
Lead	-0.790 ± 0.017	0.10–2.0	0.995	4.6	0.278 ± 0.13
Antimony[a]	-0.391 ± 0.017	0.1–2	0.992	16	0.235 ± 0.39
Copper	-0.317 ± 0.021	0.05–1.0	0.999	4.2	0.009 ± 0.004
OGSR					
2,4-Dinitrotoluene[a]	-0.148 ± 0.025	1.0–10	0.998	14	0.061 ± 0.09
Diphenylamine	0.417 ± 0.008	1.0–8.0	0.999	29	0.152 ± 0.44
Nitroglycerin	0.523 ± 0.007	0.50–8.0	0.995	33	0.438 ± 1.46
Ethyl centralite	0.945 ± 0.004	2.0–10	0.926	30	0.566 ± 1.67

[a]Antimony and 2,4-DNT were assessed as peak current height, whereas all other analytes were assessed as peak current area.

potentiostat, with the exception of ethyl centralite (0.92) due to oxidation of the analyte near the edge of the electrode potential window.

The largest difference between the two instruments was the repeatability. For the benchtop potentiostat, repeatability for all analytes was below 10%. However, the portable instrument demonstrated values under 16% for IGSR, with lead and copper below 5%, but for the OGSR analytes, repeatability ranged from 14% to 33%, significantly higher than observed for the benchtop instrument. This difference is attributed to the different specifications of the instruments or variation in the SWASV parameters between instruments [35,36]. It is important to note that since quantitative measurements are not performed in this qualitative screening, the effect is not as critical.

The final difference noted was within the limit of detection for the analytes. Although generally comparable, various differences across the two instruments can be observed. Overall, there was no trend related to IGSR or OGSR in terms of improvements or decreases in the calculated LOD values. For example, the LODs for DNT, DPA, Cu, and Sb demonstrated improvements with the portable instrument (one-sided t-test where Prob $< t$, p-values of 0.0005, <0.0001, 0.0007, and 0.0109, respectively). The alternative can be said for Pb and NG, which demonstrated inferior sensitivity to the benchtop unit where the one-sided t-test (Prob $> t$) resulted in p-values < 0.001 and 0.0074, respectively. The only analyte with a comparable LOD value was EC with a p-value of 0.1314 (Prob $> t$). Overall, the LODs were in the sub/low part-per-million range with a majority of analyte LOD values less than 0.300 µg/ml and all under 0.600 µg/ml. While various trends and differences were seen in the analytical performance measures, the detection limit windows for lead, copper, and nitroglycerin were within ranges typically observed in authentic shooter samples, while the other analytes are typically detected at levels below the LOD values for these electrochemical methods, although some instances of DNT were observed [17,18]. However, the true measure of the performance of each instrument relies on the assessment and comparison of authentic samples in order to screen for GSR analytes, and the assessment of quality controls.

Quality controls were run with these screening methods to ensure the proper functioning of the instrument and that there was no contamination present within any steps of the analysis process. The electrochemical quality controls were analyzed on both instruments and overlaid for comparison purposes. Figure 3 demonstrates the voltammogram comparison of the four quality control mixtures. As suggested by the analytical metrics, the mixture voltammograms were comparable to those obtained using the benchtop potentiostat, with the only differences being in terms of sensitivity and repeatability. In general, peak currents were similar for the majority of analytes; however, one important note is that the method for the portable potentiostat resulted in larger antimony signals for the standards. Based on previous work, it has been shown by our research group that this method is capable of correctly identifying GSR based on lead, copper, and nitroglycerin.

3.2 | Comparison of authentic samples

In this study, a data set of 350 samples was collected to represent background samples (nonshooter, 200 samples) and authentic shooters (150 samples) consisting of 100 leaded samples and 50 lead-free samples. Each of these samples was analyzed by both the portable and benchtop instruments for direct comparison, which was performed by first assessing the current signals obtained in the voltammogram against the critical threshold values. Critical threshold values were obtained from our previous study using a 350 background nonshooter set [17]. The prevalence of each of the three most commonly detected analytes (lead, copper, and nitroglycerin) above the critical threshold values was assessed and can be seen graphically in Figure 4. As expected, very low instances of lead and nitroglycerin were observed in the background population, with copper levels being the most identified analyte in the samples, at an average of 14% of the background nonshooter samples for both the benchtop and portable instruments. Lead and nitroglycerin were rare in the background population at averages of 1% and 2.5% for the two instruments. Clearly, the electrochemical profile for background samples is generally absent of GSR markers.
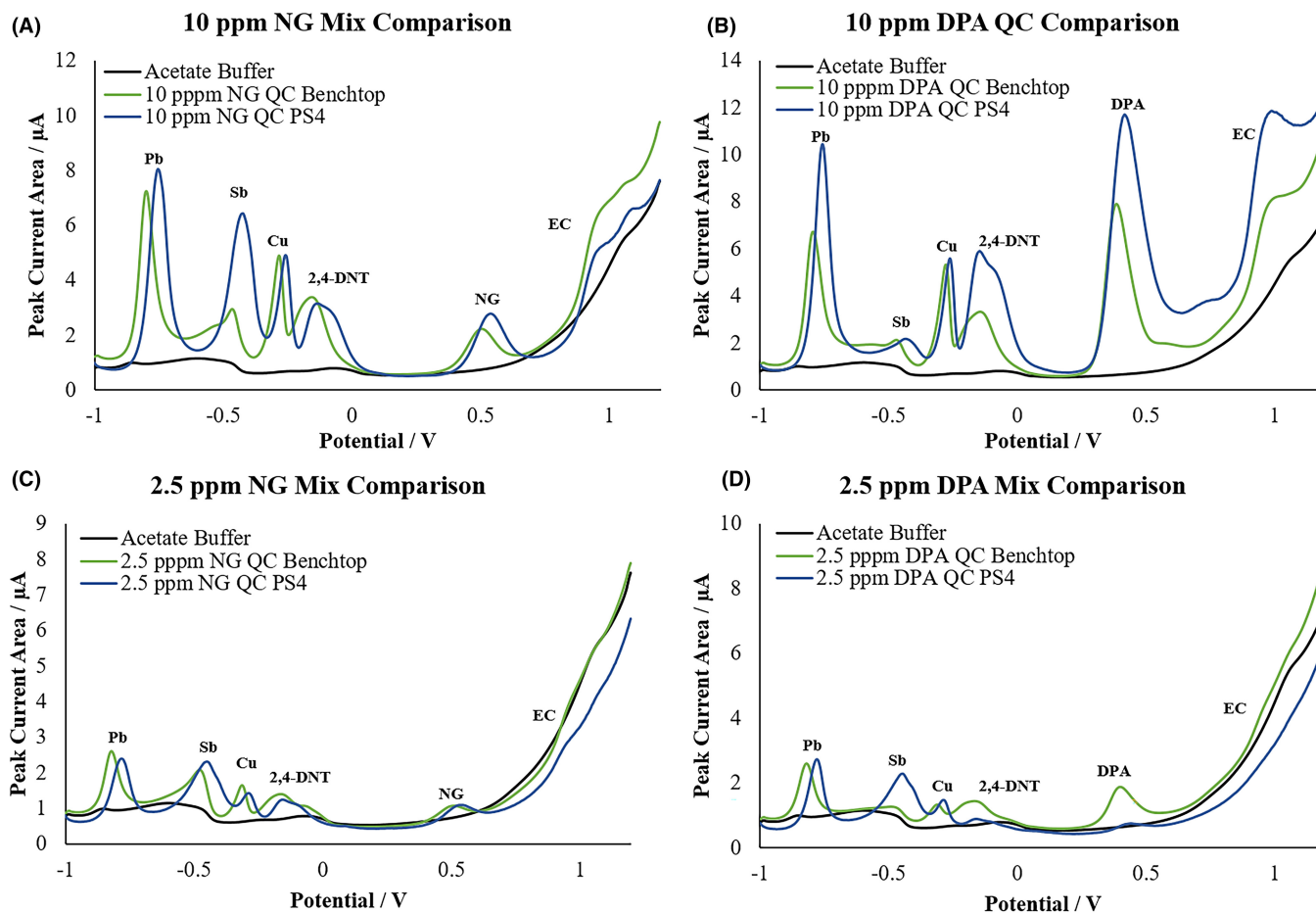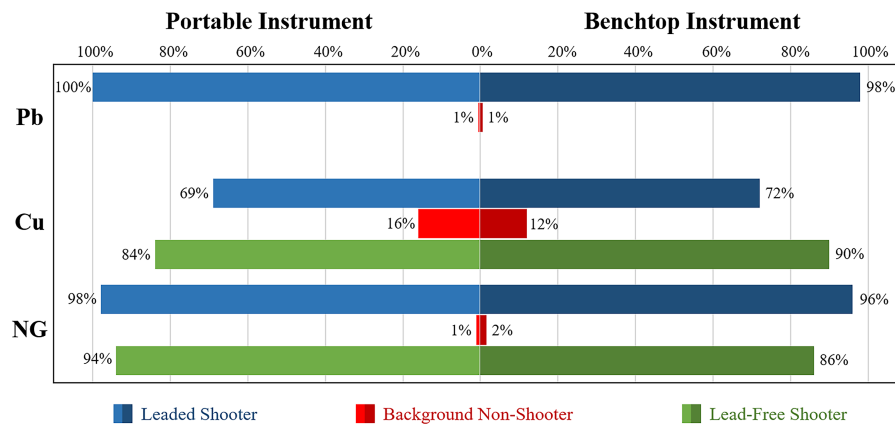
FIGURE 3 Comparison voltammograms of the quality control mixtures for the (A) 10 ppm NG QC, (B) 10 ppm DPA QC, (C) 2.5 ppm NG QC, and (D) 2.5 ppm DPA QC for the portable and benchtop instruments

FIGURE 4 Graphical comparison between the positive analyte identifications from the leaded and lead-free shooter and background populations for both the portable PalmSens4 instrument and benchtop Autolab instrument

This was in contrast to the leaded shooter samples, where approximately 70% of the samples contained copper. More significantly, an average of 97% of the leaded shooter samples contained nitroglycerin, and 99% contained lead. The high prevalence of nitroglycerin demonstrates the significance of detecting OGSR when many other GSR detection methods focus solely on IGSR. In relation to the comparison of the two instruments, it is important to observe that the largest difference in analyte identifications on leaded data sets between the benchtop and portable potentiostats was 3%, where lead and nitroglycerin were separated by 2% or less. Figure 4

shows the direct comparison between both instruments and both populations.

Additionally, the lead-free population can be seen in green in Figure 4. Due to the ammunitions being considered as lead-free, lead was not plotted in this figure but can be seen in Figure S1. The lead-free ammunition demonstrated difficulty in the proper cycling of the firearm, resulting in problems with the ejection of the cartridge cases, causing the shooters to handle the slide of the firearm and sometimes reload cartridges that have fallen on the floor of the shooting range. Additionally, the ammunition used was reloaded

in-house with lead-free primers; however, the projectiles available were lead bullets that were copper plated. Therefore, it is reasonable to assume that low-level lead contamination may have arisen from the high heat and pressure needed to propel these projectiles from the firearm in combination with contamination from the range floor itself. This was believed to result in possible lead contamination from the range environment, where an average of 77% of the lead-free samples were positive for lead. However, it is of importance to note that the lead signal size (peak current area) was significantly smaller for the lead-free ammunition than for the leaded ammunition, as can be seen in Figure 5 (one-sided t-test, Prob < t, p-value < 0.0001 and 0.0005 for the benchtop and portable instruments, respectively). The signals for lead resulting from the lead-free ammunition were significantly smaller and closer to the critical threshold cut-off than the leaded ammunition, providing evidence for possible firearm handling contamination rather than the presence of lead in the lead-free formulation. Memory effect from the barrel is not considered the major contributor, as the firearm barrel and mechanism were cleaned between ammunition types; however, as mentioned previously, low levels of lead may have been introduced during safety procedures during misfires, the range environment, or the projectile. Figures S2 and S3 provide the box plots for the comparison of copper and nitroglycerin signals between the leaded and lead-free populations, where no significant difference was found (t-test, p-values > 0.05). The lead-free shooter samples demonstrated positive copper results in 84% and 90% of samples for the portable and benchtop instruments, respectively. This is in comparison with the leaded samples at an average of 70% positive for copper, demonstrating a similar response for leaded and lead-free ammunition with a slight increase in positive copper signal. Interestingly, the mean and median signals were similar between the two populations (Figure S2). However, a
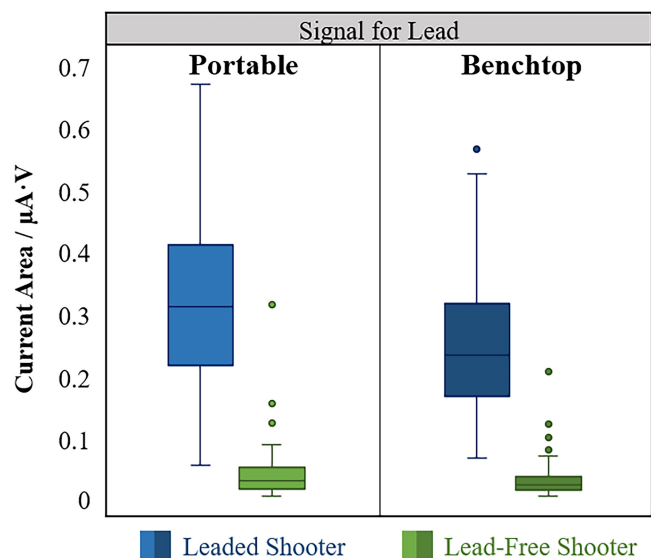
different trend was noted for nitroglycerin, where 94% and 86% of lead-free samples were above the critical threshold with the portable and benchtop instruments, respectively, which was lower than what was observed in the leaded samples. Additionally, the mean and median signals for the lead-free samples were visually slightly lower than the leaded samples for nitroglycerin, although this difference was not statistically significant (Figure S3).

These results support the utility of portable instrumentation for GSR detection, strengthening our previous evidence showing the importance of electrochemistry for the analysis of GSR and demonstrating that the portable potentiostat is capable of accurate and reliable screening as an alternative for on-site testing.

During the collection of the background nonshooter samples, volunteers were asked a series of questions to ensure they did not handle or discharge a firearm in the past 24h or participate in activities considered to be high-risk for detection of GSR-type residues. Additionally, a note was taken if the participant had any pen ink, tattoos, or other residues, or if the individual was wearing any rings or nail polish as those could lead to potential interferences or false-positive calls in the background population. Of the 38 samples that demonstrated one IGSR or OGSR analyte, 45% had an additional comment during the collection. An interesting finding regarding these comments showed that of those 69% and 72% of calls (Table S1) for copper by the benchtop and portable instruments, respectively, 38% of calls had the note of the individual wearing a ring during collection.

More importantly, a single analyte does not represent a positive identification of GSR. For the electrochemical screening, we defined the criteria that at least two different analytes (one IGSR, and one OGSR) must be present for positive identification of GSR. In this study, lead, copper, and nitroglycerin were the GSR identifiers used due to their prevalence in the sampled populations. While additional OGSR indicators would increase the reliability, nitroglycerin is a category one compound as defined by the OSAC classification of OGSR, increasing the value when present in a sample. Additionally, these methods are meant for screening, where laboratories could perform further confirmation of other OGSR analytes by methods like mass spectrometry [18,23].

When assessing the leaded shooter samples, an average of 70% of samples were positive for all three analytes as depicted in Figure 6. The next two most common calls were for lead and nitroglycerin at 25% of samples for the benchtop potentiostat and 30% of samples for the portable potentiostat. Furthermore, just 1% of samples contained only the IGSR combination of lead and copper being present with no OGSR. This is a significant finding since the majority of positive samples contained a mixture of IGSR and OGSR analytes (>96%), a fact that improves the reliability in the identification of GSR in a sample.

Following the identification of analytes above the critical threshold, performance measures were calculated based on the presence of two or more analytes as described above. Performance measures demonstrate the true positive, true negative, false-positive, false-negative, and accuracy calculated for each population analyzed by

FIGURE 5 Box plot comparison of the lead peak current area signal between leaded and lead-free populations for the benchtop and portable potentiostats

both electrochemical methods. Table 4 demonstrates the performance measures for the background and leaded shooter samples with a direct comparison between the benchtop and portable instrument. Both instruments were able to accurately assess all 200 background samples as not having the presence of GSR compounds, resulting in a 100% true negative rate. In the case of the leaded shooter samples, a small difference was seen between the benchtop and portable instruments; however, this difference may be attributed

to the loss of two samples due to an electrical failure within the instrument cable of the benchtop potentiostat. Due to this error, two samples were unable to be analyzed properly and were therefore considered negative for this comparison. Despite this, the true positive results for the leaded shooter samples were 97% for the benchtop and 99% for the portable instrument. Additionally, lead signals were not considered for the lead-free population in order to assess the strength of the method in the absence of lead and to account for the possible contamination as described previously. Therefore, the lead-free samples were considered positive if both copper and nitroglycerin were present above the critical threshold. Figure S4 provides the percentage of samples called with copper and nitroglycerin, and samples, which were false negatives for only copper or only nitroglycerin identified in the sample. By these criteria, the true positive results were 78% for the portable instrument and 76% for the benchtop instrument for the lead-free sample population.

High true positive rates and low false-negative rates were seen for both instruments for all populations, giving an average true positive rate of 88.5% and 86.5% for the portable and benchtop instruments when the different ammunition types were considered, respectively. The overall accuracy of the method was 96.5% for the portable instrument and 95.7% for the benchtop method, demonstrating the strength of electrochemistry for the screening of GSR and the ability of the portable instrument to produce results that were as accurate as the benchtop model. Further, excellent reproducibility between portable methods and benchtop instruments was demonstrated, along with high accuracy for a screening method for the correct classification of the samples. Moreover, most instances of false negatives occurred on the same samples when analyzed by both methods.
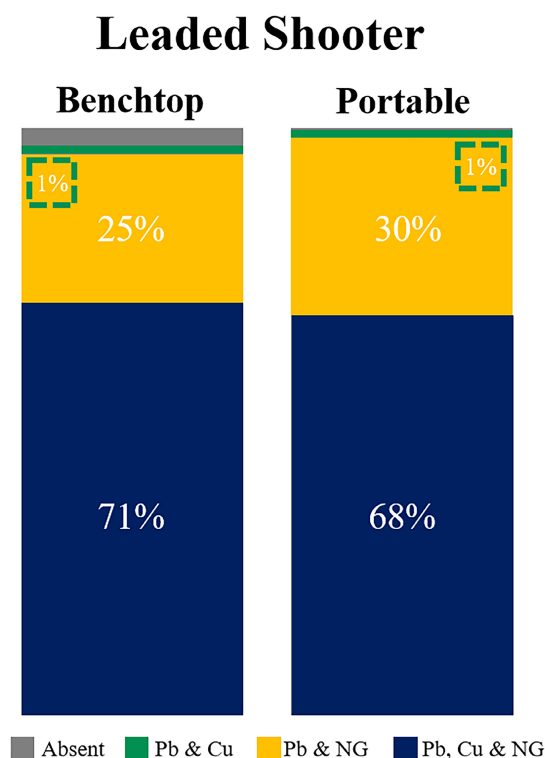

FIGURE 6 Comparison between the benchtop and portable potentiostats for positive call combinations of Pb+Cu (navy), Pb+NG (yellow), and Pb+Cu+NG (green) in the leaded shooter population

4 | CONCLUSION

The fast-paced innovation of technology has emphasized the need for testing portable devices to ensure the quality of results from

TABLE 4 Comparison of performance measures for the three populations between the benchtop (green) and portable (blue) instrumentation

Background and shooter samples performance rates by critical threshold						
	Metrohm benchtop instrument			PalmSens4 portable instrument		
	Background	Leaded shooter	Lead-free shooter	Background	Leaded shooter	Lead-free shooter
Number of sets	200	100	50	200	100	50
True positive (Sensitivity)	N/A	97 (97%)[a]	38 (76%)	N/A	99 (99%)	39 (78%)
False negative	N/A	3 (3%)	12 (24%)	N/A	1 (1%)	11 (22%)
True negative (Specificity)	200 (100%)	N/A	N/A	200 (100%)	N/A	N/A
False positive	0 (0%)	N/A	N/A	0 (0%)	N/A	N/A
Accuracy	95.7%			96.5%		

[a]Electrical issue caused the loss of two samples.

analysis to identification and interpretation of evidence. The purpose of this study was to compare the sensitivity, reliability, and selectivity of a field-portable potentiostat to a laboratory benchtop instrument for electrochemical screening of GSR. The results demonstrate equivalent identification of GSR between the two instruments, which provides a foundation for further implementation for preliminary testing of suspected GSR at forensic laboratories and the crime scene.

The sample preparation method provided the ability to analyze the same specimens on both instruments with ease of analysis taking under 10 min per sample and resulting in data directly comparable between instruments for the authentic samples.

Electrochemical performance characteristics demonstrated the comparable specificity and sensitivity between the benchtop and portable potentiostats for simultaneous IGSR and OGSR detection with limits of detection below 0.6 μg/ml for both instruments. The most significant difference was that the benchtop potentiostat demonstrated better repeatability.

Most importantly, both instruments provided GSR identification for lead, copper, and nitroglycerin using critical threshold approaches with accuracies over 95% for classification of samples as shooter or nonshooter based on combined IGSR/OGSR profiles. This demonstrates the scientific reliability of the portable electrochemical method for casework-like samples. Assessing the application of the portable potentiostat lays the groundwork for this screening approach as a future tool for forensic laboratories. The advantage of this portable system is that it provides a rapid and sensitive GSR field-screening method to minimize the disconnect of decisions between the crime scene and laboratory analysis within the discipline. Additionally, portable devices help in triage, both at crime scenes and laboratories, to provide a cost-efficient screening method that can decrease backlogs and allow for further confirmatory testing when needed. Most importantly, fast decision-making at crime scenes can significantly aid the collection of relevant information. This application contributes to the necessary developments in forensic technology with dual IGSR and OGSR detection in addition to low sensitivity with reliability comparable with laboratory instrumentation. The main findings of this work demonstrate not only the speed and convenience of simultaneous IGSR and OGSR detection but also the effectiveness of the portable technology.

This study furthers the information needed for forensic laboratories to implement electrochemical screening methods as a portable detection instrument for GSR. Continued research in portable electrochemical potentiostats by our research group will include demonstrating the convenience of the method at mock crime scenes and testing with authentic casework samples and collaboration with practicing forensic laboratories to showcase the importance and efficiency of on-site GSR screening.

ORCID

Kourtney A. Dalzell https://orcid.org/0000-0002-3559-3278
Colby E. Ott https://orcid.org/0000-0002-8059-2581
Tatiana Trejos https://orcid.org/0000-0001-9928-1022
Luis E. Arroyo https://orcid.org/0000-0003-0391-3967

REFERENCES

1. ASTM International. E1588-20 standard guide for gunshot residue analysis by scanning electron microscopy/energy dispersive X-ray spectrometry. Conshohocken, PA: ASTM International; 2020.
2. de Araujo WR, Cardoso TMG, da Rocha RG, Santana MHP, Muñoz RAA, Richter EM, et al. Portable analytical platforms for forensic chemistry: a review. Anal Chim Acta. 2018;1034:1–21. https://doi.org/10.1016/j.aca.2018.06.014
3. Maitre M, Kirkbride KP, Horder M, Roux C, Beavis A. Thinking beyond the lab: ORGANIC gunshot residues in an investigative perspective. Aust J Forensic Sci. 2018;50(6):659–65. https://doi.org/10.1080/00450618.2018.1457718
4. Gassner AL, Ribeiro C, Kobylinska J, Zeichner A, Weyermann C. Organic gunshot residues: Observations about sampling and transfer mechanisms. Forensic Sci Int. 2016;264:369–78. https://doi.org/10.1016/j.forsciint.2016.06.029
5. Maitre M, Kirkbride KP, Horder M, Roux C, Beavis A. Current perspectives in the interpretation of gunshot residues in forensic science: a review. Forensic Sci Int. 2017;270:1–11. https://doi.org/10.1016/j.forsciint.2016.09.003
6. Dalby O, Butler D, Birkett JW. Analysis of gunshot residue and associated materials – a review. J Forensic Sci. 2010;55(4):924–43. https://doi.org/10.1111/j.1556-4029.2010.01370.x
7. Feeney W, Vander Pyl C, Bell S, Trejos T. Trends in composition, collection, persistence, and analysis of IGSR and OGSR: a review. Forensic Chem. 2020;19:100250. https://doi.org/10.1016/j.forc.2020.100250
8. Goudsmits E, Sharples GP, Birkett JW. Preliminary classification of characteristic organic gunshot residue compounds. Sci Justice. 2016;56(6):421–5. https://doi.org/10.1016/j.scijus.2016.06.007
9. Goudsmits E, Sharples GP, Birkett JW. Recent trends in organic gunshot residue analysis. Trends Analyt Chem. 2015;74:46–57. https://doi.org/10.1016/j.trac.2015.05.010
10. Gunshot Residue Subcommittee and Chemistry/Instrumental Analysis Scientific Area Committee. Standard practice for the collection, preservation, and analysis of organic gunshot residues. Oganization of Scientific Area Committees for Forensic Science. 2020. https://www.nist.gov/system/files/documents/2020/05/22/OSAC%20GSR%20SC%20Organic%20GSR%20Document_May%202020.pdf. Accessed 18 Apr 2022.
11. Ali L, Brown K, Castellano H, Wetzel SJ. A study of the presence of gunshot residue in Pittsburgh police stations using SEM/EDS and LC-MS/MS. J Forensic Sci. 2016;61(4):928–38. https://doi.org/10.1111/1556-4029.13077
12. Blakey LS, Sharples GP, Chana K, Birkett JW. Fate and behavior of gunshot residue—a review. J Forensic Sci. 2018;63(1):9–19. https://doi.org/10.1111/1556-4029.13555
13. Meng H, Caddy B. Gunshot residue analysis–a review. J Forensic Sci. 1997;42(4):553–70. https://doi.org/10.1520/JFS14167J
14. Trejos T, Vander Pyl C, Menking-Hoggatt K, Alvarado AL, Arroyo LE. Fast identification of inorganic and organic gunshot residues by

LIBS and electrochemical methods. Forensic Chem. 2018;8:146–56. https://doi.org/10.1016/j.forc.2018.02.006

15. Shrivastava P, Jain VK, Nagpal S. Gunshot residue detection technologies—a review. Egypt J Forensic Sci. 2021;11:11. https://doi.org/10.1186/s41935-021-00223-9

16. Speaker PJ. Project FORESIGHT annual report, 2019-2020. WVU Res Repos. 2021. https://researchrepository.wvu.edu/faculty_publications/3008. Accessed 18 Apr 2022.

17. Ott CE, Dalzell KA, Calderón-Arce PJ, Alvarado-Gámez AL, Trejos T, Arroyo LE. Evaluation of the simultaneous analysis of organic and inorganic gunshot residues within a large population data set using electrochemical sensors. J Forensic Sci. 2020;65(6):1935–44. https://doi.org/10.1111/1556-4029.14548

18. Feeney W, Menking-Hoggatt K, Vander Pyl C, Ott CE, Bell S, Arroyo L, et al. Detection of organic and inorganic gunshot residues from hands using complexing agents and LC-MS/MS. Anal Methods. 2021;13(27):3024–39. https://doi.org/10.1039/d1ay00778e

19. O'Mahony AM, Samek IA, Sattayasamitsathit S, Wang J. Orthogonal identification of gunshot residue with complementary detection principles of voltammetry, scanning electron microscopy, and energy-dispersive X-ray spectroscopy: sample, screen, and confirm. Anal Chem. 2014;86(16):8031–6. https://doi.org/10.1021/ac5016112

20. Erden S, Durmus Z, Kiliç E. Simultaneous determination of antimony and lead in gunshot residue by cathodic adsorptive stripping voltammetric methods. Electroanalysis. 2011;23(8):1967–74. https://doi.org/10.1002/elan.201000612

21. Salles MO, Naozuka J, Bertotti M. A forensic study: lead determination in gunshot residues. Microchem J. 2012;101:49–53. https://doi.org/10.1016/j.microc.2011.10.004

22. Wang J, Tian B, Wang J, Lu J, Olsen C, Yarnitzky C, et al. Stripping analysis into the 21st century: faster, smaller, cheaper, simpler and better. Anal Chim Acta. 1999;385(1–3):429–35. https://doi.org/10.1016/S0003-2670(98)00664-3

23. Feeney W, Menking-Hoggatt K, Arroyo LE, Curran J, Bell S, Trejos T. Evaluation of organic and inorganic gunshot residues in various populations using LC-MS/MS. Forensic Chem. 2021;27:100389. https://doi.org/10.1016/j.forc.2021.100389

24. Menking-Hoggatt K, Arroyo L, Curran J, Trejos T. Novel LIBS method for micro-spatial chemical analysis of inorganic gunshot residues. J Chemometr. 2019;35(1):e3208. https://doi.org/10.1002/cem.3208

25. Vander Pyl C, Martinez-Lopez C, Menking Hoggatt K, Trejos T. Analysis of primer gunshot residue particles by laser induced breakdown spectroscopy and laser ablation inductively coupled plasma mass spectrometry. Analyst. 2021;146:5389–402. https://doi.org/10.1039/D1AN00689D

26. Vuki M, Shiu KK, Galik M, O'Mahony AM, Wang J. Simultaneous electrochemical measurement of metal and organic propellant constituents of gunshot residues. Analyst. 2012;137(14):3265–70. https://doi.org/10.1039/c2an35379b

27. Olson EJ, Isley WC, Brennan JE, Cramer CJ, Bühlmann P. Electrochemical reduction of 2,4-dinitrotoluene in aprotic and pH-buffered media. J Phys Chem C. 2015;119(23):13088–97. https://doi.org/10.1021/acs.jpcc.5b02840

28. O'Mahony AM, Wang J. Electrochemical detection of gunshot residue for forensic analysis: a review. Electroanalysis. 2013;25(6):1341–58. https://doi.org/10.1002/elan.201300054

29. Woolever CA, Dewald HD. Differential pulse anodic stripping voltammetry of barium and lead in gunshot residues. Forensic Sci Int. 2001;117(3):185–90. https://doi.org/10.1016/S0379-0738(00)00402-3

30. O'Mahony AM, Windmiller JR, Samek IA, Bandodkar AJ, Wang J. Swipe and scan: Integration of sampling and analysis of gunshot metal residues at screen-printed electrodes. Electrochem Commun. 2012;23(1):52–5. https://doi.org/10.1016/j.elecom.2012.07.004

31. Harshey A, Srivastava A, Das T, Nigam K, Shrivastava R, Yadav VK. Trends in gunshot residue detection by electrochemical methods for forensic purpose. J Anal Test. 2021;5(3):258–69. https://doi.org/10.1007/s41664-020-00152-x

32. Menking-Hoggatt K, Martinez C, Vander Pyl C, Heller E, Pollock E, Arroyo L, et al. Development of tailor-made inorganic gunshot residue (IGSR) microparticle standards and characterization with a multi-technique approach. Talanta. 2021;225:121984. https://doi.org/10.1016/j.talanta.2020.121984

33. Mocák J, Janiga I, Rábarová E. Evaluation of IUPAC limit of detection and ISO minimum detectable value – electrochemical determination of lead. Nov Biotechnol Chim. 2021;9(1):91–100. https://doi.org/10.36547/nbc.1291

34. Lavagnini I, Antiochia R, Magno F. A calibration-base method for the evaluation of the detection limit of an electrochemical biosensor. Electroanalysis. 2007;19(11):1227–30. https://doi.org/10.1002/elan.200703847

35. Colburn AW, Levey KJ, O'Hare D, Macpherson JV. Lifting the lid on the potentiostat: a beginner's guide to understanding electrochemical circuitry and practical operation. Phys Chem Chem Phys. 2021;23(14):8100–17. https://doi.org/10.1039/d1cp00661d

36. Gamry Instruments. Understanding the specifications of your potentiostat. 2016. https://www.gamry.com/application-notes/instrumentation/understanding-specs-of-potentiostat/. Accessed 18 Apr 2022.

SUPPORTING INFORMATION

Additional supporting information may be found in the online version of the article at the publisher's website.